METABOLITES ISOLATED FROM *MOOREA PRODUCENS, NOSTOC SPHAERICUM,* AND *SPONGIA* SP.

A THESIS SUBMITTED TO THE GRADUATE DIVISION OF THE UNIVERSITY OF HAWAI'I AT MĀNOA IN PARTIAL FULFILMENT OF THE
REQUIREMENTS FOR THE DEGREE OF

MASTER OF SCIENCE

IN

CHEMISTRY

MAY 2013

By

Stephen M. Parrish

Thesis Committee:

Philip G. Williams, Chairperson
Thomas K. Hemscheidt
Ho L. Ng

Keywords: Natural Products, BACE1, Aromatase, QR1, Diterpenes, Spongians, Pyridine

We certify that we have read this thesis and that, in our opinion, it is satisfactory in the scope and quality as a thesis for the degree of Master of Science in Chemistry.

THESIS COMMITTEE

Philip G. Williams, Chairperson

Thomas K. Hemscheidt

Ho L. Ng

ACKNOWLEDGMENTS

First and foremost I would like to thank my advisor Dr. Philip Williams for his seemingly limitless patience and advice. For letting me be a part of his group and go SCUBA diving around many of the Hawaiian Islands, and for not scolding me when I'm the first to run out of air. I would also like to thank Wesley Yoshida for taking the time to perform the countless NMR experiments run for me and later for all the patience in teaching me how to operate the software and run the experiments myself. A big thanks goes out to all my group members, in particular Dr. Jingqui Dai for her technical as well as emotional support; continually reminding me to have patience. Finally I would like to thank Dr. Thomas Hemscheidt and Dr. Ho Ng for being a constant source of information and taking the time to help me with this enduring task.

ABSTRACT

Mankind has been interacting with natural products for centuries. The metabolites held within organisms have been the most valuable source of drug leads and continue to develop a complex scaffolding and bioactivity. In my thesis, I present data from a cyanobacterium strain, *Moorea producens*, in the bioactivity-guided isolation of a new lipophilic molecule, trans-7-methoxytetradec-5-ene-4-oneioic acid (**2.1)** and a few known non-active molecules majusculamides A and B (**2.2, 2.3**). Next, another cyanobacterium, *Nostoc sphaericum*, is extracted to obtain three known indolocarbazoles (**2.4-2.6**), separating two similar regioisomers for the first time allowing us to obtain distinct IR data.

I will also present the isolation and characterization of one known (**3.4**) and three new spongians (**3.1-3.3**). One novel diterpene, spongiapyridine (**3.3**), has a unique pyridine ring in the D ring of the molecule. Its structure elucidation was complicated by a methylene that exchanged its proton with the deuterated solvent. 19-nor-3,5α,17-trihydroxyspongia-3,13(16),14-triene-2-one (**3.2**) showed weak aromatase inhibition at 34 μM and moderate quinone reductase induction with a CD of 11.2 μM. Data of these structures are presented via NMR and LC-MS spectroscopic data, as well as the bioactivity, biosynthesis and implications associated with these molecules.

TABLE OF CONTENTS

List of Figures

List of Tables

List of Abbreviations

$[\alpha]_D^T$	specific rotation at 589 nm and temperature T in ºC
$AB_{40/42}$	alpha beta amyloid protein fragments contacting 40 or 42 amino acids
AChEI	acetylcholinesterase inhibitor
ACN	acetonitrile
AD	Alzheimer's disease
AI	aromatase inhibitor
AMU	atomic mass unit
APP	amyloid precursor protein
BACE1	beta amyloid cleavage enzyme one
brd	broad doublet
brs	broad singlet
c	concentration in g/100 mL
°C	degrees in Celsius
C8	octyl
calcd	calculated
CD	concentration of doubling
$CDCl_3$	deuterated chloroform
CH_2	methylene
^{13}CNMR	nuclear magnetic resonance of carbon isotope with mass 13 Daltons
COSY	correlation spectroscopy

δ	chemical shift
d	doublet
1D	one dimensional
2D	two dimensional
DCM	dichloromethane
dd	doublet of doublets
ddd	doublet of doublet of doublets
dddd	doublet of doublet of doublet of doublets
ddt	doublet of doublet of triplets
DMSO	dimethyl sulfoxide
DNA	deoxyribonucleic acid
dq	doublet of quartets
dt	doublet of triplets
EFC	enzyme fragment complementation
ESI	electrospray ionization
EtOAC	ethyl acetate
FDA	Food and Drug Administration
H_2O	water
Hex	hexanes
HMBC	heteronuclear multiple bond coherence
^{1}HNMR	nuclear magnetic resonance of carbon isotope with a mass of 1 Dalton
HPLC	high pressure liquid chromatography
HSQC	heteronuclear single quantum coherence
IC_{50}	inhibitor concentration of 50%
IR	infrared
^nJ	coupling constant via n bonds
LC-MS	liquid chromatography mass spectrometry
m	multiplet
$[M+H]^+$ /$[M+Na]^+$	pseudo molecular ions
m/z	mass to charge ratio
MeOH	methanol

MHz	megahertz
MS	mass spectrometry
MW	molecular weight
NaCl	sodium chloride
NF-κB	nuclear factor kappa B
NIH	National Institute of Health
NMR	nuclear magnetic resonance
NOE	nuclear Overhauser effect
[O]	oxidation
p*	pi antibonding orbital
q	quartet
qC	quaternary carbon
qd	quartet of dublets
QR1	quinone reductase one
ROESY	rotating frame Overhauser effect spectroscopy
RXRE	retinoid X receptor response element
s	singlet
S	sinister (descriptor in Cahn-Ingold-Prelog system)
sAPP	soluble amyloid precursor protein
SCUBA	self-contained underwater breathing apparatus.
Si	silica
sp	species
sp^2	sp^2
t	triplet
tdd	triplet of doublet of doublets
THF	tetrahydrofuran
TOCSY	total correlation spectroscopy
TRPM7	transient receptor potential cation channel, subfamily M, member 7
UV	ultra violet

CHAPTER 1

1. Introduction

1.1 A Brief History of Natural Products

For centuries, mankind has looked towards Nature for inspiration. We have used Nature's chemistry to increase our effectiveness in both taking and preserving life. In warfare, tribes would coat their weaponry in toxins to make them more dangerous. For example, native Hawaiians on Maui would dip their spears in a sacred pool, rubbing the tips against the seaweed-like soft coral, thereby coating them with the deadly toxin palytoxin.[1] This is not an isolated example, as South America natives would rub the ends of their weapons on poison dart frogs, essentially applying lethal or paralysis inducing alkaloids like epibatidine,[2] to help ensure the kill.

The use of Nature's bounty as traditional medicines has flourished, as well. Almost all ancient civilizations used plants and herbs as a means to remedy their ailments and/or enhance other characteristics. Ancient Egyptians would apply honey to wounds knowing that it helped promote healing and prevent festering.[3] Other cultures, such as the Incans, used plants to combat hunger and fatigue, unaware they were ingesting the powerful narcotic cocaine by chewing on coca leaves[4]. While the use of these traditional medicines flourished, one thing was certain, most knew nothing about the antibiotics these medicines contained.

As civilizations and technology became more advanced, scientists began isolating and identifying the bioactive components of these traditional medicines and poisons. This work led to many of the well-known molecules that are still used today. These were molecules like

morphine,[5] extracted from opium poppy, or salicin,[6] a precursor to the drug aspirin from willow bark. During the early to mid-1900's, a variety of molecules were isolated and identified, yielding many of the families of antibiotic compounds still prescribed today, including the penicillins[7] and tetracyclines.[8] The discovery of these compounds fundamentally changed modern medicine. With these antibiotics widely available, mortality rates gradually decreased,[9] as influenza and pneumonia were no longer within the top five leading causes of death.[10]

Buoyed by these successes, screenings campaigns were conducted using these sources to identify compounds that could alleviate other ailments, such as hypertension, malaria, and cancer. This work produced many drug leads and a plethora of FDA approved drugs such as the anticancer drugs paclitaxel,[11] daunorubicin,[12] and camptothecin.[13] Artemisinin[14] (an antimalarial agent) and lovastatin[15] (cholesterol lowering agent) are fruits of natural product chemistry that currently bring in billions of dollars every year.

Up until the 1950's, most natural product research was conducted on terrestrial organisms. It was not until the advent of SCUBA that researchers began to investigate the marine environment. Being able to spend prolonged periods underwater allowed researchers to find and collect new organisms, such as sponges, tunicates, mollusks, and marine cyanobacteria. These organisms have become extremely productive sources of new chemistry.[16] Having this "new" environment to peruse yielded seven marine drugs[17] such as the anticancer alkaloid trabectedin,[18] isolated from a tunicate, and ziconotide,[19] a peptide obtained from a cone snail's poison used to treat severe chronic pain. Success has continued, as there are almost a dozen other marine-derived compounds, from a variety or organisms,[20] currently in clinical trials.

As discussed by Newman and Cragg in a 2012 review, approximately 57% or 767 drugs are natural products or derived from such.[21] This indicates that screening Nature's creations for molecular scaffolds is a viable strategy for the discovery of new leads. Given this impressive

track-record, it is no wonder that we still look to Mother Nature to cure us.

While these examples prove natural products are a suitable source of drug leads, there is another reason to look to Nature for inspiration. This argument is based off the idea of conservation of protein fold topology (PFT). Protein fold topology describes cavity recognition points unrelated to their sequence of domain fold similarity, and are similar through the binding of common ligands.[22] During the biosynthesis of a metabolite, both the substrate and product of a given reaction must interact with the producing enzyme. In this hypothesis, a metabolite made by an enzyme with a particular PFT should interact with other enzymes with the same PFT, regardless of the enzymes primary structure or its overall function.[23,24] This hypothesis justifies screening all organisms' metabolites against any pathology and why organisms with no nervous system, such as sponges or cyanobacteria, could produce compounds relevant to treating neurodegenerative targets.

All of these success stories in the realm of natural products chemistry are highly encouraging. Mortality rates decreased and, drug by drug, we are able to fight the diseases we are faced with. However, life expectancies are increasing and a consequence of longer lifespans is that people die by new pathologies. Cancer and neurodegenerative diseases, such as Alzheimer's disease, are two examples that are currently the 2nd and 6th leading cause of death in the US, respectively.[25, 38]

1.2 Selected Targets of Current Pathologies: Alzheimer's Disease and Cancer

As mentioned earlier, an increase in expected human lifespan due to advances in modern medicine, led to the development of other pathologies, some which take a longer time to manifest. One such disease is Alzheimer's disease (AD). In the United States alone, an estimated

5.4 million people have AD and in the year 2012, it was expected to have cost over $200 billion in expenses (not including the enormous amount of unpaid family care).[25]

While the exact cause of AD is not known, there are a few hypotheses that are being investigated. The two major hallmarks of AD are tau tangles and Aβ plaques located in the brain. One hypothesis being investigated deals with the development of tau tangles in the brain,[26,27] which are caused by hyperphosphorylation of tau protein abundant in neurons of the central nervous system.[28] When this hyperphosphorylation occurs, the tau proteins can self-assemble tangles, or if the protein is misfolded, the usually soluble protein can now become insoluble and form aggregates.[29] These tangles, which occur within the neuron, are thought to be toxic to neurons by preventing intracellular transport of nutrients and other essential molecules throughout the cell.[30] The jury is still out on whether the tau tangles are a causative function of AD, or if it is an effect.

A second hypotheses existing for the cause of AD, the Amyloid Cascade hypothesis, is strongly supported.[31,32,33] In this hypothesis, amyloid precursor protein (APP) is cleaved by the enzyme β-secretase, also known as BACE1 (beta-amyloid cleavage enzyme one), which may then be cleaved by γ-secretase to form 40 or 42 amino acid insoluble proteins. These insoluble proteins then aggregate, forming $A\beta_{42}$ plaques within the brain (**Figure 1.1**). The $A\beta_{42}$ plaques can block neuronal connections and at elevated levels become toxic to the neurons, leading to neuronal degeneration and overall loss of cognitive function. Therefore BACE1 is a suitable target for the treatment of Alzheimer's; the inhibition of BACE1 would lead to diminished levels of insoluble Aβ proteins, preventing the formation of new plaques in the brain and hopefully slowing/halting the onset of Alzheimer's disease. While γ-secretase is not a good drug target, because it plays a major role in the NOTCH signaling pathway that is important in cell

differentiation, neuronal function, and cell-cell communication,[34] BACE1 is a suitable target for the treatment of Alzheimer's. Supports for this includes that knockout mice deficient of BACE1 don't have any overtly abnormal phenotypes.[35] The inhibition of BACE1 would lead to diminished levels of insoluble Aβ proteins, preventing the formation of new plaques in the brain and hopefully slowing/halting the onset of Alzheimer's disease.

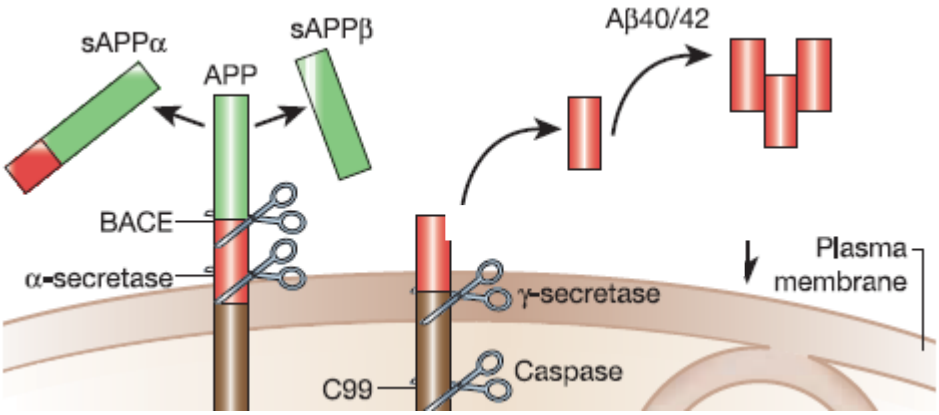

Figure1.1 Formation of amyloid plaques found in AD. Cleavage of amyloid precursor protein (APP) by a-secretase forms soluble fragments where-as cleavage by both BACE and γ-secretase yields insoluble Aβ40/42 proteins that aggregate to form plaques. Image modified from Mattson, M. P. *Nature*. **2004**, 430, 631.

Currently, five drugs are approved by the FDA to treat AD. However, these drugs only treat the cognitive symptoms, and none are targeting the possible cause. For instance, four of the drugs, including galantamine, a natural product drug derived from the bulbs of the lily, daffodil and related plants, are acetylcholinesterase inhibitors. AChEIs works by inhibiting the hydrolysis of acetylcholine, allowing for the neurotransmitter to continue activating neurons.[36] The fifth, memantine, is an *N*-methyl D-aspartate antagonist, which works by regulating glutamate levels in the brain, preventing them from rising to cytotoxic levels.[37] Since these drugs do not treat the cause, neurological deterioration due to AD continues, and unless a medical breakthrough occurs, the incidence rate of AD will be doubled in twenty years.[25]

Cancer is another pathology that affects nearly everyone's life and is becoming more

prevalent with the increase of life expectancy. It is currently the second leading cause of death in the US, and in 2008, the costs of cancer were $201.5 billion. In 2013, an estimated 1.66 million new cases will be discovered, while over 580,000 people are estimated to die from cancer.[38] While much progress has been achieved in the field of treating cancer once it has been diagnosed, the best way to deal with cancer is prevention. Chemoprevention is an idea that may be achieved by up regulating anti-carcinogenic enzymes. Of particular relevance to the work in this thesis, are quinone reductase and aromatase which can produce anti-carcinogenic and carcinogenic species respectively (**Figure 1.2**).

Aromatase, or estrogen synthase, is an attractive drug target, because estrogens are important in the growth of breast cancer.[39,40,41] Estrogens participate in redox cycles that produce oxidative stress and cause DNA damage.[42] Estrogens can also form depurinated adducts and detach from DNA leaving behind apurinated sites. These sites may be erroneously repaired creating DNA mutations that can lead to cancer.[43] In postmenopausal women, the major source of estrogen is from the enzyme aromatase, a monooxygenase responsible for the aromatization of androgens into estrogens. Thus aromatase is a suitable drug target because aromatase inhibitors (AI) would decrease the amount of estrogen available, lowering ones risk for breast carcinogenesis.

Quinone reductase 1 (QR1) is an enzyme that protects cells from the cytotoxic effects of free radicals. QR1 catalyzes the reduction of many quinones into hydroquinones, which can then be excreted safely.[44] Importantly, some of these hydroquinones act as radical scavengers. Thus, an upregulation of this enzyme produces more radical scavengers, and reduces the amount of oxidative stress in the cells, resulting in less DNA damage.[45] In addition, a reduction in the levels of estrogen quinones will decrease the amount of depurinating adducts created, thus reducing ones risk for carcinogenesis

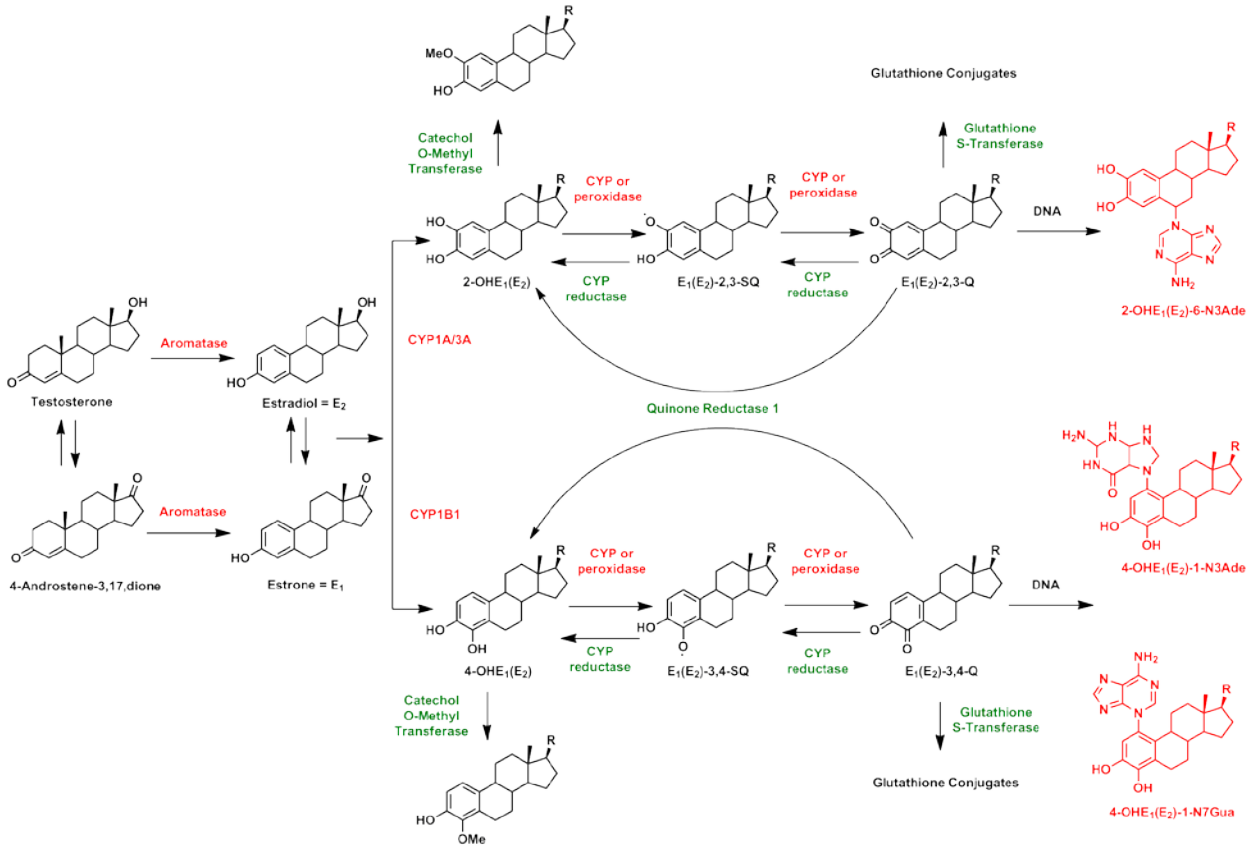

Figure 1.2. Formation, metabolism and DNA adducts of estrogens. The activating enzymes and depurinating adducts are in red, while protective enzymes in green. CYP's are different cytochrome P450 enzymes. Major strategies in this line of chemoprevention revolve around the reduction of estrogen quinones available for creating depurinating adducts. Image was modified from Cavalieri, E.L.; Rogan, E.G. *J. Steroid Biochem Mol. Bio.* **2011**, 125, 169–180

While many drugs have been approved for the treatment of breast cancer, few have been approved for the prevention. Much like the use of aspirin to prevent coronary heart disease,[46] drugs such as tamoxifen[47,48] have been used both for treatment and preventative purposes in high risk breast cancer patients. Currently there are a few FDA approved AI[49] (anastrozole, letrozole, and exemestane), but no QR1 inducers. However, a large number of QR1 inducers from fruits and vegetables has been found, which may lead the chemoprevention argument in favor of developing better diets. Inducers of QR1 have been isolated from green onions,[50] garlic,[51] and red grapes (resveratrol[45]). If drugs can be found with chemopreventative properties, we could

incorporate them into health supplements for high-risk cancer patients, and it would be possible to save many of the lives and money that is lost to cancer each year.

1.3 Research Objectives and Strategies

Our objectives have been to investigate organisms for their bioactive and/or interesting secondary metabolites. We have followed two paths in identifying bioactive compounds. The first was large scale screenings of marine samples against BACE1, identifying the active samples and then pursuing the compounds responsible via bioactivity-guided fractionation. The second was the isolation and structure elucidation of new molecules and then screening the pure compounds for potential bioactivity, based on structural similarities to known bioactive molecules, as well broadly screening in various assays.

In this second route, molecules were deemed "interesting" based upon both mass spectrometry and NMR spectroscopy. If an NMR spectrum was more than just a fatty acid or sugar resonances, and showed a range of signals, both aromatic and heteroatomic, it was considered "interesting". In addition LCMS data was used to help determine interesting metabolites by looking for halogenation, large molecular weights, and distinctive UV chromophores.

This thesis will discuss my research of three organisms: The cyanobacterium *Moorea producens* (formerly known as *Lyngbya majuscula*[52]), as well as the cyanobacterium *Nostoc sphaericum*, and the marine sponge *Spongia* sp. The first case will discuss bioassay-guided fractionation to identify a new fatty acid (believed to be a false positive), and the identification of two known majusculamides. The second case will demonstrate the isolation of two bioactive compounds that have only previously been reported as a mixture. The final case will focus on

three new compounds, their bioactivity, and potential biosynthesis.

CHAPTER 2

2. New and Known Metabolites Isolated from Cyanobacteria

2.1 Overview of *Moorea producens* metabolites

Moorea producens, formerly known as *Lyngbya majuscula*[52], is a species of marine cyanobacteria that consistently produces interesting new chemicals. Curacin A[53], jamaicamide A[54], and lynbyatoxin A[55] are three well-studied molecules isolated from this species, which are potent cytotoxins. These archetypes demonstrate *M. producens*' ability to produce molecules that affect human biological systems.

Bioassay-guided fractionation of the cyanobacterium collected from Black Point, Oahu in 2008, led to the isolation of a new 15-carbon fatty acid (**2.1**). **2.1** was an inhibitor of BACE1, which inhibited BACE1 activity by 58% at a concentration of 74 μM in our primary EFC assay system. However, because of a consistency in activity after every level of purification, and inconclusive results involving our secondary affinity assay, our active compound is thought to be a false positive (vide infra).

Two known compounds, majusculamides, A and B (**2.2** and **2.3**), were isolated based on an NMR-guided process. While the epimers **2.2** and **2.3** constituted an inseparable mixture, analysis of the data from TOCSY experiments enables identification of the resonances belonging to each epimer.

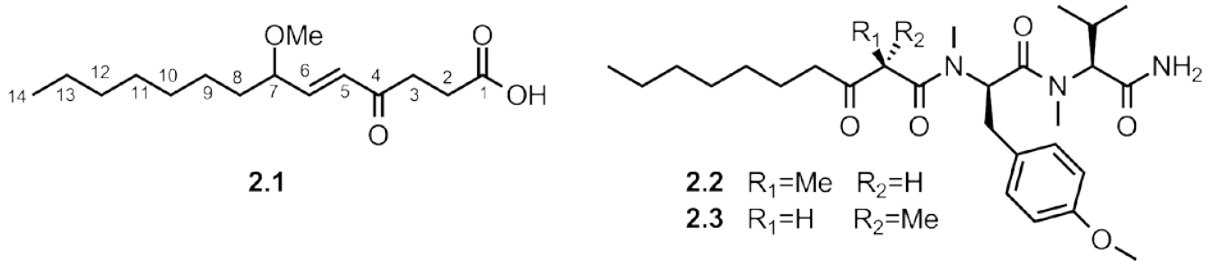

Figure 2.1 Metabolites isolated from *Moorea producens*

2.1.1 Isolation and Structure determination of Trans-7-methoxytetradec-5-ene-4-oneioic acid

BACE1 screening of a sample of *Moorea producens* showed that many of the nonpolar portions thought to contain fats were active. That is, after a modified Kupchan partitioning, the hexane portion inhibited BACE1 activity by 52% at a concentration 30 µg/ml, while the DCM portion was slightly less active against BACE1, inhibiting 42% of its activity at the same concentration. The more potent hexane partition fraction was investigated first.

Separation by HPLC of the 50% EtOAC fraction from the hexane partition led to the isolation of **2.1**. Analysis of the low resolution ESI-MS data gave a molecular weight of 270 AMU consistent with the molecular formula $C_{15}H_{26}O_4$, indicating three degrees of unsaturation. The ^{13}CNMR spectrum displayed two carbonyls (δ_{C-1}181.0, δ_{C-4} 202.3), two other sp^2 carbons (δ_{C-5} 131.2, δ_{C-6} 147.6), two oxygenated carbons (δ_{C-7} 82.1, δ_{C-OMe} 57.3), and 9 aliphatic carbons. These resonances accounted for all three degrees of unsaturation. The chemical shift of C-1 (δ_{C-1} 181.0) indicated a carboxylic acid, as no proton resonances were present indicating the oxygen linkage of an ester functional group. Only position 7 shows the downfield proton and carbon resonances needed for an ester functional group, and these resonances were determined to belong to a different spin system (vide infra).

The ^{1}HNMR spectrum showed a methyl signal under the residual methanol, indicating an oxygenated methyl group that accounted for the third oxygen (OMe). Also apparent was a doublet of doublets at δ_{H-6} 6.70 coupling both to the doublet at δ_{H-5} 6.25 and the quartet at δ_{H-7} 3.79 suggesting the below fragment (**Figure 2.2 A)**. The olefin was in a *trans*-configuration as indicated by the large coupling constant (16.1 Hz) between δ_{H-5} 6.25 and δ_{H-6} 6.70. Since the "free" end of the methine giving rise to the doublet at δ_{H-5} 6.25 must be attached to an atom with no protons, it was connected to the quaternary carbonyl at δ_{C-4} 202.3, giving rise to an α,β−unsaturated ketone moiety. The methylene triplet at δ_{H-3} 2.88 was coupled to the methylene triplet at δ_{H-2} 2.43, and their downfield chemical shifts suggested that they were both adjacent to sp^2 centers, which could only occur if they were sandwiched between the two carbonyls. Due to the stronger inductive effects of a ketone than that of a carboxylic acid, the more downfield methylene was placed nearer to it. Finally, since all degrees of unsaturation and heteroatoms were accounted for, and the methyl triplet at δ_{H-14} 0.89 suggested an aliphatic chain, the remaining six CH_2 carbons were placed in a linear sequence.

Table 2.1 NMR Data of Trans-7-methoxytetradec-5-ene-4-oneioic acid in MeOH-d_4

Position	δ_C[a], Type	δ_H[b], mult	*J* (Hz)	HMBC (^{1}H-^{13}C)[c]
1	181.0, qC			
2	30.6, CH_2	2.43, t	6.7	C-4, C-1
3	37.8, CH_2	2.88, t	6.7	C-4, C-1
4	202.3, qC			
5	131.2, CH	6.25, d	16.1	C-7, C-4
6	147.6, CH	6.70, dd	16.1, 6.5	C-7, C-4
7	82.1, CH	3.79, q	6.5	C-8, C-5, OMe
7OMe	57.3, CH_3	3.29, s		C-7
8	35.8, CH_2	1.55, m		
9-13*	33.0, CH_2	1.29, m		
9-13*	32.8, CH_2	1.29, m		
9-13*	30.3, CH_2	1.29, m		
9-13*	26.2, CH_2	1.29, m		
9-13*	23.7, CH_2	1.29, m		
14	14.4, CH_3	0.89, t	6.9	

[a] Recorded at 125 MHz [b] Recorded at 500 MHz [c] Spectrum taken in $CDCl_3$
*Unable to distinguish due to intensive overlap in the proton spectrum

Additional 2D NMR spectra were obtained to support the proposed structure. Key COSY and HMBC correlations are highlighted in **Figure 2.2 B.** The HMBC correlations originating from H-7 to the OMe carbon, and the lack of correlations from H-7 to either of the carbonyls, support the previous assignment of C-1 as a carboxylic acid. Of particular importance are the HMBC correlations from the protons H-2, H-3, H-5, and H-6 to the ketone C-4 which connect the assembled fragment (**Figure 2.2A**) to the carboxylic acid moiety.

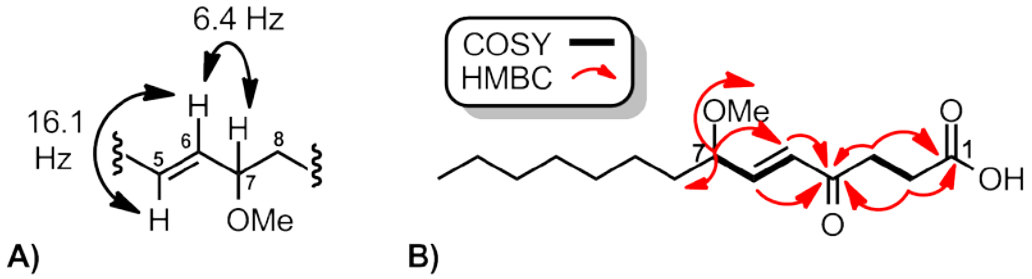

Figure 2.2 A) A large fragment of compound **2.1** obtained by coupling constant analysis. B) Key COSY and HMBC (proton to carbon) correlations of compound **2.1**

2.1.2 Bioactivity of (E)-7-methoxytetradec-5-ene-4-oneioic acid

Compound **2.1** reduced the activity of BACE1 to 58% at approximately 74 μM. However, before obtaining an IC_{50} value, the compound was tested against an affinity assay system designed for BACE1 due to suspicion, based upon its molecular structure, that the inhibitor was a false positive.

The affinity assay, based on the work by Annis et al,[56] filters out small molecules that do not complex to the enzyme. In this system, the inhibitor is incubated with the enzyme and then the solution is filtered by size over a size exclusion column. At this point only molecules over 6 kDa, such as the enzyme-ligand complex, elute from the stationary phase. Eluent containing the

enzyme-inhibitor complex is collected and injected onto an LC-MS system, where the complex dissociates to provide the inhibitor's retention time and mass spectrometric profile. A positive control of just the sample, a negative control of only the sample spun on the size exclusion column, are also performed for each trial. All three trials were run in duplicate.

The results showed the inhibitor in every sample. The small molecule appearing in the negative control indicates that it did not enter the pores of the size exclusion column. This voids the validity of the affinity assay and may be attributed to the detergent-like effects of the fatty acid forming larger aggregates which are then large enough to bypass the pores of the size exclusion particles. This suggests that the form of inhibition is via sequestration of enzyme by aggregates of **2.1**, a mechanism that is well documented to create false positives[57,58].

2.1.3 Isolation of Majusculamides A and B

The DCM fraction also showed activity against BACE1. However, when a reversed-phase flash column was performed, only the 100% methanol fractions retained activity. The ^{1}HNMR spectrum suggested a molecule with no downfield protons similar to **2.1**. Therefore, we shifted our focus to a NMR-guided fractionation based upon aromatic and heteroatomic signals. Of all the fractions, the only interesting NMR resonances occurred in the DCM partition fractions and specifically the 75% fractions. Extensive reversed-phase HPLC led to the isolation of majusculamides A and B (**2.2**, **2.3**).

Although already known, the structure elucidation of these molecules presented some difficulty. That is, they epimerize at elevated temperatures and therefore interconvert between majusculamide A and B [62]. Secondly, the tertiary amide group allows for two distinct conformers, causing a minor set of signals in the NMR spectrum. Therefore, when carrying out

the structure elucidation, the spectra consisted of four overlapping sets of signals to sift through.

At the time of structure determination, this mixture of compounds was thought to be one compound with multiple conformers. 2D NMR data was collected on the mixture of compounds, COSY, HMBC, and TOCSY experiments, in order to determine the structure of these molecules.

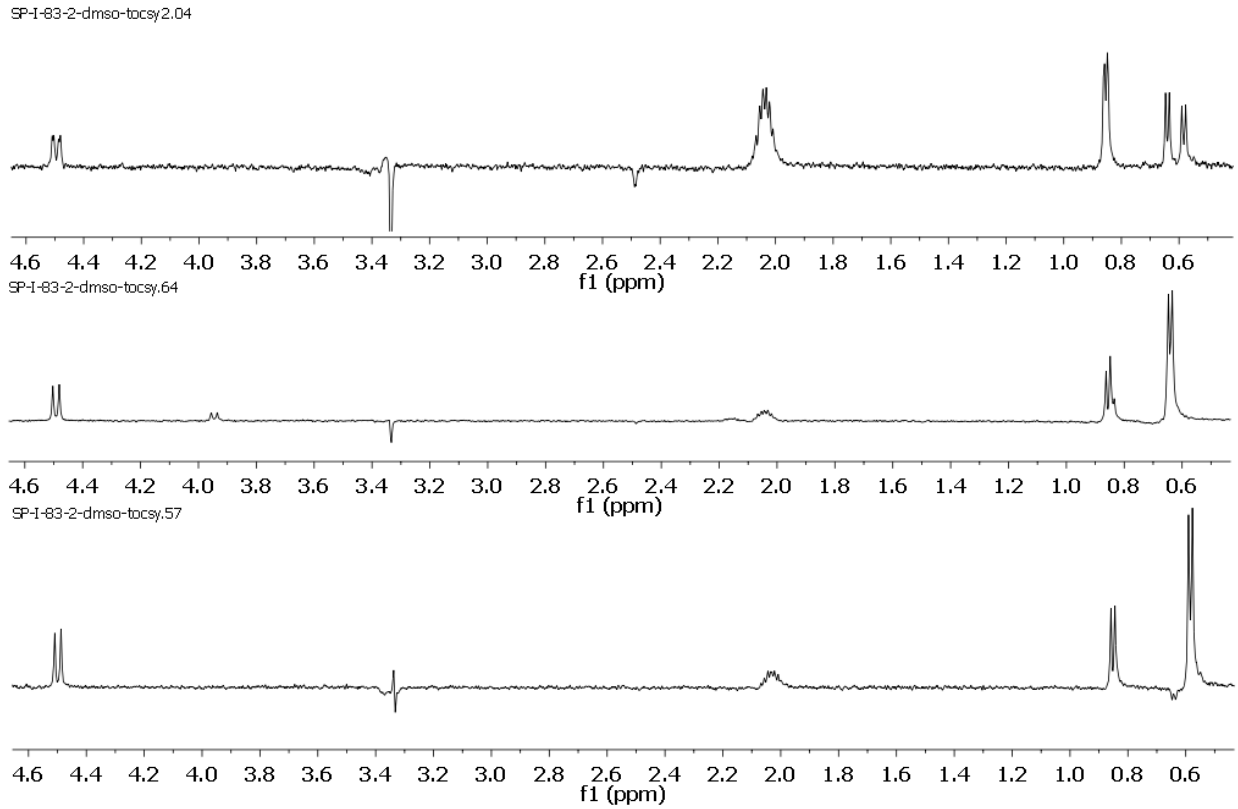

Figure 2.3 TOCSY experiments on the mixture of majusculamides, irradiating the proton signals at 2.04 (top), 0.64 (middle), and 0.57 (bottom) belonging to the valine unit. Irradiating either of the upfield methyl doublets did not transfer energy to each other, indicating that they were actually separate spin systems, which suggested the sample was a mixture of two compounds.

TOCSY experiments were performed on nearly all resolved proton resonances which linked resonances to the spin system that they belong to. It was through TOCSY experiments that it became apparent that the spectra contained duplicate spin systems that were isolated from each other suggestive of two related molecules. For instance, a valine residue was suspected due to a series of upfield methyl doublets, and an octet signal δ_H 2.04 ppm. A TOCSY experiment performed at the octet signal at δ_H 2.04 ppm showed correlations to an alpha proton at δ_H 4.49

and 3 methyl doublets (δ_H 0.86, 0.64, 0.57) when there should have only been two methyl doublets for the suspected valine moiety (**Figure 2.3**). Subsequent TOCSY experiments irradiating either of the upfield methyl doublets indicated that they were not part of the same spin system as they did not transfer energy to each other as would be expected. Therefore, there were two molecules where the alpha hydrogen, the octet, and the downfield methyl doublet at δ_H 0.87 ppm of one molecule had identical resonances with the respective signals of the other molecule.

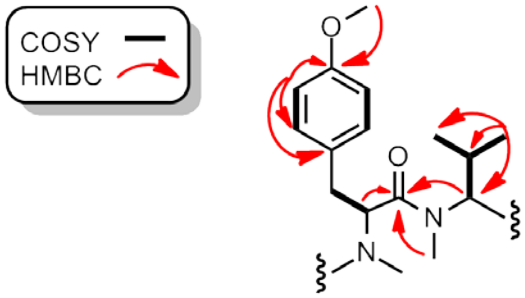

Figure 2.4 Key COSY and HMBC correlations of the complex mixture of majusculamides A and B leading to the OMe tyrosine and NMe valine dipeptide. With this partial structure, and AntiMarin dereplication database, the compounds were identified before the entire structure was elucidated.

With the simplifications made by the TOCSY experiments, the COSY, and HMBC data were now decipherable. The analyses of the COSY and HMBC experiments as seen in **Figure 2.4** led to the construction of two sets of O-methylated tyrosine residues and N-methylated valine residues, one belonging to each epimer. These amino acids were linked together via HMBC correlations from each alpha hydrogen to the same carbonyl to form the dipeptide. At this point the molecular mass of 503 Daltons, the partial structure, and the proton and carbon resonances were used to dereplicate the compounds using the database AntiMarin,[59] which identified the compounds as majusculamide A and B (**2.2** and **2.3**).

2.1.4 Comments on *Moorea producens* metabolites

Trans-7-methoxytetradec-5-ene-4-oneioic acid has only one stereocenter requiring absolute stereochemistry determination. The lack of similar structures in the literature rendered optical rotation comparison inconclusive. With too little compound to demethylate and then do derivations such as Mosher's analysis, we are left to only speculate on the answer. Compound **2.1** is similar to lyngbic acid also isolated from *Moore*a *producens*, in which C-7 has been determined to have the *S* configuration[60]. Interestingly, the configuration of this center is conserved in the over 30 metabolites belonging to the large family of malyngamides containing the lyngbic acid precursor. The only reported exception having the 7*R* configuration is malyngamide X[61] isolated from a Thai sea hare. Due to the structural similarities between lyngbic acid and **2.1**, it is thought that **2.1** is produced by the same biosynthetic pathway (vide infra) and most likely has the 7*S* stereochemistry as well.

The structure of **2.1** is likely a product of polyketide synthesis. The 14 carbon chain and the positioning of the oxygens connected to C-1 and C-7 are consistent with the idea of repeating acetyl-CoA building blocks. Attack of acetyl-CoA by another acetyl-CoA building block via a Claisen condensation briefly forms a tetrahedral intermediate that collapses to create a ketone and free coenzyme A. The resultant ketone is reduced to the alcohol where it is dehydrated to form a trans double bond. That double bond is then reduced to the saturated carbon chain. This happens three times and on the fourth, the alcohol is methylated before dehydration can occur. The C-5 trans double-bond could be formed by the dehydration of an alcohol unit on C-5. The ketone probably arises via a dehydration of an alcohol on the C-3 position, followed by oxidation of the resultant diene at C-4.

Although majusculamides A and B are nontoxic and show no biological activity towards

BACE1, they have served an important purpose. That is, they have served as a chemotaxonomic identifier[62], linking the biological material to the organism *Lyngbya majuscula*, recently renamed as *Moorea producens*. Both dermatitis and non-dermatitis (swimmers-itch) producing varieties contain both of these lipophilic molecules, which to the best of the author's knowledge, have yet to be isolated from any other species.

2.2 Overview of *Nostoc sphaericum* Metabolites Isolated

Nostoc sphaericum is a cyanobacterium that has three major UV active metabolites. By UV detection methods, we were only able to isolate the three known compounds which have moderate activity against herpes simplex virus type 2 and nonselective cytotoxicity against murine and human cell lines[63].

As part of an effort to expand the NIH's molecular libraries small molecule repository, a strain of the cyanobacterium *Nostoc sphaericum* was grown. Of three mildly cytotoxic metabolites harvested, two (**2.4** and **2.5**) have only been reported as a mixture with coincidental resonances for all major chemical shifts, excluding N-H protons, in DMSO[63]. After extensive experimentation, we were able to separate the regioisomers using normal-phase HPLC with THF:hex on a Si column and/or reversed-phase HPLC with MeOH:H_2O on a C8 column, such that the characterization of each distinct molecule could be accomplished.

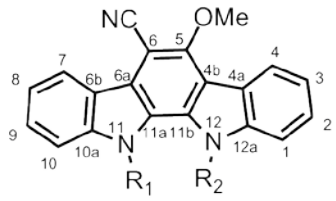

2.4 R_1= H R_2=Me
2.5 R_1=Me R_2=H
2.6 R_1= H R_2=H

Figure 2.5 Metabolites isolated from *Nostoc sphaericum*

2.2.1 Isolation of Indolocarbazoles (2.4-2.6)

70% EtOH and also DCM extracts of the biological material were separated over Si gel starting with pure hexanes and then a step gradient of increasing THF in hexanes. The resulting fractions containing the compounds of interest, as determined by LC-MS, were subjected to normal-phase HPLC with an isocratic solvent composition of 33% THF in hexanes to give a mixture of regioisomers as well as 6-cyano-5-methoxyindolo[2,3-a]carbazole (**2.6**). ^{1}HNMR analysis of the mixture in deuterated pyridine then showed a 4:1 ratio of regioisomers such that the purity of the mixture could be accessed during purification. Due to the low solubility of the compounds that led to broad, overlapping elution peaks, extensive HPLC was performed using small sequential injections in order limit the degree of overlap, resulting in separation of the two regioisomers to approximately 90% purity.

While most of the structure was easily deduced from comparison of the resonances to the literature and through some additional 2D NMR data, determining which regioisomer was which depended on NOE experiments. HRESI-TOFMS analysis of **2.4** determined it to be one of the methylated regioisomers due to yielding a pseudomolecular ion of 326.1281 $[M+H]^+$ consistent with the molecular formula of $C_{21}H_{15}N_3O$. The position of the NMe group was determined by NOE energy transfer from NMe to H-1 and from OMe to H-4. Since H-1 and H-4 are on the

same ring structure, as verified by COSY correlations, the NMe and the OMe in this molecule must be on the same side of the molecule. Therefore, **2.4** was determined to be the 6-cyano-5-methoxy-12-methylindolo[2,3-a]carbazole regioisomer.

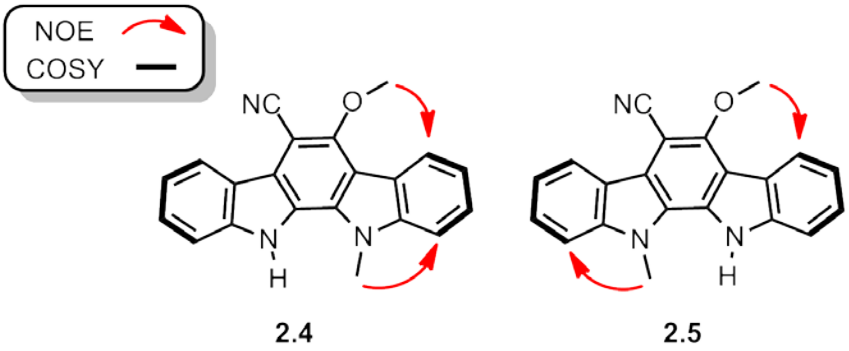

Figure 2.6 Key NOE and COSY correlations for the determination of each regioisomer. In **2.2.4**, and OMe NOE and the NMe NOE shows correlations to protons on the same ring system. In **2.2.5** the correlations are to different ring systems.

Compound **2.5**, had the same mass and major proton resonances as **2.4** and was determined to be the other regioisomer based upon nearly identical NMR and LC-MS data. The position of the NMe group in **2.5** was determined due to an NOE energy transfer from NMe to H-10 and from OMe to H-4. Since H-10 and H-4 are on different indole rings as confirmed by COSY correlation, the NMe and the OMe in this molecule must be on opposite sides of the molecule. Thus **2.5** was the 6-cyano-5-methoxy-11-methylindolo[2,3-a]carbazole regioisomer.

Known compound **2.6** was isolated and its structure deduced to be 6-cyano-5-methoxyindolo[2,3-a]carbazole by comparison of its NMR and MS data. A pseudomolecular ion of 312.1140 $[M+H]^+$ was consistent with the MW of the desmethylated molecule. The ^{1}HNMR showed the addition of a downfield NH proton, and the lack of an NMe group. It also showed the same aromatic proton signals of the indole rings, as well as the OMe group.

2.2.2 Comments Isolation of Indolocarbazoles (2.4-2.6)

Indolocarbazoles systems are found in many bioactive natural products obtained from a variety of sources. Staurosporine[64] from the bacterium *Streptomyces staurosporeus*, arcyriflavins from the slime mold *Arcyria denudata*[65], and compounds **2.4-2.6** from the cyanobacterium *Nostoc sphaericum*[63] are a few of the compounds that demonstrate the diversity of sources and scaffolding.

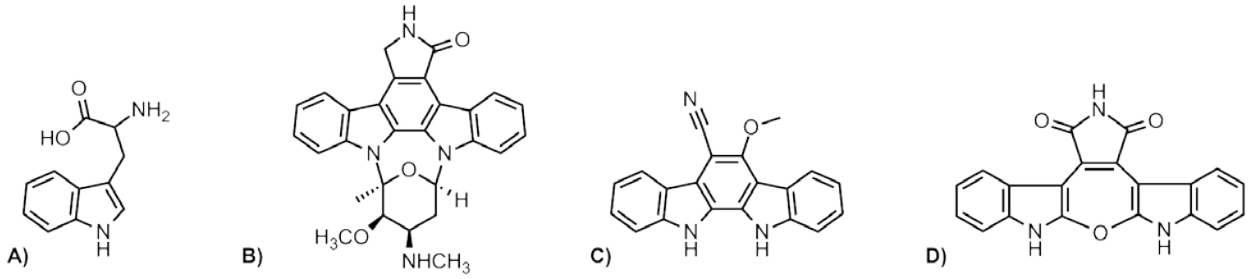

Figure 2.7 A comparison of indole containing structures. **A** is the amino acid tryptophan, **B** is staurosporine from bacterium *S. staurosporeus*, and **C** is our isolated compound **2.6** from *N. sphaericum*, and **D** is arcyroxepin from the slime mold *Arcyria denudata*

Although it may seem obvious to some that the indole ring would be derived from tryptophan, Meksuriyen and Cordell conducted labeling studies to confirm that the indolocarbazole ring system was formed by tryptophan in the case of staurosporine[66]. In these feeding studies, radioactive tryptophan was first fed to the cyanobacteria to determine that there was radioactivity incorporated in the staurosporine metabolite. Next, a mixture of L-[5-^{3}H] tryptophan and L-[β-^{14}C] tryptophan was fed to the cyanobacterium which led to an indolocarbazole ring with the same ratio of radioactivity. This indicated that an intact tryptophan unit (or two) was incorporated, and not an indole ring from tryptophan that was modified. Furthermore, feeding DL-[α-^{13}C] tryptophan led to specific incorporation of both carbons adjacent to the nitrogen in the lactam ring, indicating that two intact tryptophan moieties are used in the biosynthesis. Since compounds **2.4-2.6** also contain this [2-3α] indolocarbazole moiety

(**Figure 2.7**), they are thought to arise from the same biosynthetic pathway, owing their indole ring structures to two tryptophan residues.

The regioisomers **2.4** and **2.5** have been isolated and characterized when previously have only been reported as a mixture. This was partially due to the fact that, when placed in d_5-pyridine, many of the formerly identical NMR proton resonances were resolved. Many of the physical characteristics were the same between the regioisomers, and because these molecules are planar and have no chiral centers, there is no optical rotation correlated with them.

There are, however, slight differences in the IR spectra. The difference in the IR spectra between the major (**2.4**, 2206.6 cm^{-1}) and minor (**2.5**, 2214.3 cm^{-1}) regioisomers could be explained by the small donation of electron density provided by the NMe group. This, essentially, places an electron donor group in the para position to the nitrile group. A resonance structure shows that the donation of the lone pair electrons of the nitrogen can disrupt the nitrile, giving it more double bond character and decreasing the energy of the bond. The greater inductive effect of the methyl group relative to a hydrogen atom provides more stability of the positive charge on the nitrogen, making this resonance structure a slightly larger contributor in **2.4** than is in **2.5**. The desmethylated (**2.6**) and the minor regioisomer (**2.5**) have identical IR values for the nitrile group, suggesting that the NMe group at position 11 doesn't have the same effect as one might suspect.

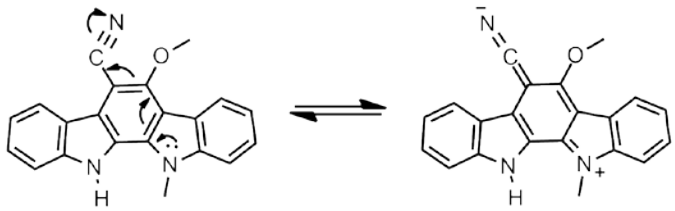

Figure 2.8 Compound **2.4** demonstrating how electron density on the indole nitrogen para to the cyano group could affect the bond strengths. A resonance structure of **2.4** can be drawn that shows more double bond character. The inductive effect of the methyl group provides a small stabilizing interaction that is not available in the other structures.

The separation of the mixture into two pure compounds may allow for a more accurate assessment of their bioactivity. However, even if the NIH's broad screening efforts show promising activity, their potential as a drug candidate seems bleak owing to the compounds' poor solubility in most solvents. Additional efforts would have to be made to modify the compound to improve its pharmokinetic and pharmodynamic properties.

2.3 Conclusion on Metabolites isolated from Cyanobacteria

Cyanobacteria are an incredible source of bioactive metabolites. The same species can produce different biologically active metabolites in geographically different locales and some researchers such as Dr. William Gerwick and the late Dr. Richard Moore have made their career out of working with these organisms, which seem to consistently produce new chemicals.

In this chapter we demonstrate an example of bioactivity-guided fractionation. Starting with a crude active sample of *Moorea producens* and repetitively purifying and testing the sample against BACE1 led to a potential inhibitor. After solving the structure based upon NMR and LC-MS data, the bioactivity was suspected to be due to detergent-like effects and thus the compound may be a false positive. We were also able to identify a set of known compounds (majusculamides A and B) and use them to help confirm the taxonomy of our strain of cyanobacteria. We then showed the separation of two previously inseparable compounds of *Nostoc* sp. by HPLC, in order to help fully characterize them individually, a process that will give more accurate bioactivity results when screened.

CHAPTER 3

3. Metabolites Isolated From Sponges

3.1 Overview of Spongians Isolated from *Spongia* sp.

Since the beginning of marine natural products, sponges have been a major producer of new chemistry[67]. Being sessile, these organisms are easy to prey upon and therefore have evolved to develop chemical or physical (spicules) defenses in order to protect themselves. *Spongia* sp. have been well studied with over 260 unique structures identified, a majority of them being terpenoids[68]. A subset of these terpenoids fall into the class of spongians, which are diterpenes with a cholesterol-like ABCD ring structure where the D ring is almost always a furan.

Two norditerpenes (**3.1, 3.2**), one novel diterpene (**3.3**), and one known diterpene (**3.4**) were isolated from a tropical Suluwesi sponge of the genus *Spongia* sp. (Order Dictyoceratida, Family Thorectidae). The structures of **3.1-3.3** were deduced by analyses of the spectrometric and spectroscopic data. Diterpene **3.3** contains a unique pyridine moiety as the D ring and its structure elucidation was complicated by the rapid exchange of the axial proton at the C-11 position with deuterium from methanol-d_4. Norditerpene **3.2** weakly inhibited aromatase at with an IC_{50} of 34 μM and induced quinone reductase 1 activity with a CD of 11.2 μM.

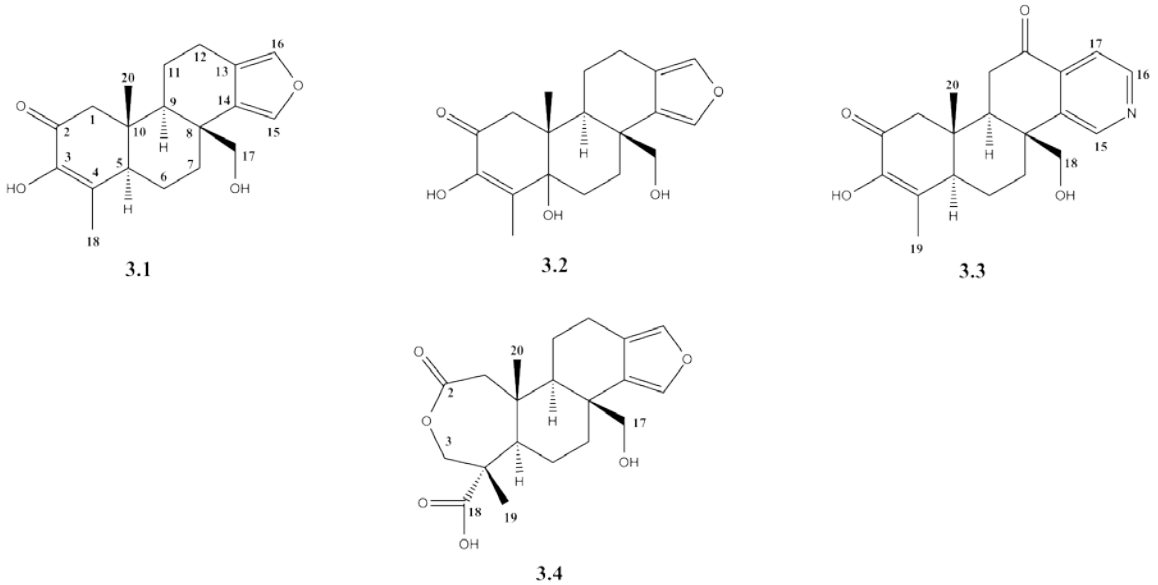

Figure 3.1 Metabolites isolated from *Spongia* sp.

3.1.1 Isolation and Structure Elucidation of Spongians 3.1-3.4

50 grams of biological material was extracted overnight with 1:1 MeOH:DCM three times. The resultant crude extract was fractionated by flash column chromatography on C8 silica gel. Select 75% MeOH fractions were then purified by HPLC to afford 12 mg (0.024% yield) of 19-nor-3,17-dihydroxyspongia-3,13(16),14-triene-2-one (**3.1**), 8 mg (0.016% yield) of 17-hydroxy-4-epispongialactone A[69] (**3.4**) and 1 mg (0.002% yield) of 19-nor-3,5α,17-trihydroxyspongia-3,13(16),14-triene-2-one (**3.2**). Extensive HPLC of one of the 50% MeOH fractions afforded 4.5 mg (0.009% yield) of spongiapyridine (**3.3**).

Compound **3.1** was isolated as a white powder. High resolution mass spectrometry gave a pseudomolecular ion at *m*/*z* 317.1747 $[M+H]^+$. This is consistent with the molecular formula $C_{19}H_{24}O_5$ and indicated eight double bond equivalents. The carbon spectrum showed seven sp^2 carbons, six of which were C=C bonds, and one of which was a conjugated carbonyl carbon ($\delta_{C\text{-}2}$ 195.4). Therefore, the compound must have four rings to account for the remaining double bond

equivalents.

3.1 was assembled by analysis of COSY and HMBC correlations. Beginning with the tertiary methyl group ($\delta_{H\text{-}19}$ 1.09), HMBC correlations to two methines, a quaternary carbon and a methylene (C-1, C-5, C-9, C-10) laid the foundation for fragment 3.1 (see **Figure 3.2)**. A methylene proton that resonated at $\delta_{H\text{-}6}$ 1.98 showed a COSY correlation to one of the established methines $\delta_{H\text{-}5}$ 2.62, along with a methylene ($\delta_{H\text{-}7}$ 1.41) elongating the alkyl chain. HMBC correlations from the proton at $\delta_{H\text{-}18}$ 1.88 indicated a chain of two sp^2 carbons connecting to C-5, but were unable to distinguish in which order. A set of HMBC correlations between the signal at $\delta_{H\text{-}1}$ 2.73 ppm and signals at $\delta_{C\text{-}2}$ 195.4 ppm and $\delta_{C\text{-}3}$ 145.7 ppm, resolved the ambiguity of the order of sp^2 carbons, creating an α,β-unsaturated ketone moiety within a six-membered ring.

The two downfield protons at $\delta_{H\text{-}16}$ 7.14 and $\delta_{H\text{-}15}$ 7.17 as well as four remaining sp^2 carbons hinted at the possibility of a heteroatomic aromatic ring. The $^1J_{C\text{-}H}$ extracted from the HMBC experiment at position 16 suggested the heteroatomic ring was a furan moiety (201 Hz vs. 202 Hz in furan[70]). With a furan moiety in mind, HMBC correlations from $\delta_{H\text{-}16}$ 7.14 to C-14 and C-15 while $\delta_{H\text{-}15}$ 7.17 correlated strongly to C-16 and C-13, but weakly to C-14 suggested the furan ring is as shown in **Figure 3.2**.

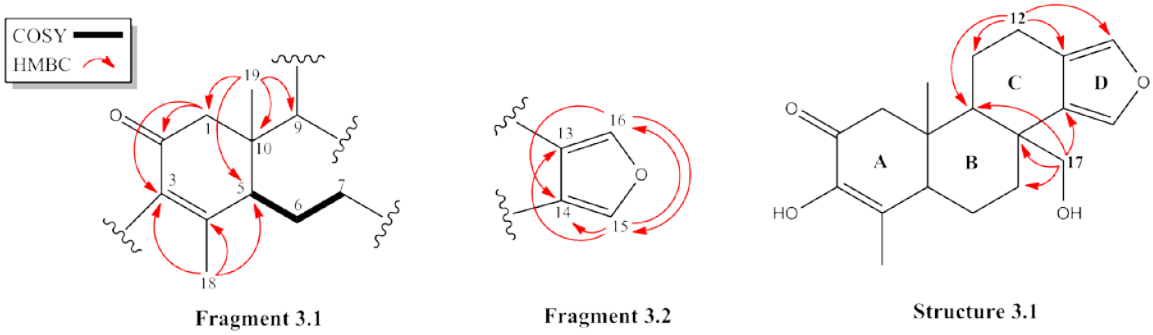

Figure 3.2 Key HMBC (^{1}H-^{13}C) and COSY correlations of **3.1**

Fragments 3.1 and 3.2 were joined based on HMBC correlations observed from the methylene protons of the primary alcohol (δ_{H-17} 3.87) to C-7, C-8, C-9, C-14. These correlations also indicated the presence of a second six-membered ring. Of the remaining two methylenes, C-12 was placed nearer the sp^2 center (C-13), being the more downfield resonances. The more shielded methylene C-11 was then attached to C-12 and C-11 in order to satisfy the last degree of unsaturation. HMBC correlations from the proton at δ_{H-12} 2.80 ppm confirmed this configuration. The remaining hydroxyl group, required by the molecular formula, was attached to C-3 based on the chemical shifts of the α,β-ketone system to provide structure **3.1**.

Table 3.1 NMR Spectra of Compound **3.1**

Position	δ_C[a], Type	δ_H[b] (*J* in Hz)	COSY	HMBC (^{1}H to ^{13}C)[c]
1	53.3, CH_2	2.18, d (16.6)	H-19, H-1	C-20, C-10, C-9, C-5, C-2
		2.73, d (16.6)	H-1	C-20, C-10, C-9, C-6, C-5, C-2, C-3
2	195.4, qC			
3	145.7, qC			
4	132.9, qC			
5	50.1, CH	2.62, ddt (12.9, 3.1 ,2.0)	H-6b	C-20, C-10, C-9, C-6, C-4, C-3, C-2
6	21.7, CH_2	1.91, dq (13.4, 3.1)	H-6	C-10, C-8, C-7, C-5, C-4,
		1.62, qd (13.4, 3.1)	H-6, H-5	C-10, C-8, C-7, C-5, C-4
7	34.9, CH_2	1.41, tdd (13.4, 3.7, 1.2)	H-7, H_2-6	C-17, C-14, C-8, C-6, C-5
		2.53, dt (13.4, 3.1)	H-7	C-17, C-9, C-8, C-6, C-5
8	40.8, qC			
9	54.4, CH	1.72, m		
10	42.4, qC			
11	18.9, CH_2	1.72, m		
		1.72, m		
12	21.1, CH_2	2.56, m	H-12	
		2.80, dd (16.0, 4.0)	H-12	C-16, C-14, C-13, C-11, C-9
13	120.8, qC			
14	131.3, qC			
15	139.2, CH	7.17, d (1.4)		C-16, C-14, C-13
16	138.3, CH	7.14, d (1.4)		C-15, C-14
17	62.8, CH_2	3.48, d (10.9)	H-17	C-14, C-8, C-7
		3.87, d (10.9)	H-17	C-14, C-9, C-8, C-7
18	13.3, CH_3	1.88, d (2.0)		C-5, C-4, C-3, C-2
20	15.6, CH_3	0.88, d (0.9)	H-1	C-17, C-10, C-9, C-5, C-1

[a]Recorded at 125 MHz. [b]Recorded at 500 MHz. [c]Correlations observed for $^nJ_{CH}$ = 7.

Three other analogues were identified in the extract. Diagnostic evidence for these compounds included the resonances for the primary alcohol at C-17, the two aromatic protons (H-16, H-17) of the furan ring, and the two methyl singlets (C-18, C-20). Carbon and proton

resonances for these three analogues are tabulated in **Table 3.2** and **Table 3.3**.

19-nor-3,5α,17-trihydroxyspongia-3,13(16),14-triene-2-one (**3.2**) was clearly an analogue of **3.1** as it possessed many of the same carbon and proton resonances as **3.1**. Mass spectrometry analyses suggested that its mass was 2 AMU smaller than that of **3.1**, thereby suggesting it contained an extra double bond equivalent. However, it contained a nearly identical UV trace as **3.1**, showed the same amount of carbon and proton resonances, and had no additional olefinic protons, seeming to rule out the idea of another degree of unsaturation. A closer inspection of the NMR data indicated the quaternary carbon at C-5 was shifted downfield, which suggested an alcohol functional group ($\delta_{C\text{-}5}$ 76.8). HMBC correlations from H-18 and H-20 supported C-5 being the oxygenated carbon (**Figure 3.2**). Based on these data, it appears that after passing through the UV unscathed, the molecule dehydrates under the electrospray ionization conditions to give a *m/z* of 315.1580 $[M+H-H_2O]^+$.

Table 3.2. ^{13}C NMR of Spongians at 125 MHz in CD_3OD

Position	δ_C 3.1	δ_C 3.2	δ_C 3.3[a]	δ_C 3.4
1	53.3	50.3	51.9	46.6
2	195.4	194.2	194.5	177.0
3	145.7	143.0	145.7	74.8
4	132.9	132.9	131.9	53.8
5	50.1	76.8	49.0*	58.0
6	21.7	28.7	21.8	22.7
7	34.9	36.8	33.8	35.0
8	40.8	32.8	42.5	41.7
9	54.4	48.6	50.4	55.3
10	42.4	44.0	41.8	40.2
11	18.9	22.6	35.9	19.9
12	21.1	21.4	199.1	21.6
13	120.8	122.4	139.5	120.8
14	131.3	127.0	145.6*	131.6
15	139.2	139.9	149.3	139.0
16	138.3	138.1	148.3	138.2
17	62.8	71.0	120.3	62.8
18	13.3	10.7	66.2	177.9
19			13.2	14.9
20	15.6	18.7	14.6	17.7

[a] **3.3** was dissolved in CD_3OH.
*Chemical shifts identified via HMBC correlations

Table 3.3. ^{1}H Chemical Shifts for Compounds **3.1**-**3.4** at 500 MHz in CD_3OD

Position	3.1 δ_H (*J* in Hz)	3.2 δ_H (*J* in Hz)	3.3 δ_H (*J* in Hz) [a]	3.4 δ_H (*J* in Hz)
1	2.18, d (16.6)	2.64, d (17.2)	2.62, m	2.87, m
	2.73, d (16.6)	2.57, d (17.2)	2.20, d (16.4)	2.87, m
3				4.67, brs
				3.95, brs
5	2.62, ddt (12.9, 3.1, 2.0)		2.66, d (11.4)*	2.25, d (11.9)
6	1.91, dq (13.4, 3.1)	2.00, m	2.17, brd (10.2)	1.75, m
	1.62, qd (13.4, 3.1)	2.19, ddd (13.4, 10.8, 2.2)	1.74, m	1.29, m
7	1.41, tdd (13.4, 3.7, 1.2)	2.10, dd (12.4, 6.5)	2.80, brd (9.9)	1.32, m
	2.53, dt (13.4, 3.1)	1.78, tt (11.8, 3.1)	1.73, m	2.45, brd (13.0)
9	1.72, m	1.70, brd (13.2)	2.36, dd (14.5, 4.8)	1.51, d (10.7)
11	1.72, m	1.62, td (12.8, 4.2)	2.60, m	1.83, dd (13.5, 6.9)
	1.72, m	1.84, m	3.04, dd (18.5, 14.5)	1.74, m
12	2.56, m	2.76, dt (15.2, 3.1)		2.82, m
	2.80, dd (16.0, 4.0)	2.31, dddd (15.2, 12.8, 4.2, 1.9)		2.55, m
15	7.17, d (1.4)	7.32, d (1.2)	8.71, brs	7.14, s
16	7.14, d (1.4)	7.15, brs	8.58, d (4.8)	7.14, s
17	3.48, d (10.9)	3.70, dd (9.0, 1.6)	7.82, d (4.8)	3.49, d (11.0)
	3.87, d (10.9)	4.01, dd (9.0, 3.1)		3.88, d (11.0)
18	1.88, d (2.0)	1.83, s	4.02, d (11.4)	
			3.74, d (11.4)	
19			1.90, d (1.9)	1.25, s
20	0.88, d (0.9)	1.09, s	1.06, brs	1.03, brs

[a] **3.3** was dissolved in CD_3OH.
**J* extracted from TOCSY experiment irradiating at 1.75 ppm

Spongiapyridine (**3.3**) had an observed pseudomolecular ion in HRESI-TOFMS at (*m/z*) 342.1701 $[M+H]^+$, consistent with a molecular formula of $C_{20}H_{23}NO_4$. Comparison to compound **3.1** showed that **3.3** contained identical features in the A and B ring, as well as the primary alcohol C-17. The C and D ring, however, included a nitrogen, a second carbonyl carbon ($\delta_{C\text{-}12}$ 199.1), a third aromatic proton, as well as a downfield shift of the aromatic protons ($\delta_{H\text{-}15}$ 8.71, $\delta_{H\text{-}16}$ 8.58, $\delta_{H\text{-}17}$ 7.82). In contrast to **3.1**, the sharp doublet proton resonance at $\delta_{H\text{-}16}$ 8.58 displayed a $^{1}J_{C\text{-}H}$ of 182 Hz, which was no longer consistent with a carbon adjacent to the oxygen of a furan moiety. Instead, this one-bond coupling constant was consistent with a carbon adjacent to the nitrogen in a pyridine moiety. Consequently, a ^{1}H-^{15}N HMBC experiment was performed to help support this supposition. In this experiment, a correlation was observed from the signal at $\delta_{H\text{-}15}$ 8.58 to a nitrogen atom resonating at δ_N -68 (referenced to nitromethane), further

supporting the inclusion of a pyridine moiety in **3.3**. Additional structural modifications were deduced based on HMBC correlations from $\delta_{H\text{-}18}$ 3.74 to $\delta_{C\text{-}14}$ 145.6, which connected the pyridine ring to ring B, and between $\delta_{H\text{-}17}$ 7.82 and $\delta_{C\text{-}12}$ 199.1 that indicated the carbonyl was at C-12 (**Figure 3.3**).

The final piece left to assign **3.3**, according to our phase edited HSQC experiment, was a methine at $\delta_{H\text{-}11}$ 2.60 which showed a COSY correlation to $\delta_{H\text{-}9}$ 2.36. However, if C-11 was a methine, this would result in a molecular formula that was not consistent with the observed MW of 341, being off by one AMU. Upon closer investigation of the ^{13}C spectrum, it became clear that the carbon at $\delta_{C\text{-}11}$ 35.9 was not a singlet, as would be expected in a broad-band decoupled carbon spectrum, but instead was coupled to another nucleus, displaying a triplet with lines in a ratio of 1:1:1. The multiplicity of this carbon resonance suggests coupling with a nucleus that has a quantum spin number of one. One possible explanation for the observed coupling was that deuterium from the solvent was exchanging with one of the protons alpha to the ketone. To test this hypothesis, **3.3** was dissolved in CD_3OH and the NMR spectra were re-recorded. The result was the collapse of the carbon triplet into a singlet and the appearance of another proton at $\delta_{H\text{-}11}$ 3.04 showing the methine to actually be a methylene.

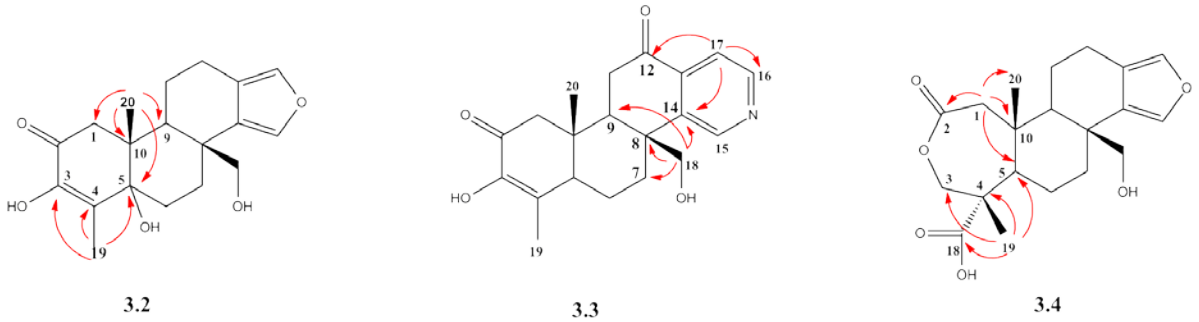

Figure 3.3 Key HMBC correlations of analogues that differ from **3.1**

HRESI-LCMS of **3.4** gave the pseudomolecular ion (*m/z*) 363.1790, consistent with the molecular formula $C_{20}H_{26}O_6$. In comparison to **3.1,** the major changes in the NMR spectra of **3.4** were all located in the A ring. These changes were two ester/carboxylic acid function groups, an oxygenated methylene, and an sp^3 quaternary carbon at the expense of the α–β unsaturated carbons and the ketone. These differences were satisfied via a seven-membered lactone ring. All of the HMBC correlations from $\delta_{H\text{-}19}$ 1.25 and also from $\delta_{H\text{-}1}$ 2.87 supported this structure (**Figure 3.3**). An NOE correlation between $\delta_{H\text{-}19}$ 1.25 and $\delta_{H\text{-}20}$ 1.03 confirmed the stereochemistry at the 3 position, ensuring that it was the known compound 17-hydroxy-4-epispongialactone A. This molecule has previously been isolated as the diacetyl derivative by Gunasekera and Schmitz from a *Spongia* sp. specimen, which inhibited our dereplication process as no proton or carbon spectra are reported in the literature for the molecule.

3.1.2 Stereochemistry of Spongians 3.1-3.3

Relative stereochemistry of **3.1** was assigned using a ROESY experiment and coupling constant analysis. Based on this data, H_3-20 and H_2-17 were both *syn* and axial. The methine H-5 was determined to be axial due to it having a large coupling constant of 12.9 Hz. Since H-5 is a methine and has no chance for geminal coupling, this large coupling constant must be due to a dihedral angle close to 0° or 180°. Since the B ring is in a chair conformation, as supported by MM2 minimized energy calculations using ChemBio3D Ultra, this can only occur if these protons are axial. For the fourth stereogenic center, H-9 was assigned as axial due to a ROESY correlation occurring with H-5. Although negative evidence should not be used to make stereochemical conclusions, as we would expect in our proposed structure, there were no ROESY correlations between H-5 and either H_3-20 or H_2-17. This is also in accordance with the

literature as all other known spongians have this relative configuration at these four stereocenters.

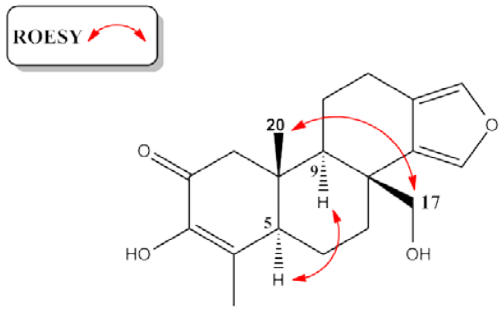

3.1

Figure 3.4 Key ROESY correlations of **3.1**

Of the four stereocenters of **3.2**, only three were able to be determined. An NOE correlation between H_3-20 and H_2-17 suggested they were *syn* and axial. H-9 had a large coupling constant of 13.2 Hz, indicating it is axial. The last stereocenter at C-5 at this point in time could not be assigned because of the alcohol proton exchanges too quickly to be seen on an NMR timescale. This includes using aprotic solvents like $CDCl_3$ and ACN-d_3, as well as variable temperature experiments going as low as -20 °C. Also, derivatizations on the alcohol were not attempted in fear of elimination of the alcohol to form a conjugated diene.

The relative stereochemistry of **3.3** was determined by *J* based analysis and NOE experiments. H-5 had a coupling constant of 11.4 Hz and H-9 which had a coupling constant of 14.4 Hz. For reasons discussed above, these protons must be axial. The other two stereogenic centers, C-8 and C-10, were determined to be *syn* and axial due to the 1,3-diaxial NOE correlations from $\delta_{H\text{-}20}$ 1.05 to $\delta_{H\text{-}17}$ 3.74 and 4.02.

Absolute stereochemistry could not be determined at this time. Of the class of spongians, no compounds have had their absolute stereochemistry solved. Crystal structures have been

obtained for zimolactone species, but without the incorporation of a heavy atom needed for absolute stereochemistry. None of the spongians we isolated contain a secondary alcohol suitable for a Mosher's analysis.

3.1.3 Plausible Biosynthetic Pathway for Spongians

A plausible biosynthetic pathway has been proposed in **Figure 3.5**. From geranyl geranyl pyrophosphate, a poly-olefin cation cyclization could give structure **3.5**. After hydrolysis of the pyrophosphate and oxidation to yield **3.6**, attack on the carbonyl carbon by the primary alcohol yields **3.7b**. Elimination of the alcohol establishes the aromaticity of the furan **3.8b,** which is followed by the required oxidations needed to yield our new compound **3.1**. Further evidence supporting this biosynthetic pathway is from similar known structures, which could be accounted for by traveling down the same route. Oxidation from **3.7b** leads to known compound zimolactone B and further oxidation of **3.7a** to a carboxylic acid before cyclization leads to the framework required for zimolactone A and C[71]. Also, from **3.8b**, partial oxidation can account for spongiadiol, spongiatriol, and their C-3 epimers[72].

3.7a could feed into an alternative pathway, being subject to transanimation in order to yield **3.10a**. Cyclization of **3.10a** via a Claisen condensation would yield **3.11a**. **3.11a** then decarboxylates, providing the electrons needed to remove the secondary alcohol and create the pyridine moiety **3.12a**. Oxidation yields our novel compound. If the transanimation of glycine occurred at the other aldehyde, the same pathway would account for the flipped pyridine ring in the known structure spongidine A[73].

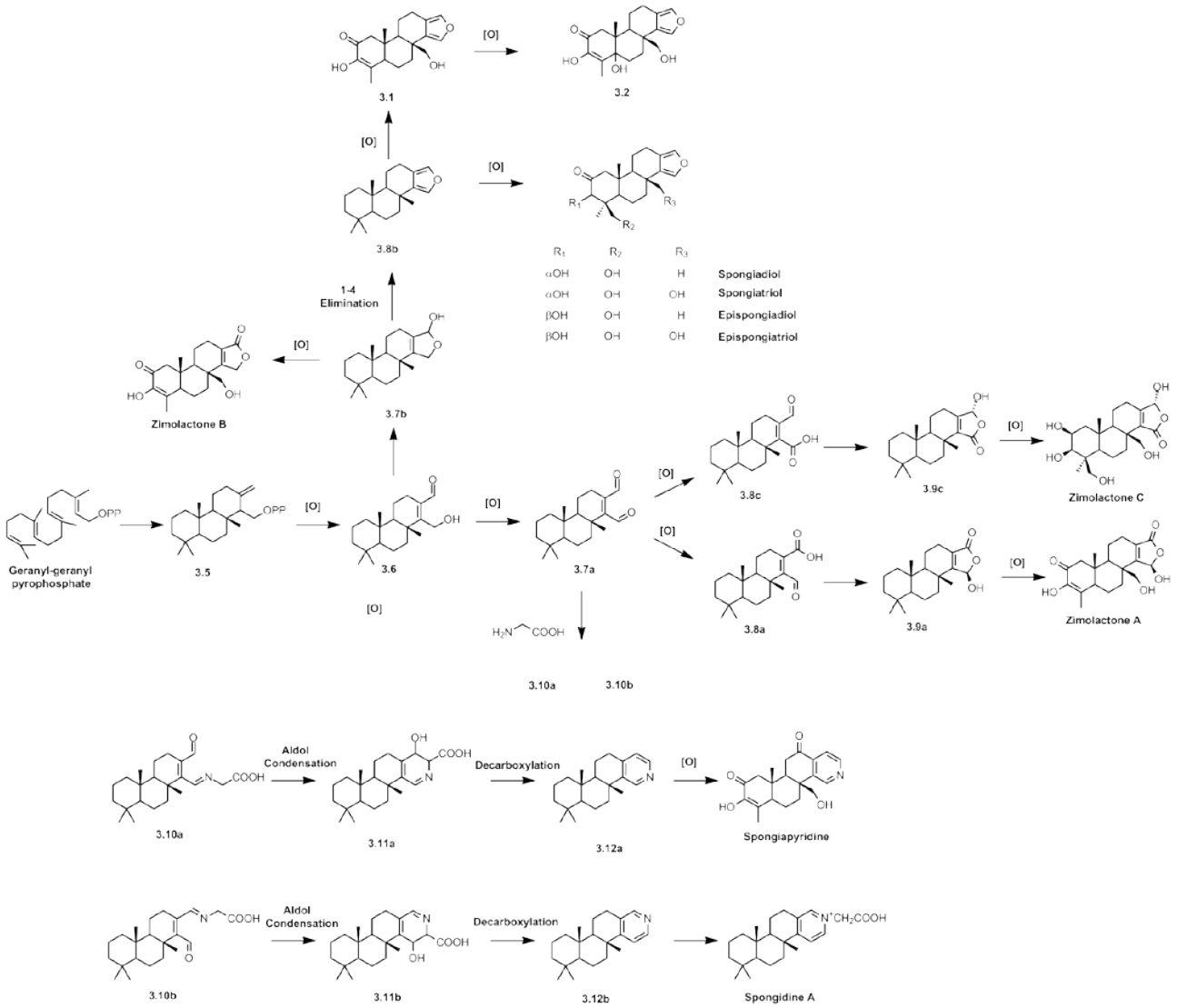

Figure 3.5 A plausible biosynthetic pathway of spongians originating for geranyl-geranyl phosphate. From **3.6**, differences in oxidation may lead to the framework for several different compounds isolated from other groups including zimolactones, spongiadiols, and spongidines.

3.1.4 Bioactivity of Spongian Compounds

The literature contained many analogues of our compounds, but few were bioactive. An analogue, epispongiatriol[74], having only slight oxidation changes in ring A was cytotoxicity against the KB cell lines, while another analogue with a lactone in the A ring shows mild

cytotoxicity vs. murine leukemia cell lines[75]. Compounds **3.1-3.4** were screened against several assay systems. We screened for NF-κB inhibition due to the α,β−unsaturated ketone moiety, which is known to be a Michael acceptor for cysteine residues of NF-κB[76,77] and then later tested opportunistically in other assays with the results discussed below.

All new compounds showed no significant activity towards TRPM7 ion channels and all isolated compounds showed no activity towards the aspartic protease BACE1 (<100 μM). In addition, no significant activity was observed against NF-κB, Nitrite, or RXRE assays. **3.2** was a weak aromatase inhibitor with an IC_{50} value of 34.4 μM and induced QR1 with a CD (the concentration needed to double a response) of 11.2 μM. Although these activities are much weaker than what would make an ideal drug candidate (nanomolar or lower IC_{50}), it does highlight the importance of oxygenation on the C-5 center of steroid-like structures.

3.1.5 Comments on Spongians.

Diterpenes from sponges offer a huge degree of structural complexity with carbon skeletons of various ring sizes. The wide range of structural diversity of diterpenes contributes to the diverse array of biological activities, which have been reported, including antibacterial, antifungal, cytotoxicity, and inhibition of development. A subset of these diterpenes are spongians, which adopt a steroid's ABCD ring system and while it has been common to find a furan group as the D ring, it is very rare to find a pyridinium moiety. Spongians are the products of terpene synthesis and many of the closely related analogues can be explained by differing degrees of oxidation. Although weakly active, spongians have shown to have potential in fighting cancer, both by having slightly cytotoxic properties as well has chemopreventative properties (inducing QR1 and inhibiting aromatase).

The unique case of **3.3** highlights an unusual problem that can complicate structure elucidation by NMR; the rapid exchange of carbon-bound hydrogen with deuterium. It also serves as a reminder that heteronuclear coupling may still be evident in a broadband proton decoupled ^{13}C NMR spectrum. In speculating why in the deuterium exchange is selective to the axial proton, the explanation is primarily due to a well-known stereoelectronic effect, overlap of the alpha C-H bond with the ketone's p*-orbital as documented by E. J. Corey[78]. However, the almost instantaneous exchange is uncanny and it was noticed that there is a potential for an internal hydrogen donor from the primary alcohol C-17. After acetylating the compound, it was noticed that exchange still occurred, however no longer instantaneously. Unfortunately, this derivative underwent spontaneous methanolysis to yield a mixture of acetylated products over a course of three days at room temperature. Due to our limited supply, we were not able to fully conduct the kinetic study to fully elucidate the role of the alcohol in the deuterium exchange.

3.2 Conclusion on Spongians

Three new and one known, oxidized diterpenes from the sponge *Spongia* sp. were isolated. The unusual structural features of some of these compounds were determined through a series of spectroscopic and spectrometric data and their bioactivities were screened against a series of assays. The secondary metabolites isolated from this organism provided insights into their respective biosynthetic pathways.

More importantly, this chapter has demonstrated an alternative to bioactivity-guided fractionation. That is, the purification of pure compounds from crude extracts and then broadly screening against assays. Based upon structural features, one can make educated guesses to which assay systems to choose, but often there is a little bit of luck involved. We have shown

that natural products from the marine environment can be an adequate source for drug leads and those molecules which don't seem to show activity in some assay systems may still be worth testing in others.

CHAPTER 4

4 Experimental

4.1 General Experimental Conditions

4.1.1 NMR

^{1}H, ^{13}C NMR and 2D NMR experiments on the natural products were carried out on Varian Unity Inova 500 MHz spectrometer. NMR spectra were referenced to the appropriate residual solvent signal (δ_H 7.26, δ_C 77.2 for $CDCl_3$; δ_H 3.33, δ_C 49.1 for MeOH-$d_{3/4}$; δ_H 7.19, and δ_C 135.5 for pyridine-d_5) with chemical shifts reported in δ units (ppm). Multiplicities are as indicated in the list of abbreviations. The HSQC experiments were optimized for $^{1}J_{C,H}$ = 140 Hz and HMBC experiments for $^{3}J_{C,H}$ = 7 Hz. Mixing times for ROESY and NOESY experiments were 500 ms and generally 80 ms for the 1D TOCSY experiments.

4.1.2 Mass Spectrometry

High-resolution ESI mass spectra were recorded in the positive or negative mode on an Agilent 1100 LC coupled to an Agilent MSD-TOF. The gas temperature was held at 325 °C, sheath nitrogen flow rate was set at 10 L/min, and the nebulizer at 30 psig. The ESI source

needle voltage was set at 3.5 kV. Low-resolution ESI mass spectra were recorded in the positive/negative mode by an Agilent 1200 LC coupled to an Agilent 6410 Triple Quad MS. In these cases, the gas temperature was held at 325 °C, sheath nitrogen flow rate was set at 10 L/min, and the nebulizer at 30 psig. The ESI source needle voltage was set at 3.5 kV.

4.1.3 IR UV optical rotations

The UV spectra were determined on a Varian Cary 50 Bio series spectrophotometer and the IR spectra were recorded on a Shimadzu IRAffinity-1 series FTIR instrument as a thin solid on either CaF_2 or NaCl disks. The optical rotations were measured on a Jasco-DIP-700 polarimeter at the sodium D line (589 nm).

4.2 Biological material

The cyanobacterium *Moorea producens* was collected from Black Point, Oahu, on September 11th, 2008. The green filamentous cyanobacterium was freeze-dried and stored at -20° C. It was identified as M. *producens* due to its morphological appearance and chemotaxonomic metabolites, majusculamide A and B.

The cyanobacterium *Nostoc sphaericum* was grown from a slant of the strain EX-5-1 of the Patterson-Moore collection. Originally isolated from a mud sample at the University of Hawaii and Manoa, it was grown in 20 L cultures grown with the modified inorganic medium designated A_3M_7, which was adjusted to pH 7.0 by adding sodium hydroxide before autoclaving. The cultures were continuously illuminated by cool-white fluorescent tubes and aerated with CO_2 at about 5 L/min. Twelve of these 20 L cultures were harvested by filtration, and freeze-

dried and stored at -20° C.

The sponge was collected from Bunaken Marine Park, Suluwesi, Indonesia, in 1992. It was freeze dried and stored at -20° C. It appears that the sponge may be thickly encrusting with prominent surface conules. The color in life is charcoal grey, with a tan interior. The texture is soft and compressible, tearing relatively easily. The skeleton is composed of slightly fasciculated primary fibres cored with foreign spicule detritus, and a light dusting of foreign spicules is found in the collagenous ectosome. The secondary spongin network is well developed. The sponge is comparable to the genus *Cacospongia* (Order Dictyoceratida, Family Thorectidae), but has the homogeneous spongin fibre structure of *Spongia* (Order Dictyoceratida, Family Spongiidae). The metabolic profile of this organism resembles many of the metabolites already identified as *Spongia* sp. A voucher specimen has been deposited at the Natural Museum, London (NHMUK2012.3.27.3). Help with identifying this organism is attributed to Dr. Michelle Kelly at the National Institute of Water & Atmospheric Research (NIWA) Ltd, Auckland, New Zealand.

4.2.1 Extraction and Isolation of Metabolites from *Moorea producens*

28 g of freeze dried cyanobacterium was extracted overnight three times with 1:1 MeOH:DCM. The resultant 2.53 g of crude extract was subjected to a modified Kupchan partitioning, yielding 84 mg of the hexane portion, 182 mg of the dichloromethane portion, 87 mg of the butanol portion, and 1.2 g of the water portion.

A silica gel flash column was performed on the hexane portion with an eluent step gradient of 10%, 50%, 75%, and 100% ethyl acetate in hexanes. The 50% portion was subjected to reversed-phase HPLC on an analytical Phenomenex column [Luna C18, 150 x 4.60 mm, 5 micron] with a concentration gradient of 30-80% ACN:H_2O over 30 min and a flow rate of 0.7

ml/min in order to receive 2 mg of pure Trans-7-methoxytetradec-5-ene-4-oneioic acid.

A C8 reversed-phase flash column was performed on the 182 mg DCM portion using a step gradient of 25%, 50%, 75%, and 100% MeOH:H_2O. The 75% fraction was then subjected to reversed-phase HPLC on a Phenomenex C8 column [Luna C8, 150 x 4.6 mm, 5 micron] on an isocratic system of 71% MeOH (aq.) with .1% FA and a flow rate of 1 ml/min to obtain 1 mg of majusculamide A and 1 mg of majusculamide B.

4.2.2 Extraction and Isolation of Metabolites from *Nostoc sphaericum*

44.01 g of freeze-dried cyanobacterium were extracted overnight three times with 70% ethanol. The resultant crude extract was dry loaded onto silica gel and a normal-phase flash column performed using a complex step gradient starting with 18%, 33%, 40%, 60%, and 100% THF:hex.

The 33% fractions were subjected to normal-phase HPLC on a Phenomenex Si column [Luna Si, 250 x 10mm, 10 micron pore size] on an isocratic system of 33% THF:hex at 4 ml/min in order to completely separate the desmethyl compound from the mixture of region isomers. This afforded 19 mg of 6-cyano-5-methoxyindolo[2,3-a]carbazole.

The mixture of regioisomers was then subjected to the same HPLC column, but now at 28% THF:hex at 4 ml/min. Small quantities had to be injected in order to resolve the two regioisomers sufficiently. Overlapping injections were made to speed up the process. This afforded 27 mg of 6-cyano-5-methoxy-12-methylindolo[2,3-a]carbazole and 4 mg of 6-cyano-5-methoxy-11-methylindolo[2,3-a]carbazole. It is to be noted that these are not complete yields as we stopped collected as we reached a 20 mg goal.

4.2.3 Extraction and Isolation of Metabolites from *Spongia* sp.

50 g of freeze-dried sponge was extracted overnight three times with a 1:1 mixture of MeOH and DCM. The resultant crude extract (7.4 g) was subjected to a liquid partitioning with hexanes, DCM, BuOH and water. The DCM partition (2.6 g) was then dry loaded onto C8 silica gel and a reversed-phase flash column (4 steps: 25%, 50%, 75%, 100% MeOH:H_2O) was performed with three fractions at each step to yield a total of 12 fractions.

The first 75% MeOH fraction (550 mg) was separated on Luna C-8 (250x10 mm, 5 micron particle size) using a flow rate of 2.75 ml/min and a solvent gradient of 30%-60% MeOH: H_2O over 30 min, then to 60%-100% over the next ten minutes for a total of 40 minutes. This afforded 12 mg of pure 19-nor-3,17-dihydroxyspongia-3,13(16),14-triene-2-one as well as 8 mg of 17-hydroxy-4-epispongialactone A.

The third 75% MeOH fraction (73 mg) was subjected to reversed-phase HPLC on the aforementioned Luna C-8 semi-prep column using a concentration gradient of 30%-80% ACN:H_2O over 30 minutes at 2.75 ml/min. This afforded 1 mg of pure 19-nor-3,5α,17-trihydroxyspongia-3,13(16),14-triene-2-one.

The second fraction of the 50% MeOH step (160 mg) underwent reversed-phase HPLC on a Luna C-18 semi-prep column (250x10 mm, 5 micron particle size) using the gradient 20%-30% ACN: H_2O over 30 minutes at 2.75 ml/min in order to yield 6 mg of pure spongiapyridine.

4.3 Assay Protocols

The HitHunter BACE1 EFC chemiluminescence assay was purchased from DiscoveRx and was run in house. The proteolytic cleavage of amyloid precursor protein was assayed as described by Naqvi[79]. Test compounds were solubilized in DMSO at the desired concentration

and incubated in triplicate with the enzyme for 16 h in 96-well plates. A DMSO control (1.5 μL) and an inhibitor standard were also tested in triplicate. The chemiluminescence signal was read using a Fluostar Optima spectrophotometer. Data were analyzed using GraphPad Prism. BACE1 activity was calculated as a percent of the positive control using a nonlinear regression analysis function that corresponded to a best one-fit model.

The BACE1 Affinity assay was run in house. 50 µL of a 0.1 µg/µL BACE1 enzyme solution in a buffer consisting of 80% 10mm NH_4HCO_3 and 20% LC-MS grade MeOH was incubated overnight with 10 µL of a 5 µg/µL MeOH solution of extract and 10 µL of a 0.005 µg/µL MeOH solution of BACE1 inhibitor IV (Calbiochem). Bio-Gel P-6 Gel (150mg) was placed in a plastic Bio-Spin column and was equilibrated with 1:4 MeOH:buffer solution. Enzyme-extract-inhibitor solution (20 µL) was added to the column and centrifuged for 1 min at 4°C and 1000 rcf. The solution in the receiving vessel was transferred to the insert in the LC-MS vial and LC-ESI-TOFMS was performed separating over a Luna C18 150 x 4.6 mm column with particle size 3 microns. A positive control of just the extract, a negative control of the extract spun down on the SEC only, and the experiment of the above described process was run for every sample.

The aromatase and quinone reductase assays was performed by Dr. Tamara Kondratyuk of Dr. John Pezzuto's lab on Hawaii. QR1 activity was assayed using Hepa 1c1c7 murine hepatoma cells as previously described[80]. Briefly, cells were incubated in a 96-well plate with test compounds at a maximum concentration of 50 µM for 48 h prior to permeabilization with digitonin. Enzyme activity was then determined as a function of the NADPH-dependent menadiol-mediated reduction of 3-(4,5-dimethylthiazo-2-yl)-2,5-diphenyltetrazolium bromide (MTT) to a blue formazan. Production was measured by absorption at 595 nm. A total protein

assay using crystal violet staining was run in parallel. Data presented are the result of three independent experiments run in duplicate. 4'-Bromoflavone (CD = 0.01 μM) was used as a positive control.

Aromatase activity was assayed as previously reported, with the necessary modifications to assay in a 384-well plate[81]. Briefly, the test compound (3.5 μL) was preincubated with 30 μL of NADPH-regenerating system (2.6 mM $NADP^+$, 7.6 mM glucose 6-phosphate, 0.8 U/mL glucose-6-phosphate dehydrogenase, 13.9 mM $MgCl_2$, and 1 mg/mL albumin in 50 mM potassium phosphate buffer, pH 7.4) for 10 min at 37 °C. The enzyme and substrate mixture (33 μL of 1 μM CYP19 enzyme, BD Biosciences, 0.4 μM dibenzylfluorescein, 4 mg/mL albumin in 50 mM potassium phosphate, pH 7.4) was added, and the plate was incubated for 30 min at 37 °C before quenching with 25 μL of 2 N NaOH. After termination of the reaction and shaking for 5 min, the plate was further incubated for 2 h at 37 °C. This enhances the ratio of signal to background. Fluorescence was measured at 485 nm (excitation) and 530 nm (emission). IC_{50} values were based on three independent experiments performed in duplicate using five concentrations of test substance. Naringenin (IC50 = 0.23 μM) was used as a positive control.

4.4 Physical Data

Trans-7-methoxytetradec-5-ene-4-oneioic acid (2.1): colorless oil. $[\alpha]_D^{23}$ 28 (c 0.2, $CDCl_3$); UV ($CDCl_3$) λ_{max} (log ε) 217 (7.71); IR (CaF_2) ν_{max} 1721. Proton and carbon data can be found in **Table 2.1,** LRESI-QQQMS (*m/z*): 293.0 $[M+Na]^+$. Notebook reference: SP-I-69, SP-I-78.

Majusculamide A (2.2): (1 mg, .003% yield) amorphous white powder. Isolated as a mixture. For full characterization see Ref: Marner, F. J.; Moore. R. E. *J. Org. Chem.* **1977***,* 42, 2815-2819. Notebook reference: SP-I-69, SP-I-79.

Majusculamide B (2.3): (1 mg, .003% yield) amorphous white powder. Isolated as a mixture. For full characterization see Ref: Marner, F. J.; Moore. R. E. *J. Org. Chem.* **1977***,* 42, 2815-2819. Notebook reference: SP-I-69, SP-I-79.

6-cyano-5-methoxy-12-methylindolo[2,3-a]carbazole (2.4): (28 mg, incomplete % yield) amorphous white solid. UV (THF) λ_{max} (log ε) 373 (9.04), 355 (8.92), 339 (9.28), 290 (10.78) 253 (9.88); IR (NaCl) ν_{max} 2206, 1628 and 1559 cm^{-1}; HRESI-TOFMS (*m/z*) 326.1281 $[M+H]^+$ (calcd for +H, 3.7 error ppm); proton and carbon data in pyridine *d*-5 can be found in Appendix 27. Notebook reference: SP-II-10.

6-cyano-5-methoxy-11-methylindolo[2,3-a]carbazole (2.5): (4 mg, incomplete % yield) amorphous white solid. UV (THF) λ_{max} (log ε) 375 (7.53), 357 (7.49), 339 (7.99), 292 (9.53), 252.5 (8.79); IR (NaCl) ν_{max} 2214 and 1581 cm^{-1}; HRESI-TOFMS (*m/z*) 326.1299 $[M+H]^+$ (calcd for +H, -1.8 error ppm); proton and carbon data in pyridine *d*-5 can be found in Appendix 27. Notebook reference: SP-II-10.

6-cyano-5-methoxyindolo[2,3-a]carbazole (2.6): (19 mg, incomplete % yield) amorphous white solid. UV (THF) λ_{max} (log ε) 365 (9.18), 348 (9.25), 336.5 (9.63), 322.6 (9.33), 287.5 (10.92), 252.4 (10.22); IR (NaCl) ν_{max} 2214, 1643, and 1566 cm^{-1}. HRESI-TOFMS (*m/z*) 312.1140 $[M+H]^+$ (calcd for +H, -1.0 error ppm); proton and carbon data in

pyridine *d*-5 can be found in Appendix 27. Notebook reference: SP-II-10.

19-nor-3,17-dihydroxyspongia-3,13(16),14-triene-2-one (3.1): (12 mg, 0.024 % yield): amorphous powder; $[\alpha]_D^{22}$ 0 (c 0.2, MeOH); UV (MeOH) λ_{max} (log ε) 281 (9.11), 202 (9.77); HRESI-TOFMS (*m/z*): 317.1747 $[M+H]^+$ (calcd for +H, error 1.9 ppm). Proton and carbon data can be found in **Tables 3.2** and **3.3**. Notebook reference: SP-I-30, re-extraction SP-I-55.

19-nor-3,5α,17-trihydroxyspongia-3,13(16),14-triene-2-one (3.2): (2 mg, 0.004 % yield): amorphous powder; $[\alpha]_D^{22}$ -7 (c 0.2, MeOH); UV (MeOH) λ_{max} (log ε) 275.9 (6.8), 202 (8.4); HRESI-TOFMS (*m/z*): 315.1580 $[M+H-H_20]^+$ (calcd for $+H–H_2O$, error 5.1 ppm). Proton and carbon data can be found in **Tables 3.2** and **3.3**. Notebook reference: SP-I-30, re-extraction SP-I-55.

Spongiapyridine (3.3): (4.5 mg, 0.009 % yield): amorphous powder; $[\alpha]_D^{22}$ -0.5 (c 0.2, MeOH); UV (MeOH) λ_{max} (log ε) 282.1 (7.8), 202.9 (8.79); HRESI-TOFMS (*m/z*): 342.1701 $[M+H]^+$ (calcd for +H, error 1.2 ppm). Proton and carbon data can be found in **Tables 3.2** and **3.3**. Notebook reference: SP-I-30, re-extraction SP-I-55.

17-hydroxy-4-epispongialactone A (3.4): (8 mg, .016 % yield): amorphous powder; $[\alpha]_D^{22}$ -2.0 (c 0.2, MeOH); HRESI-TOFMS (*m/z*): 363.1790 $[M+H]^+$ (calcd for +H, error 3.35 ppm). Proton and carbon data can be found in **Tables 3.2** and **3.3**. Notebook reference: SP-I-30, re-extraction SP-I-55.

Appendices

Appendix 1 1H NMR Spectrum of Trans-7-methoxytetradec-5-ene-4-oneoic acid (**2.1**) (CD3OD, 500 MHz**)**

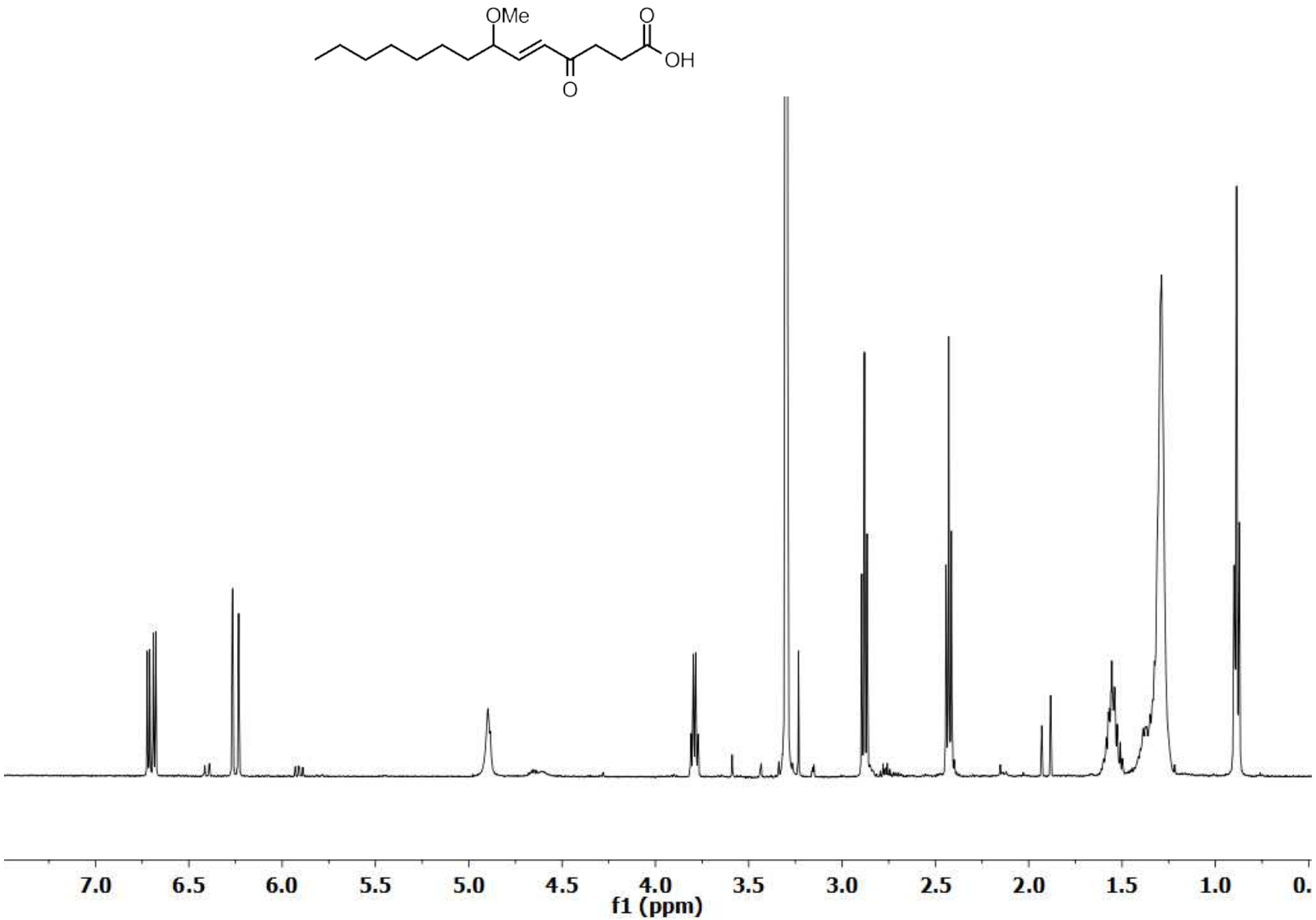

Appendix 2: 13C NMR Spectrum of Trans-7-methoxytetradec-5-ene-4-oneioic acid (**2.1**) (CD3OD, 500 MHz)

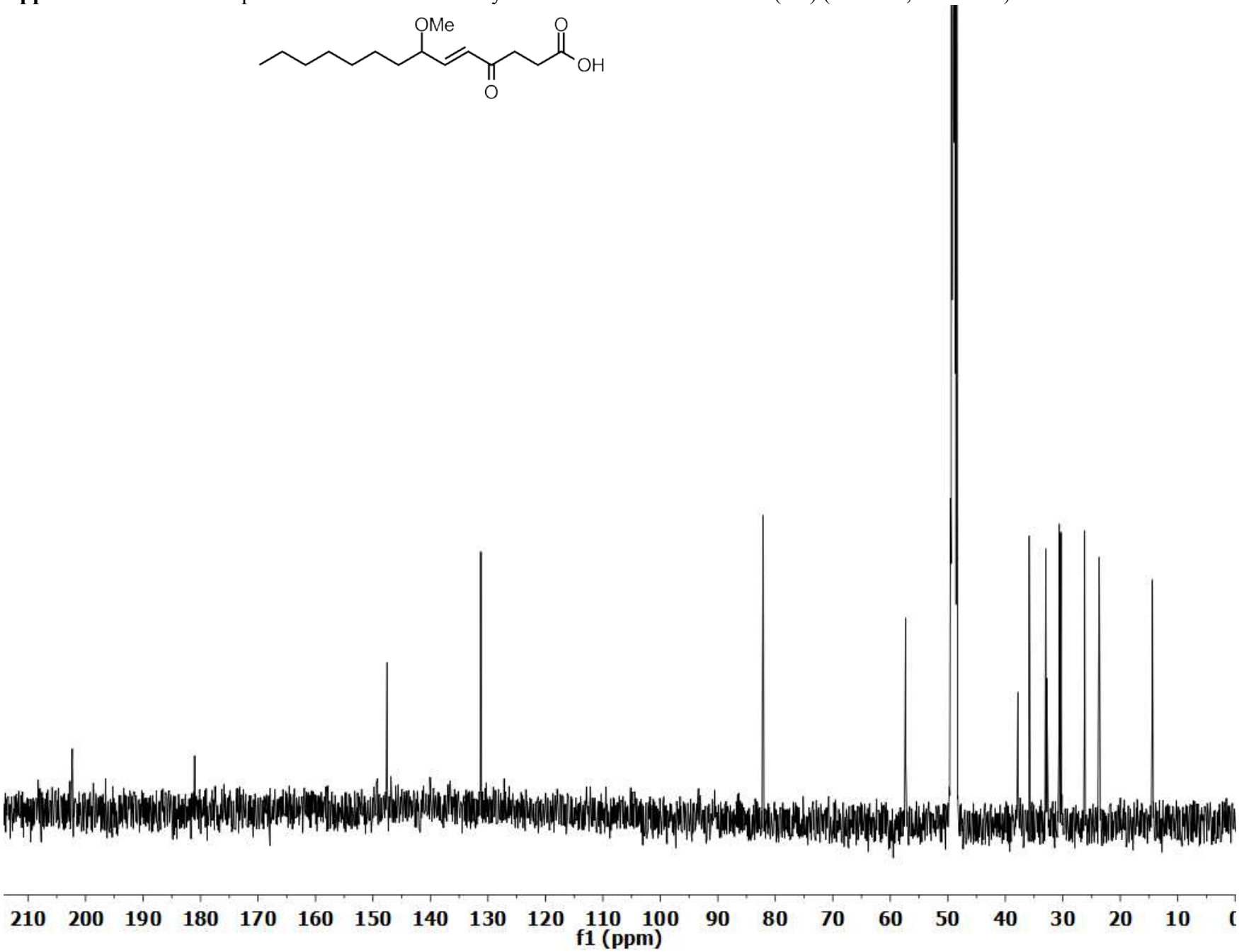

Appendix 3: ^{1}H NMR Spectrum of 6-cyano-5-methoxy-12-methylindolo[2,3-α]carbazole (**2.4**) (pyridine-d_5, 500 MHz)

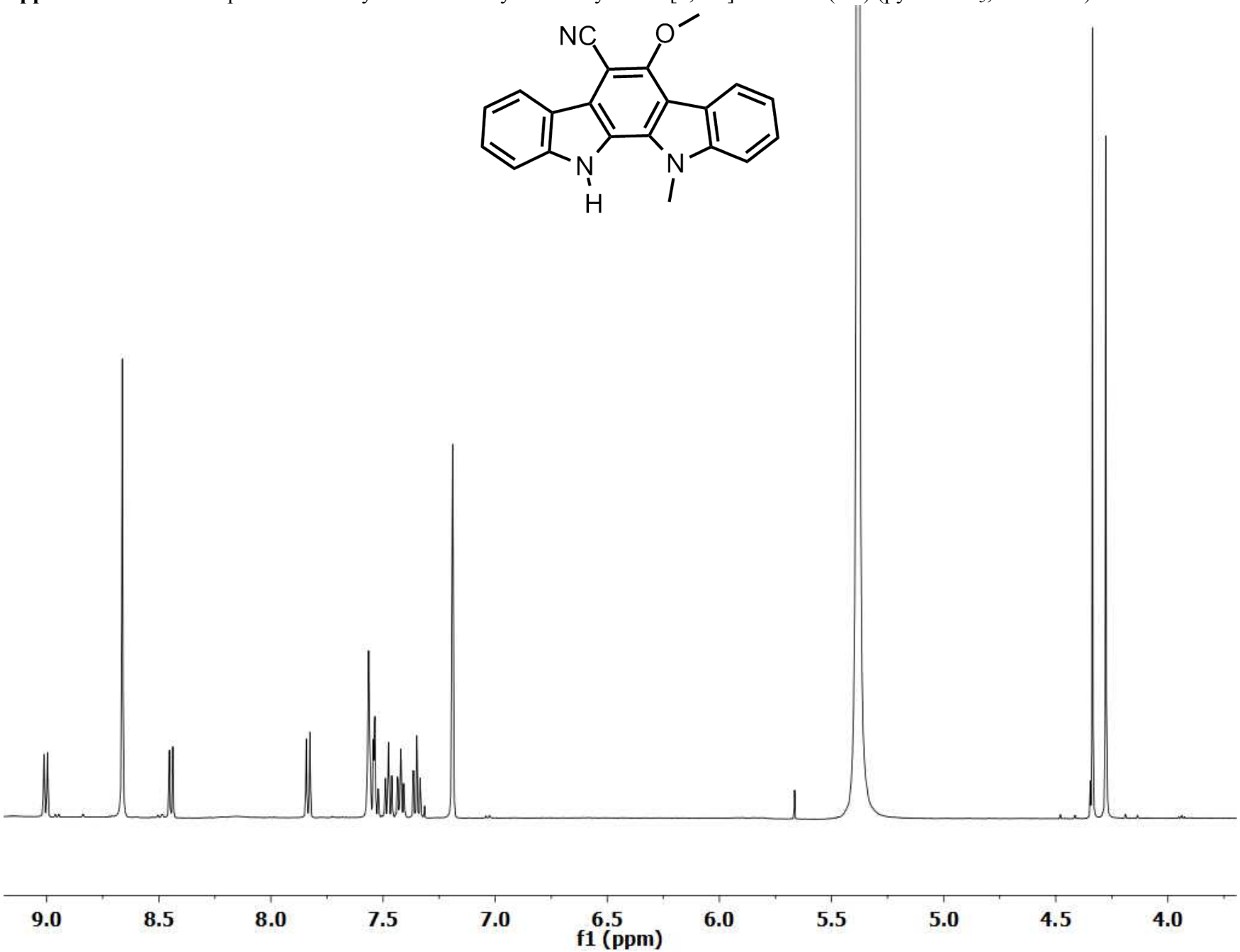

Appendix 4: ^{13}C NMR Spectrum of 6-cyano-5-methoxy-12-methylindolo[2,3-α]carbazole (**2.4**) (pyridine-d_5, 125 MHz)

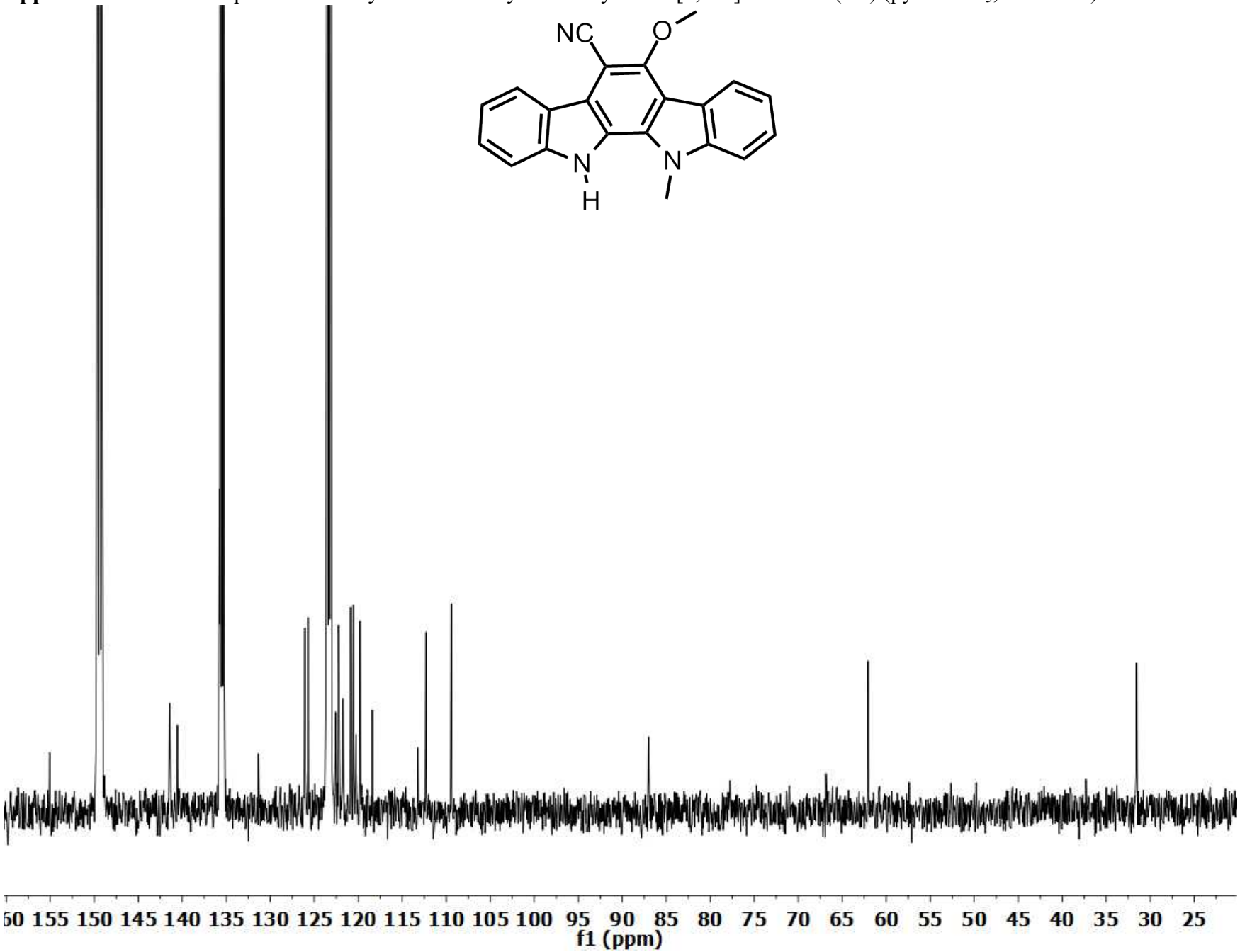

Appendix 5: NOE Experiment of 6-cyano-5-methoxy-12-methylindolo[2,3-α]carbazole (**2.4**) at δH 4.34 (pyridine-d5, 500 MHz)

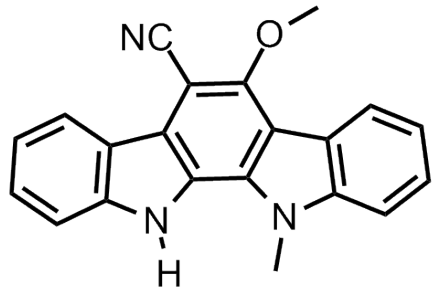

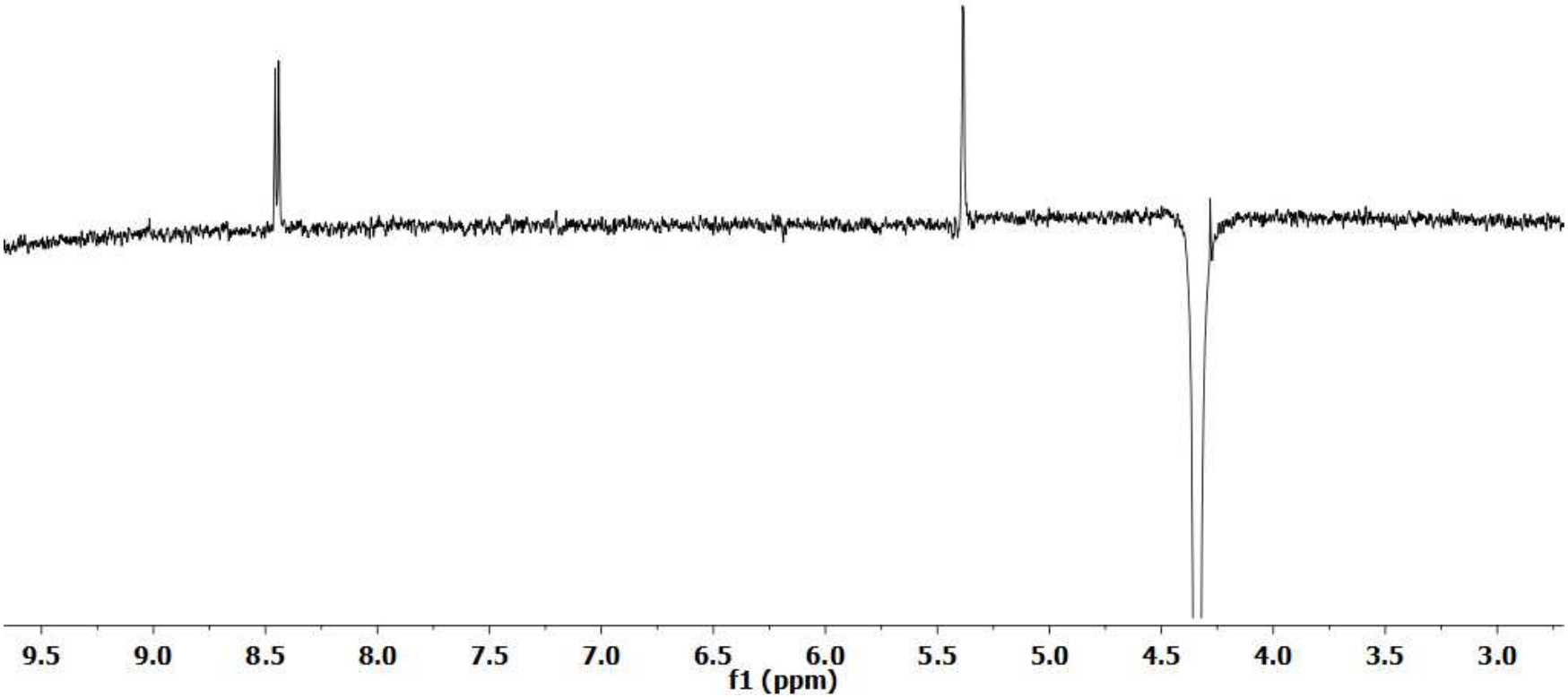

Appendix 6: NOE Experiment of 6-cyano-5-methoxy-12-methylindolo[2,3-α]carbazole(**2.4**) at δ_H 4.28 (pyridine-d_5, 500 MHz)

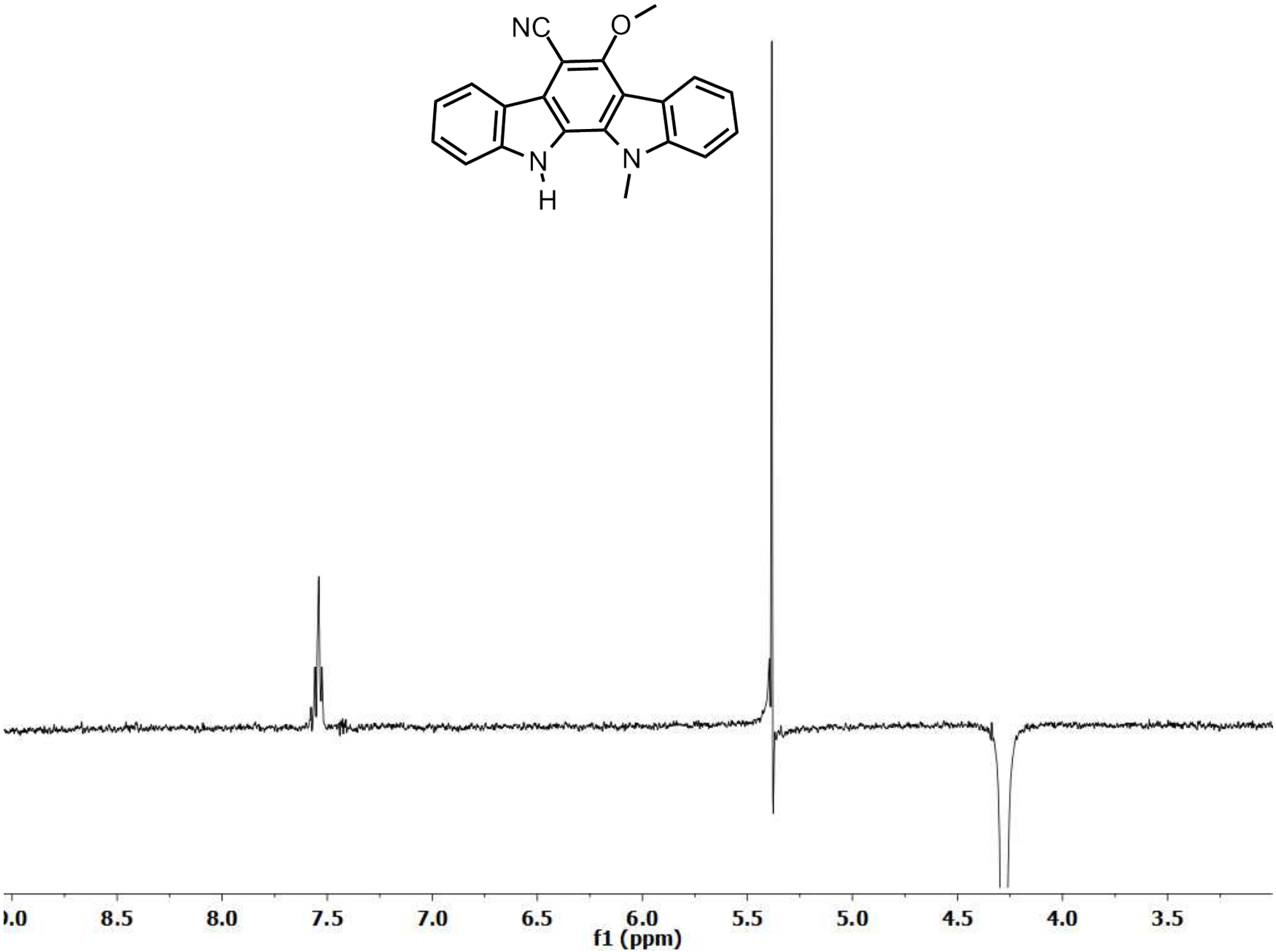

Appendix 7: ^{1}H NMR Spectrum of 6-cyano-5-methoxy-11-methylindolo[2,3-α]carbazole (**2.5**) (pyridine-d_5, 500 MHz)

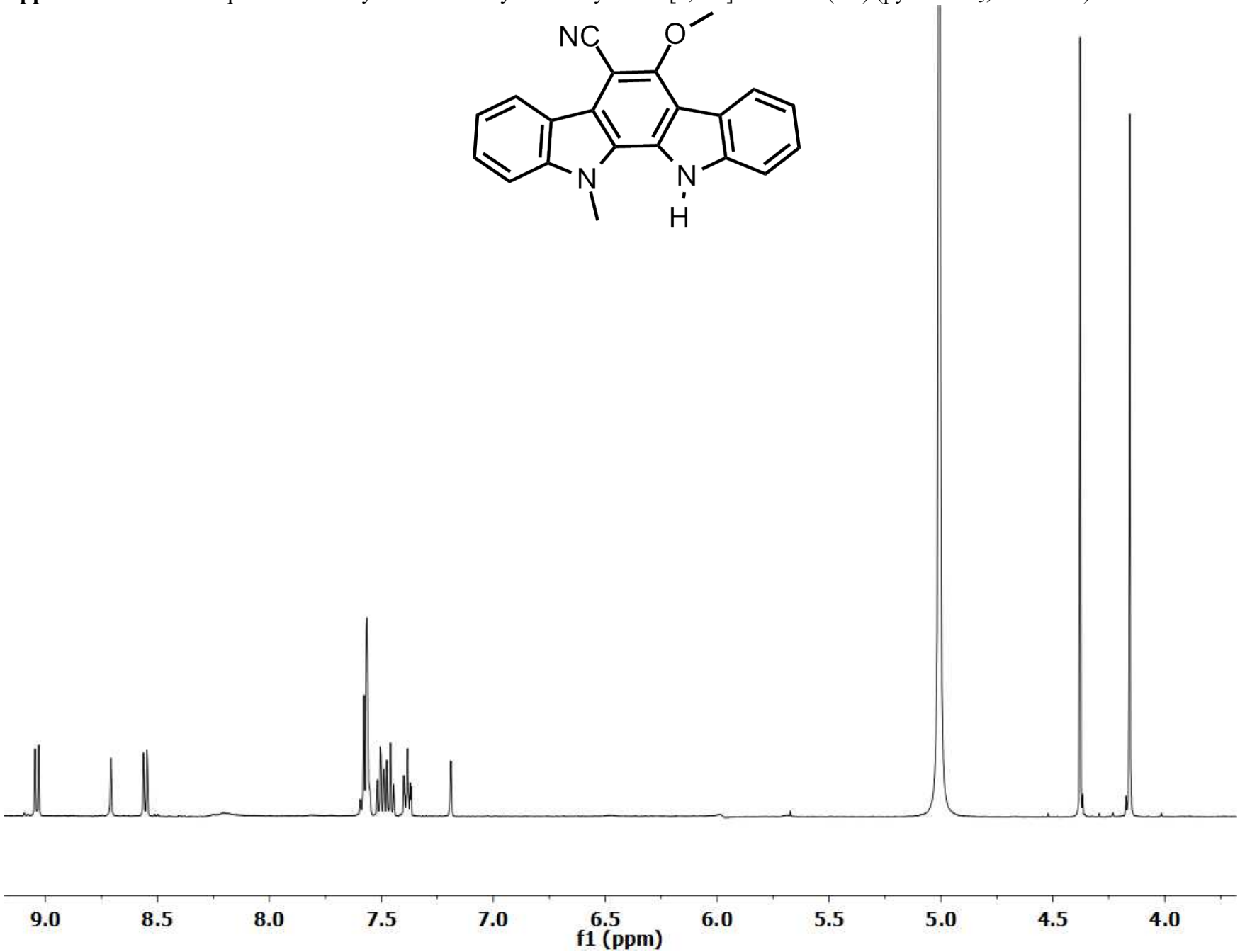

Appendix 8: ^{13}C NMR Spectrum of 6-cyano-5-methoxy-11-methylindolo[2,3-α]carbazole (**2.5**) (pyridine-d_5, 125 MHz)

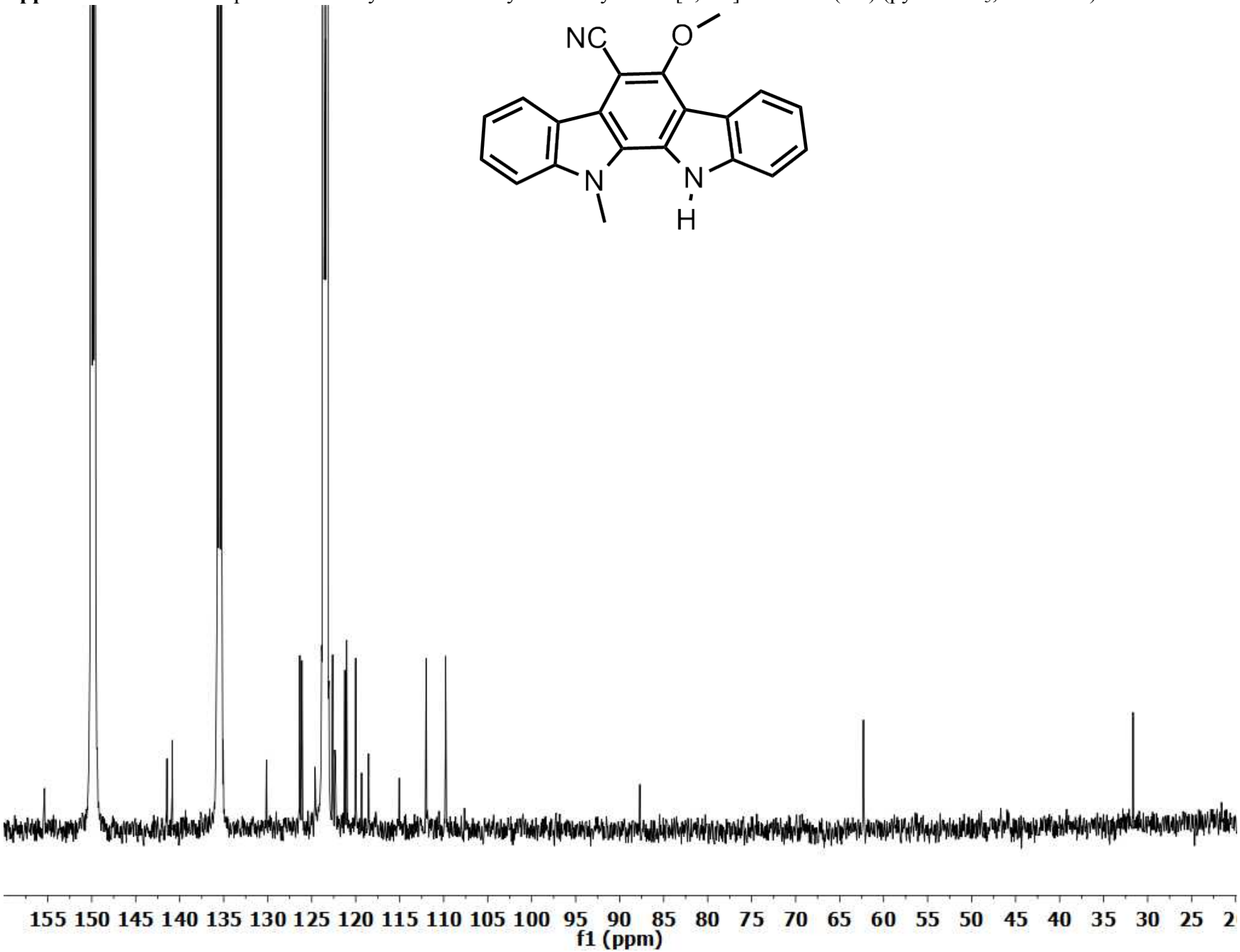

Appendix 9: NOE Experiment of 6-cyano-5-methoxy-11-methylindolo[2,3-α]carbazole (**2.5**) at δ_H 4.38 (pyridine-d_5, 500 MHz)

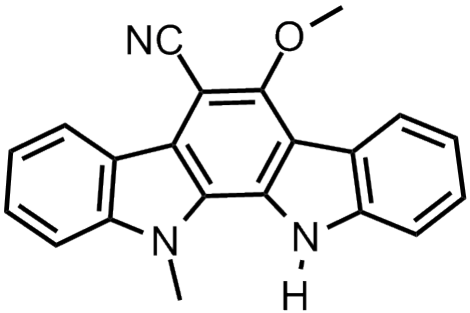

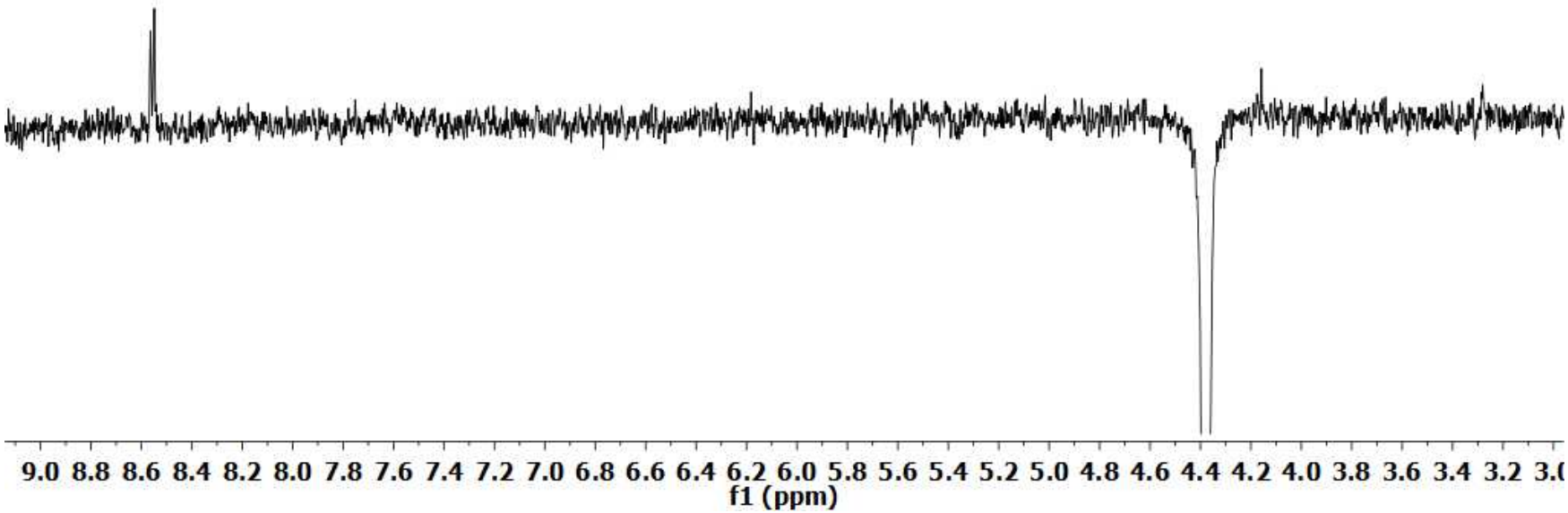

Appendix 10: NOE Experiment of 6-cyano-5-methoxy-11-methylindolo[2,3-α]carbazole (**2.5**) at δ_H 4.16 (pyridine-d_5, 500 MHz)

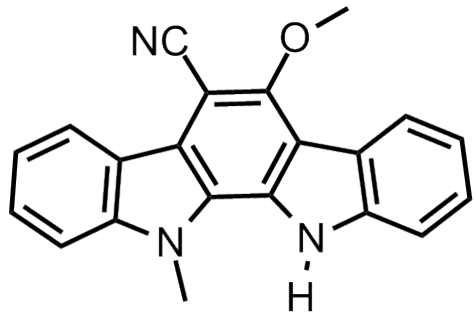

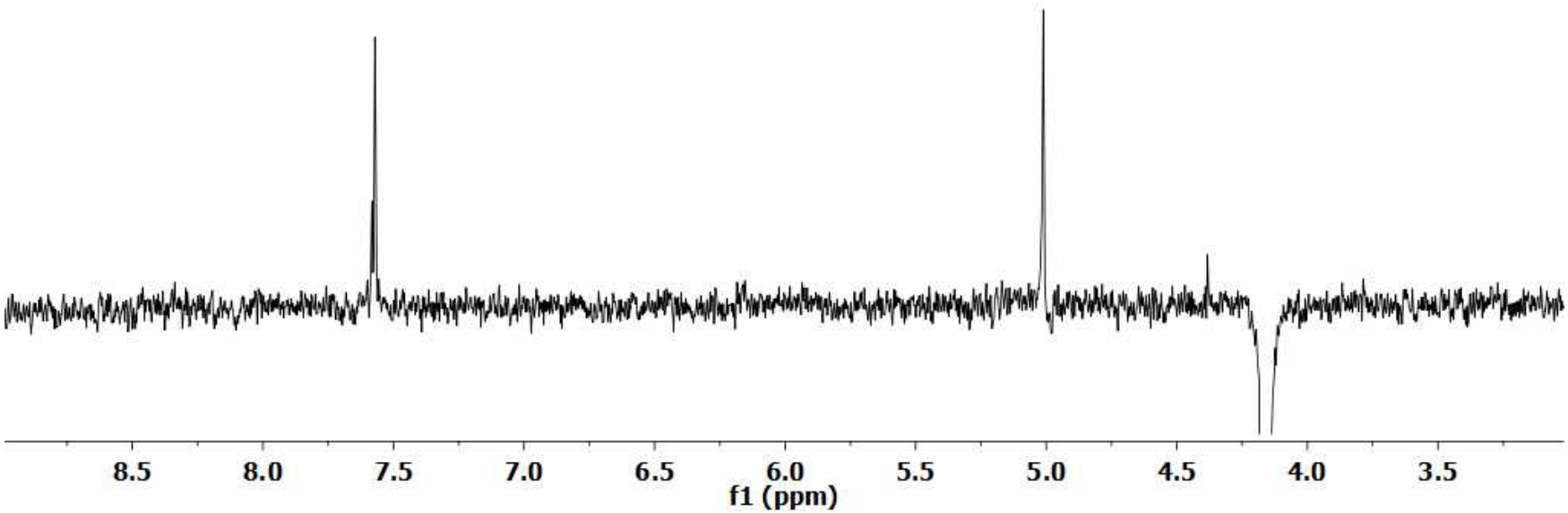

Appendix 11: ^{1}H NMR Spectrum of 6-cyano-5-methoxyindolo[2,3-α]carbazole (**2.6**) (pyridine-d_5, 500 MHz)

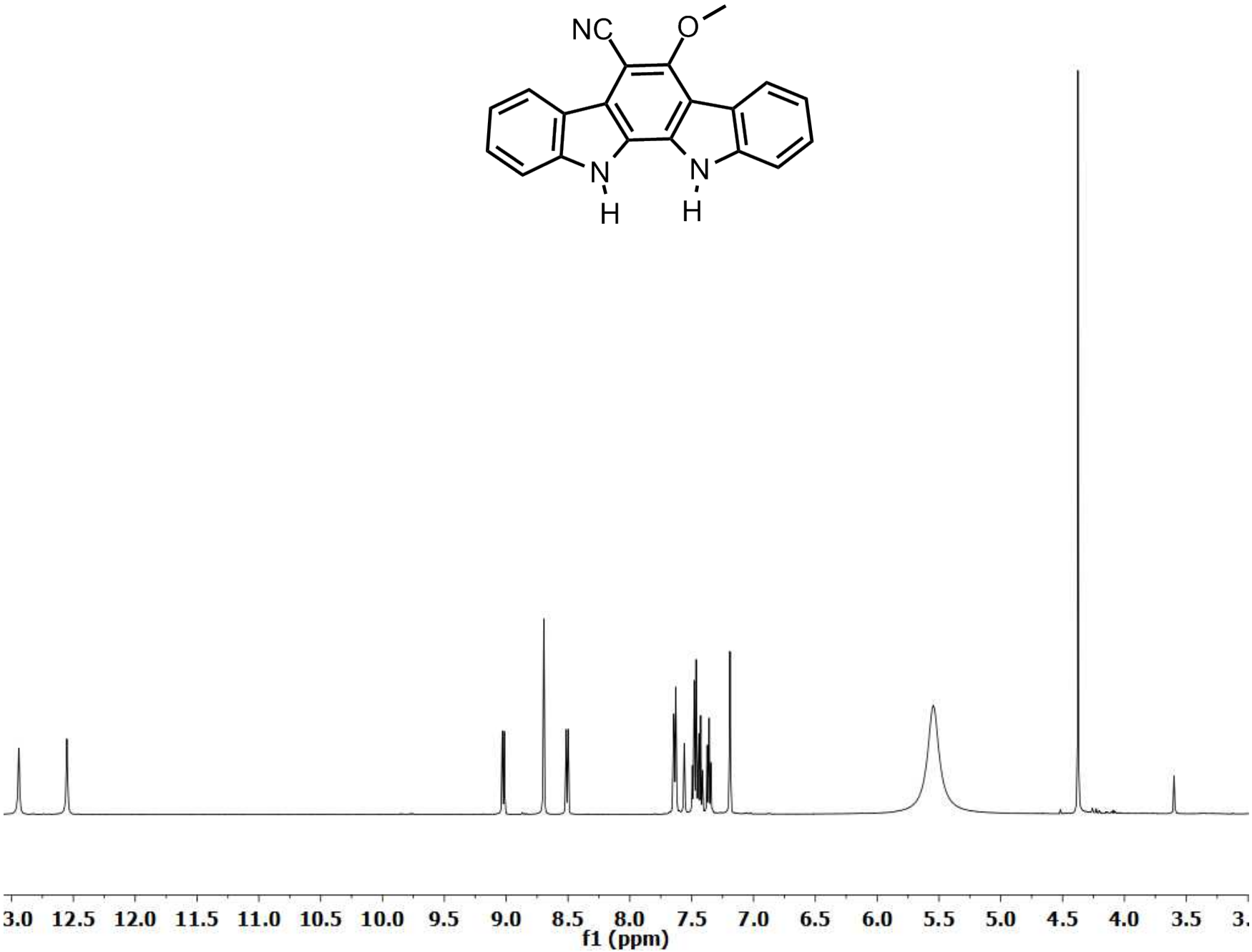

Appendix 12: ^{13}C NMR Spectrum of 6-cyano-5-methoxyindolo[2,3-α]carbazole (**2.6**) (pyridine-d_5, 125 MHz)

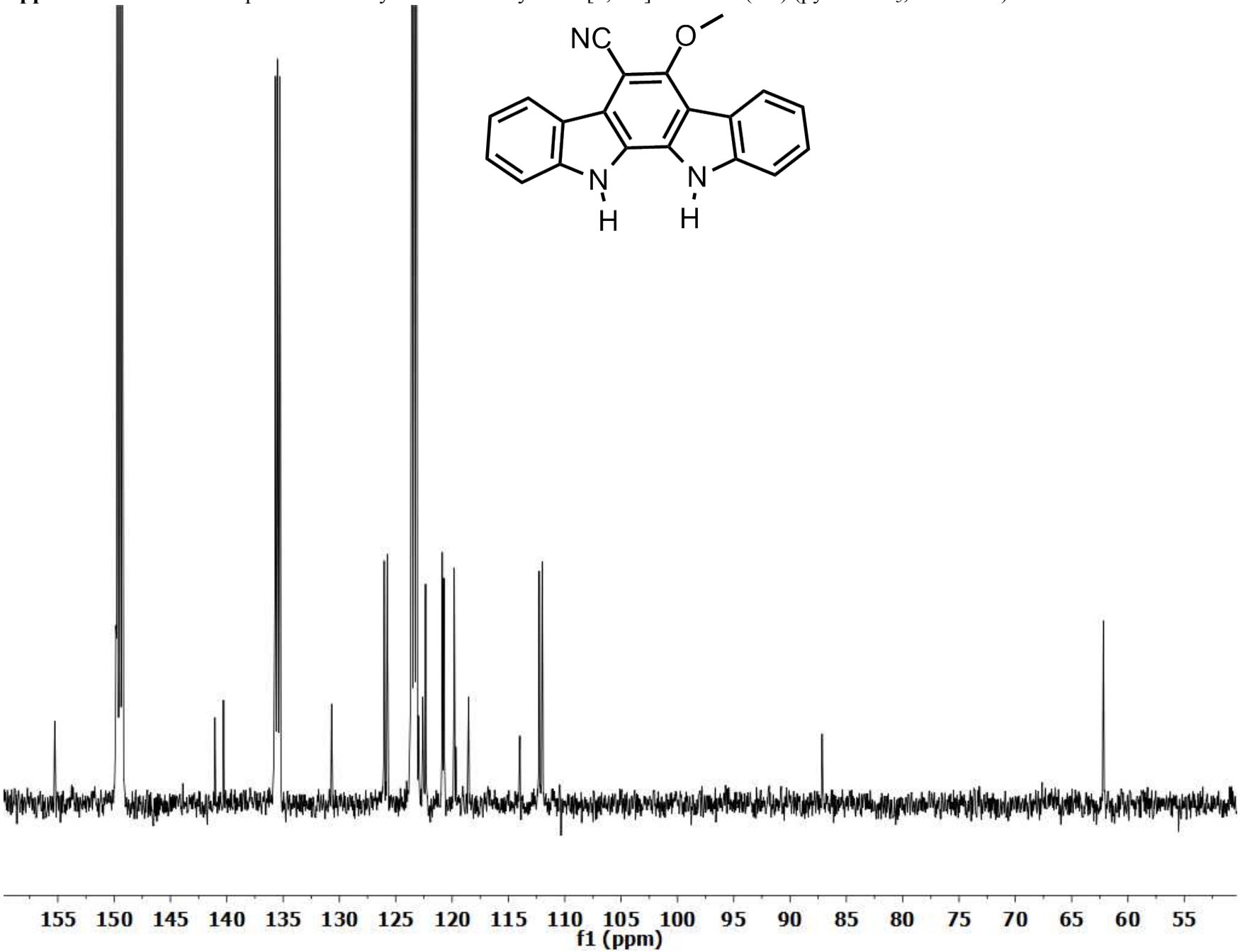

Appendix 13: ^{1}H NMR Spectrum of 19-nor-3,17-dihydroxyspongia-3,13(16),14-triene-2-one (**3.1**) (CD3OD, 500 MHz)

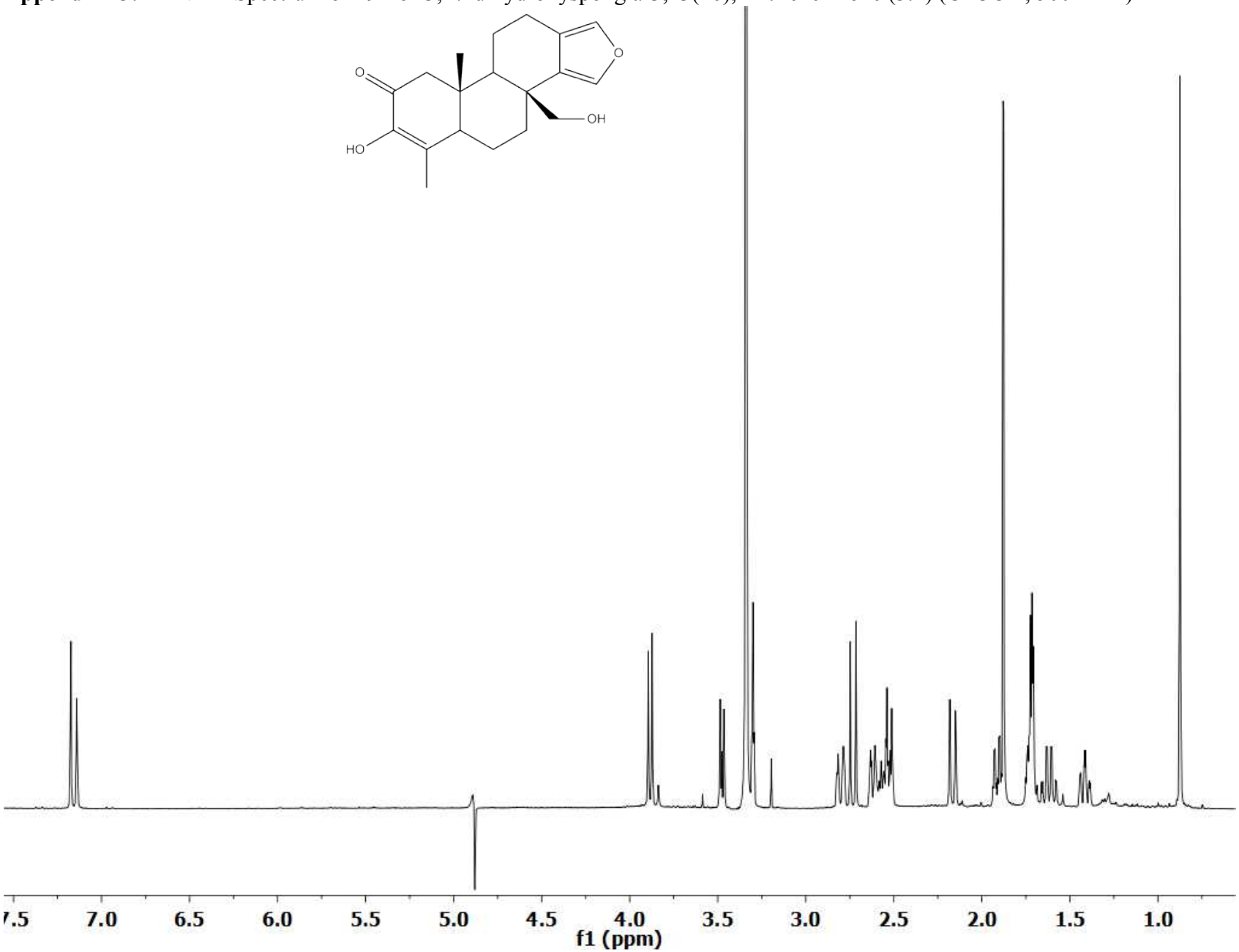

Appendix 14: ^{13}C NMR Spectrum of 19-nor-3,17-dihydroxyspongia-3,13(16),14-triene-2-one **(3.1)** (CD_3OD, 125 MHz)

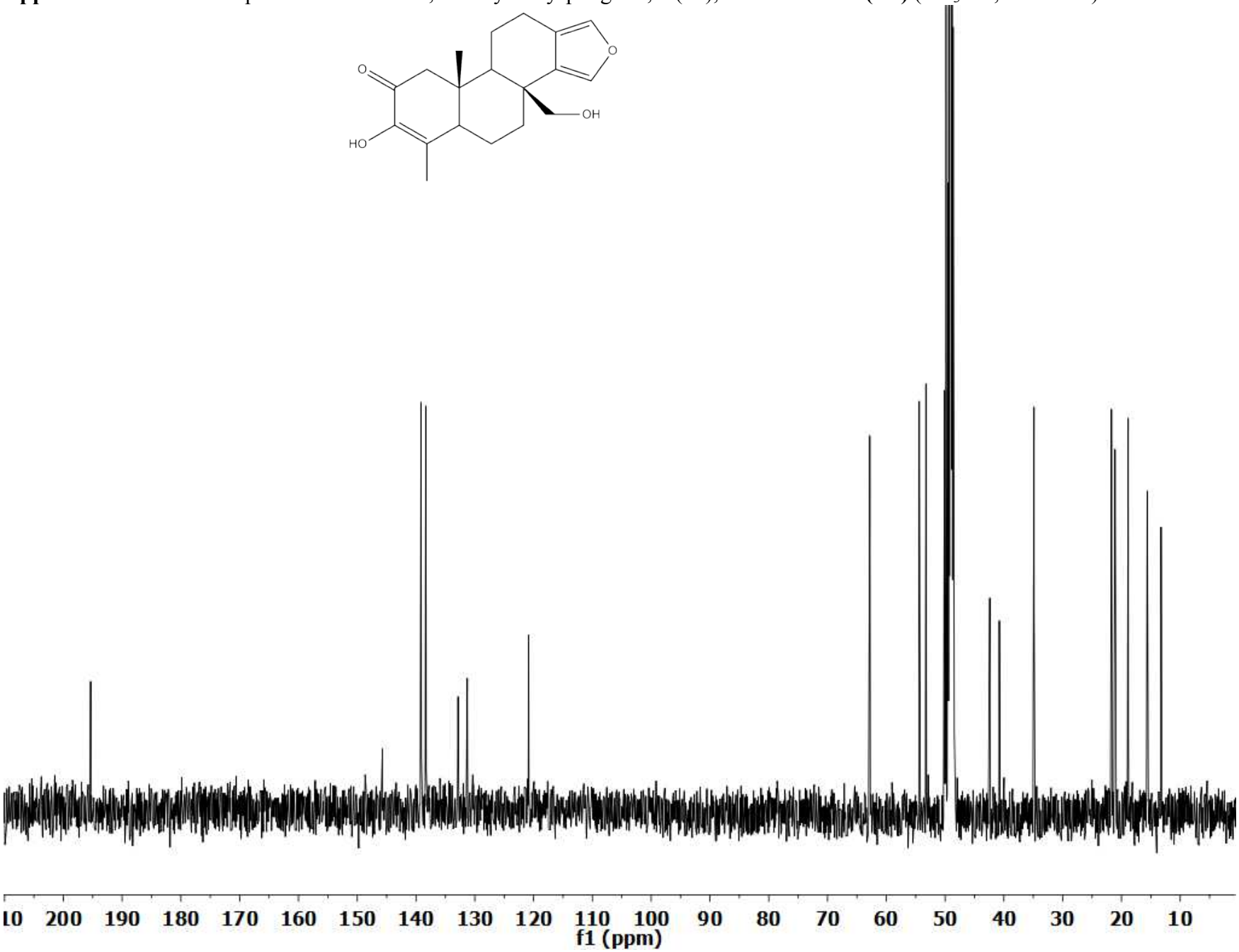

Appendix 15: ^{1}H NMR Spectrum of 19-nor-3,5α,17-trihydroxyspongia-3,13(16),14-triene-2-one (**3.2**) (CD_3OD, 500 MHz)

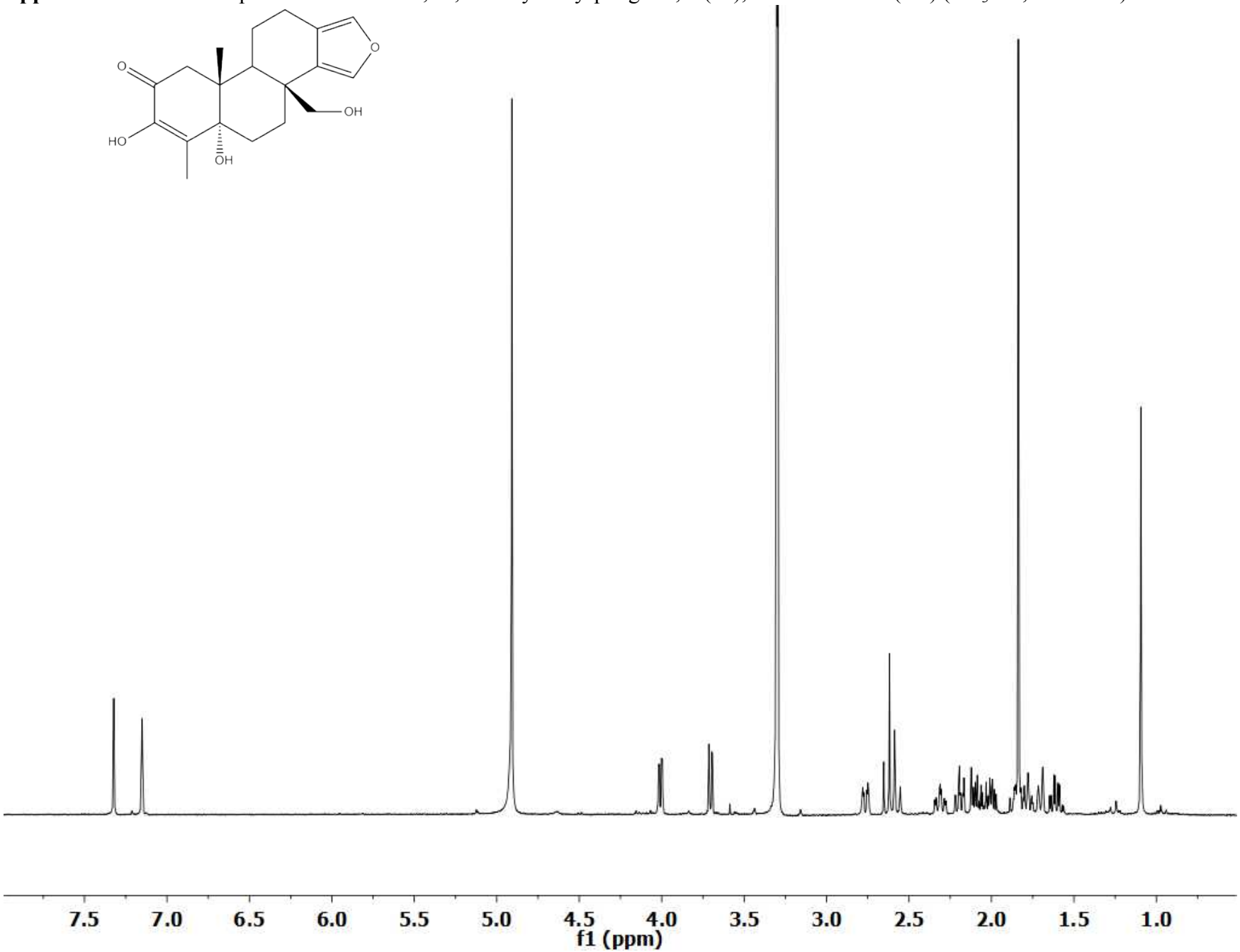

Appendix 16: ^{13}C NMR Spectrum of 19-nor-3,5α,17-trihydroxyspongia-3,13(16),14-triene-2-one (**3.2**) (CD_3OD, 125 MHz)

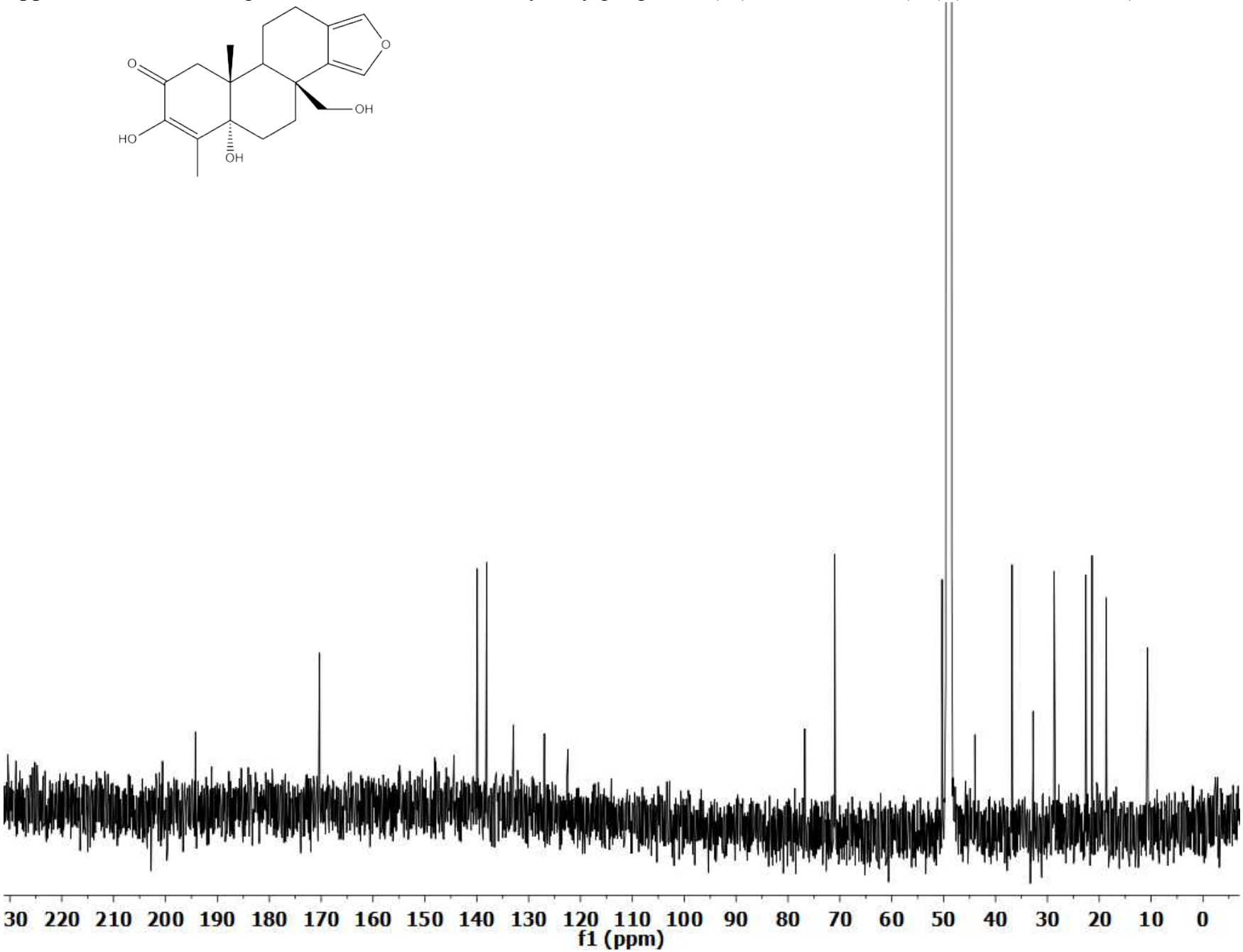

Appendix 16: NOE Experiment of 19-nor-3,5α,17-trihydroxyspongia-3,13(16),14-triene-2-one (**3.2**) at δ_H 1.09 (CD_3OD, 125 MHz)

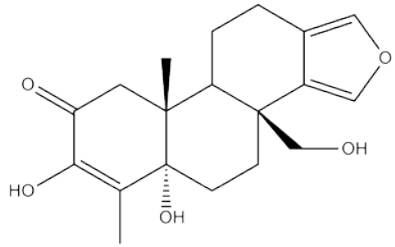

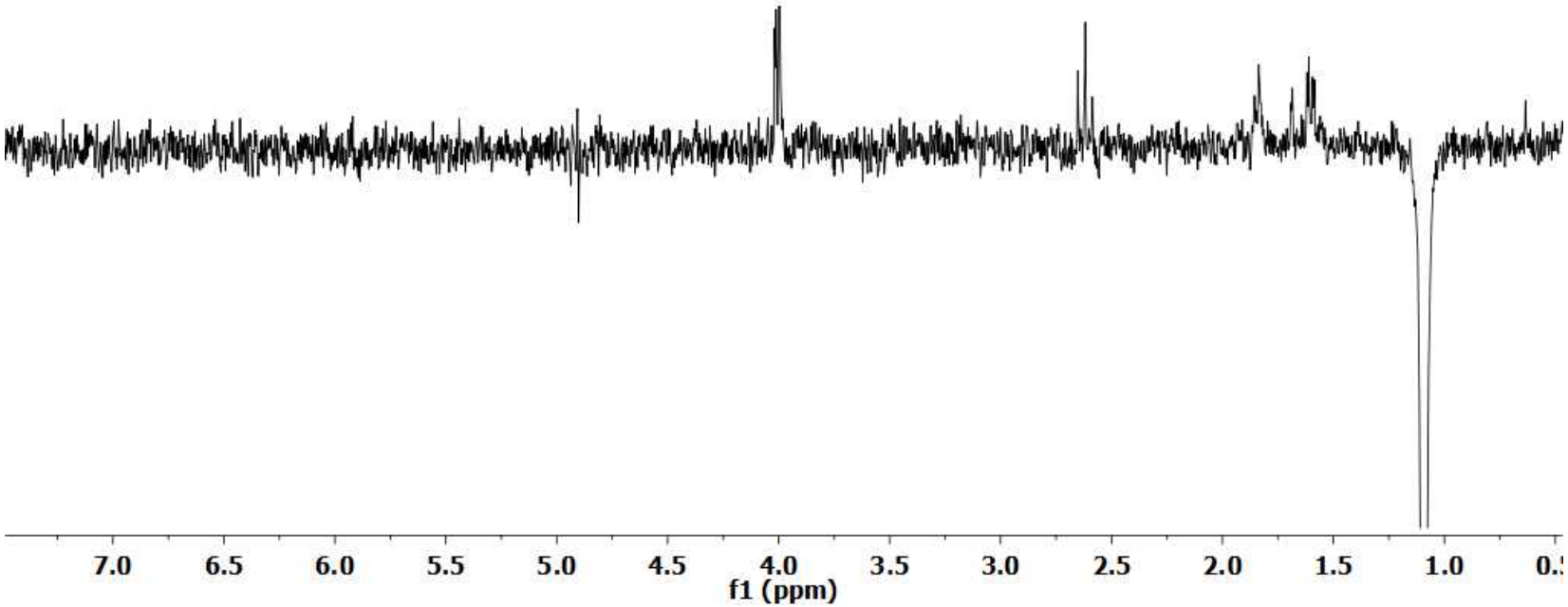

Appendix 17: ^{1}H NMR Spectrum of Spongiapyridine (**3.3**) (CD_3OD, 500 MHz)

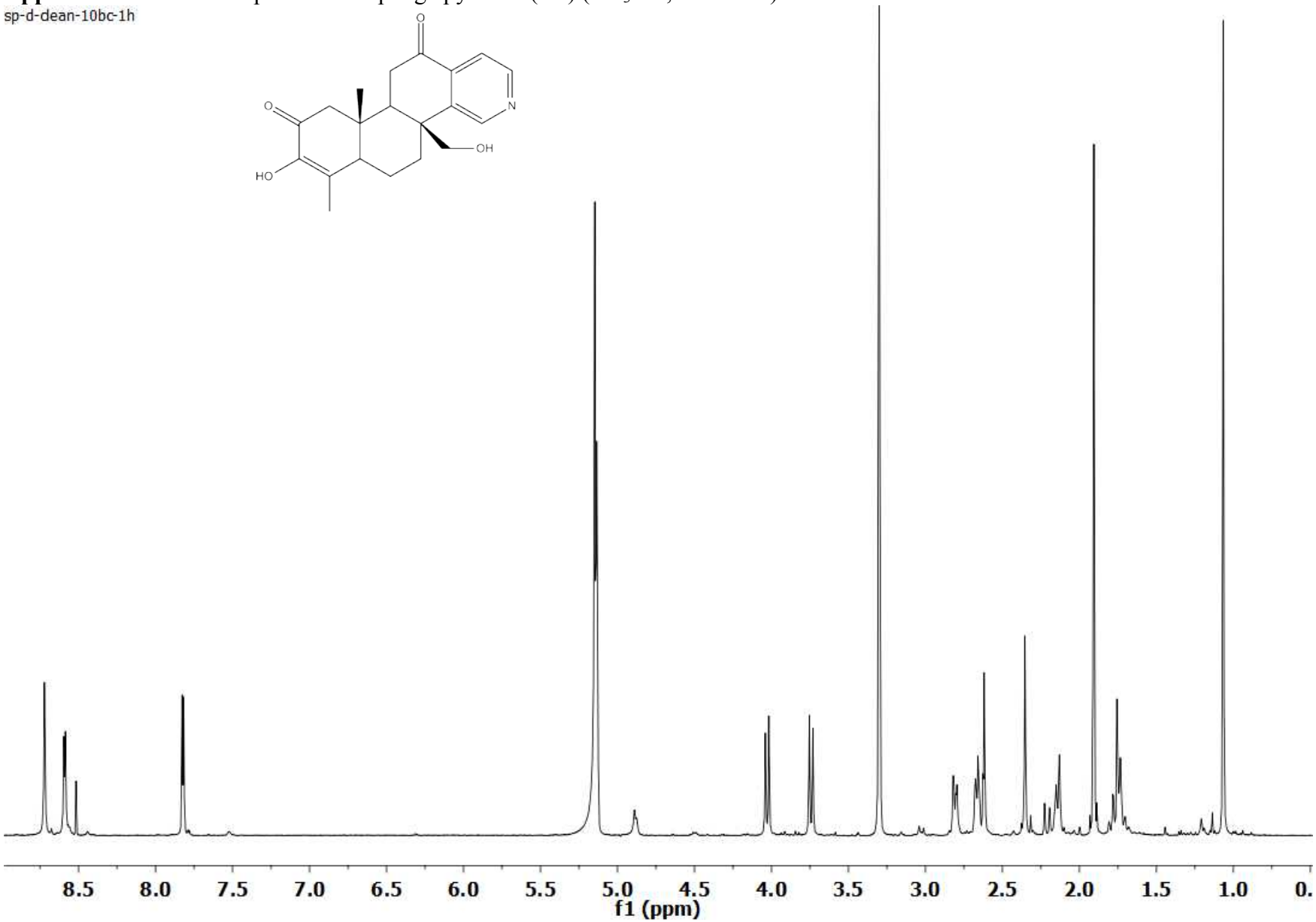

Appendix 18: ^{13}C NMR Spectrum of Spongiapyridine (**3.3**) (CD_3OD, 125 MHz)

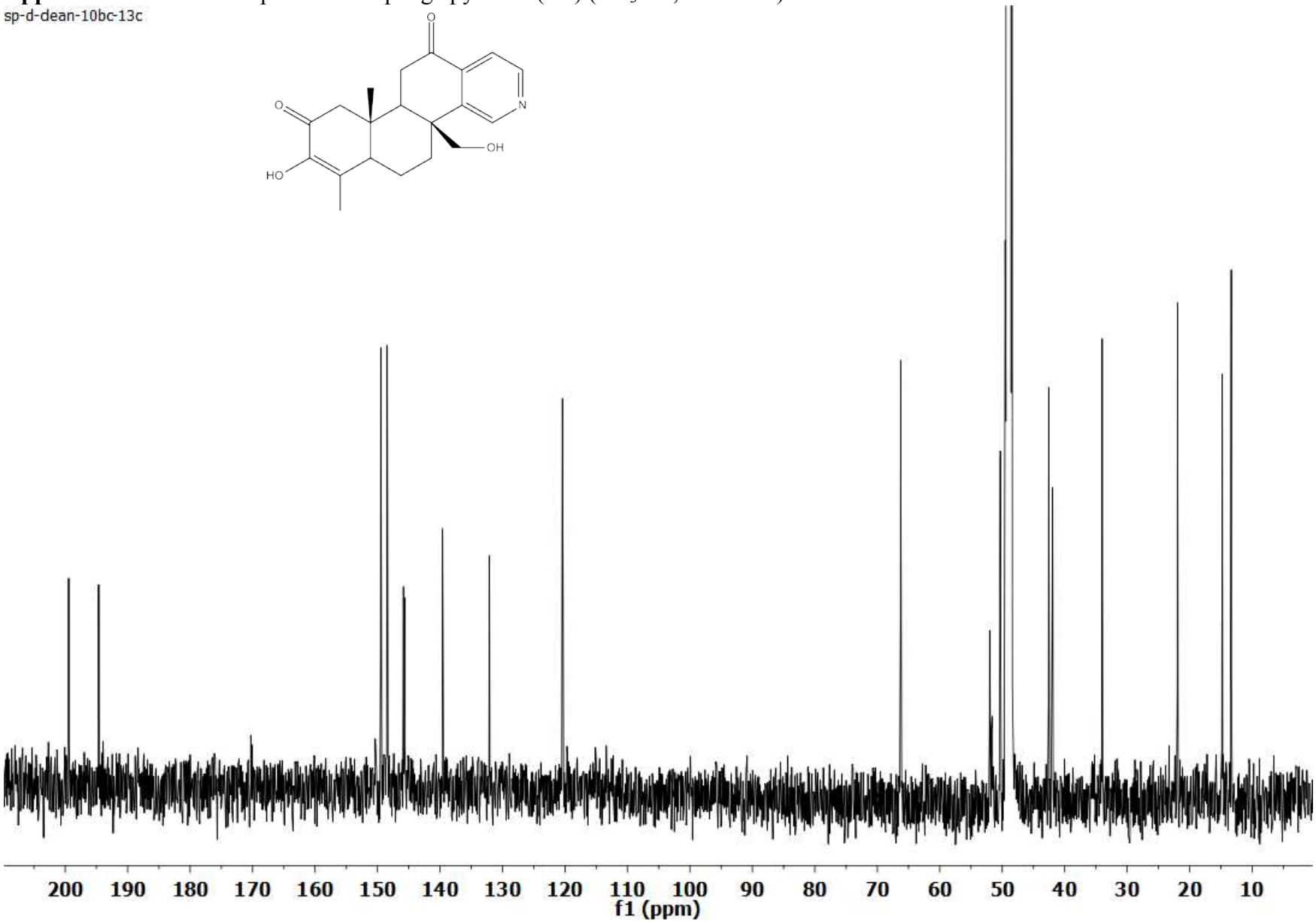

Appendix 19: Expansion of ^{13}C NMR Spectrum of Spongiapyridine (**3.3**) (CD_3OD, 125 MHz)

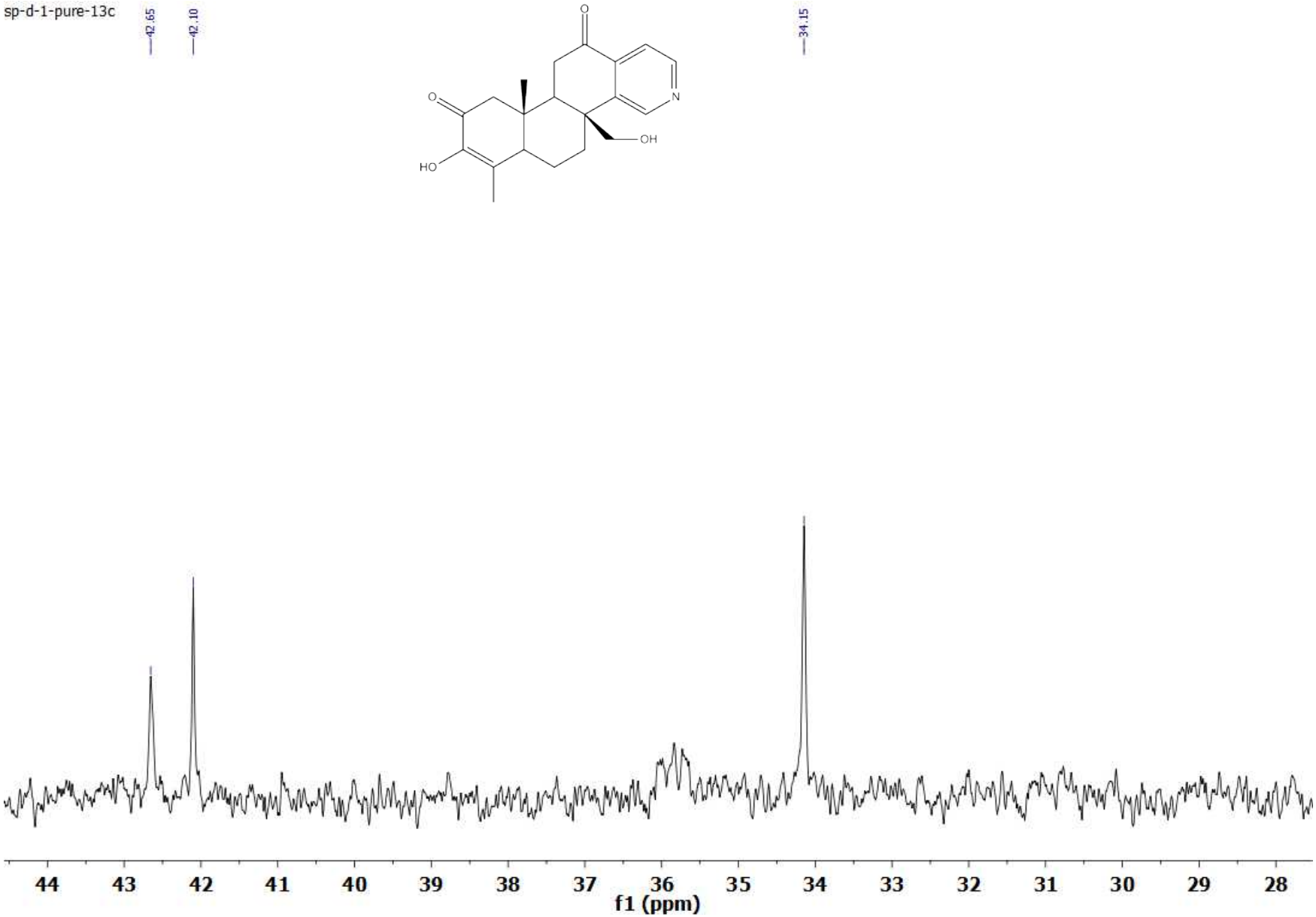

Appendix 20: ^{1}H-^{15}N HMBC NMR Spectrum of Spongiapyridine (**3.3**) (CD_3OD, 500 MHz)

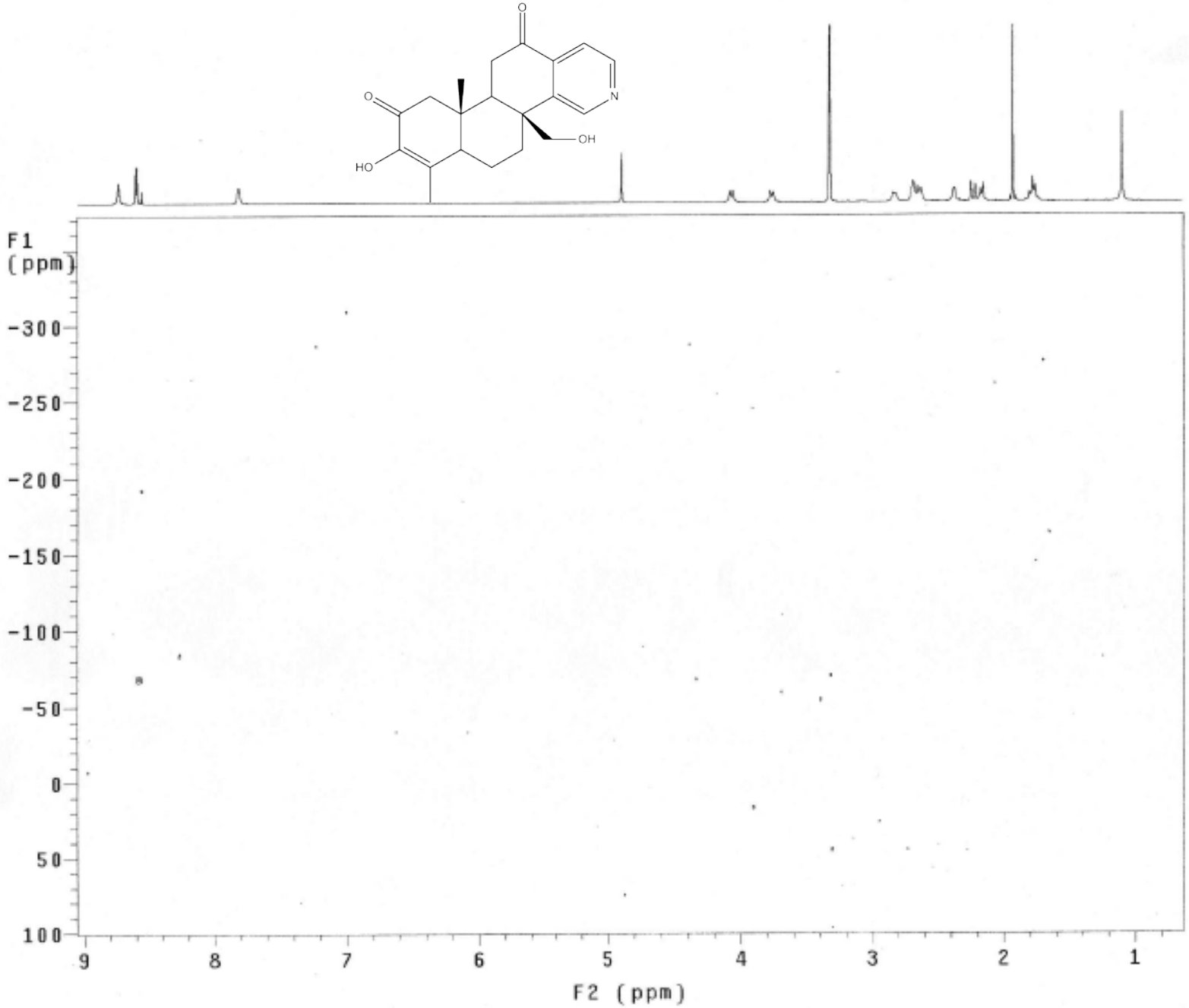

Appendix 21: ^{1}H NMR Spectrum of Spongiapyridine (**3.3**) (CD_3OH, 500 MHz)

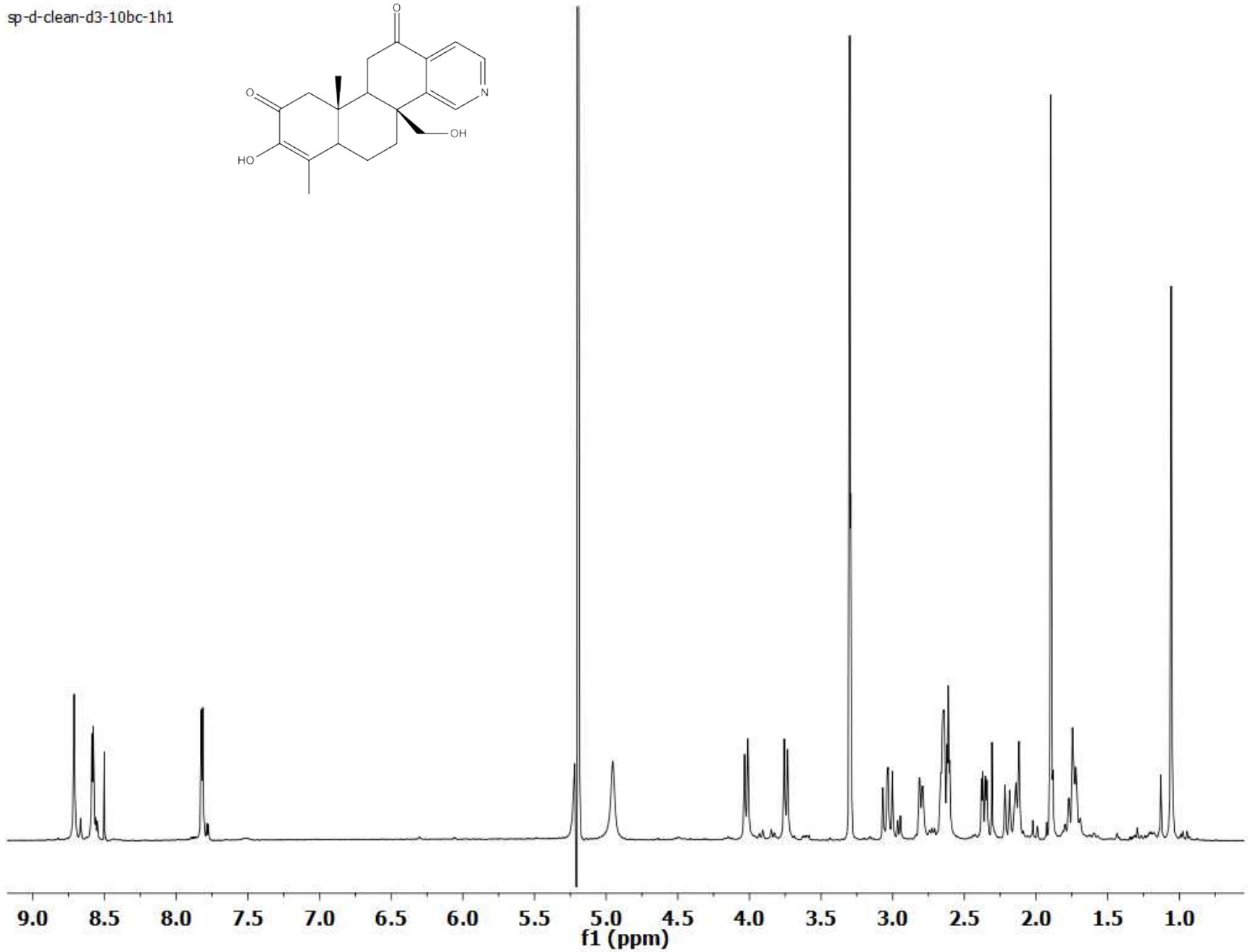

Appendix 22: ^{13}C NMR Spectrum of Spongiapyridine (**3.3**) (CD_3OH, 125 MHz)

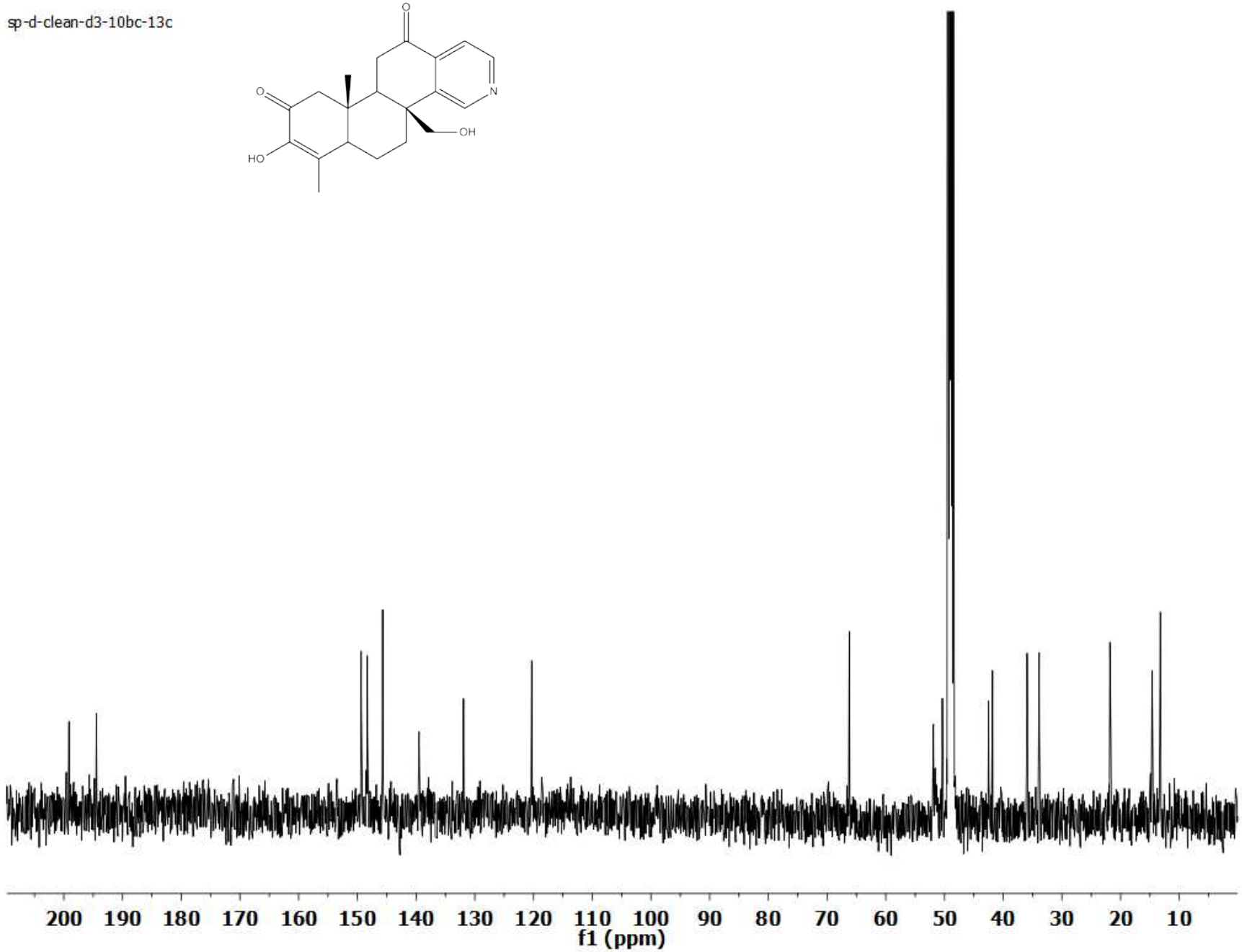

Appendix 23: Expansion of ^{13}C NMR Spectrum of Spongiapyridine (**3.3**) (CD_3OH, 125 MHz)

sp-d-clean-d3-10bc-13c

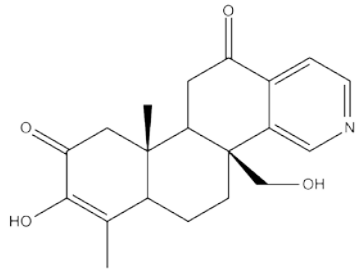

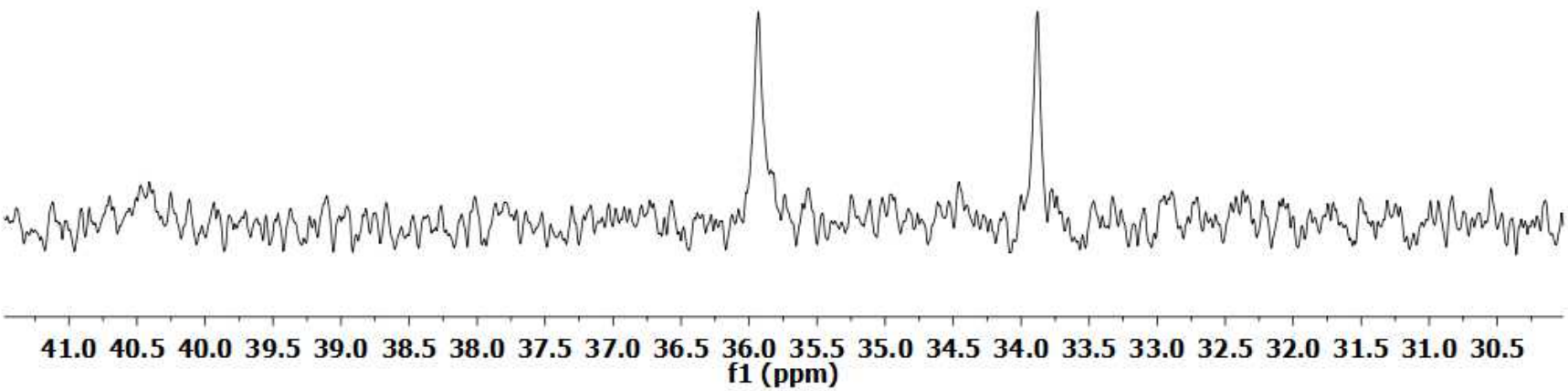

Appendix 17: NOE Experiment of Spongiapyridine (**3.3**) at δ_H 1.09 (CD_3OH, 500 MHz)

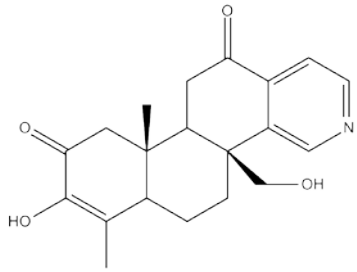

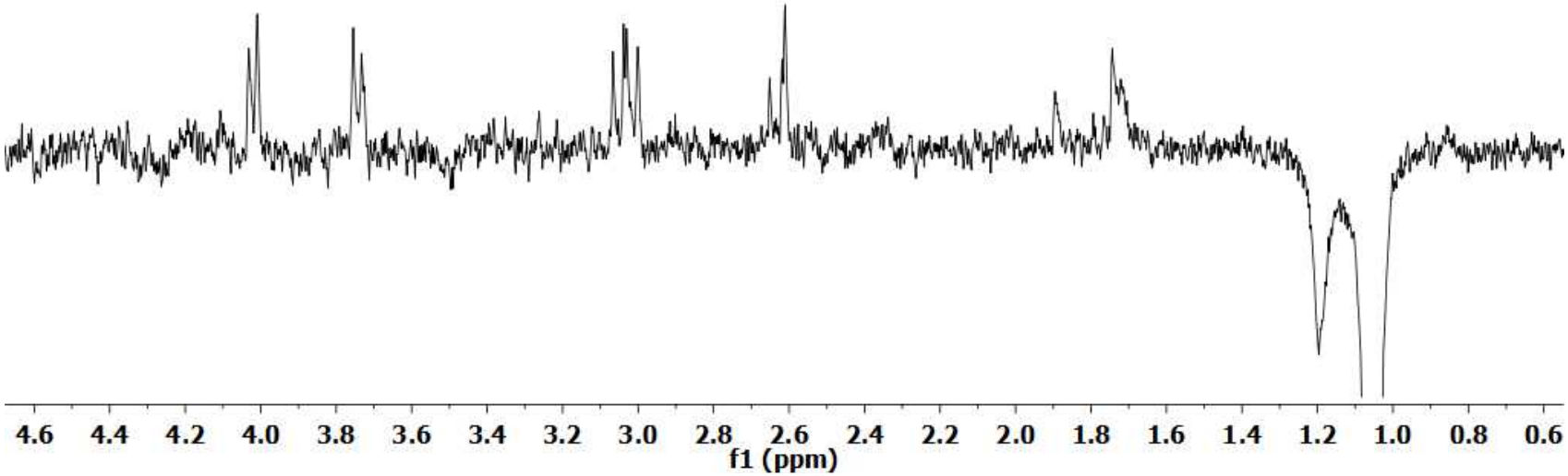

Appendix 24: ^{1}H NMR Spectrum of 17-hydroxy-4-epispongialactone A (**3.4**) (CD_3OD, 500 MHz)

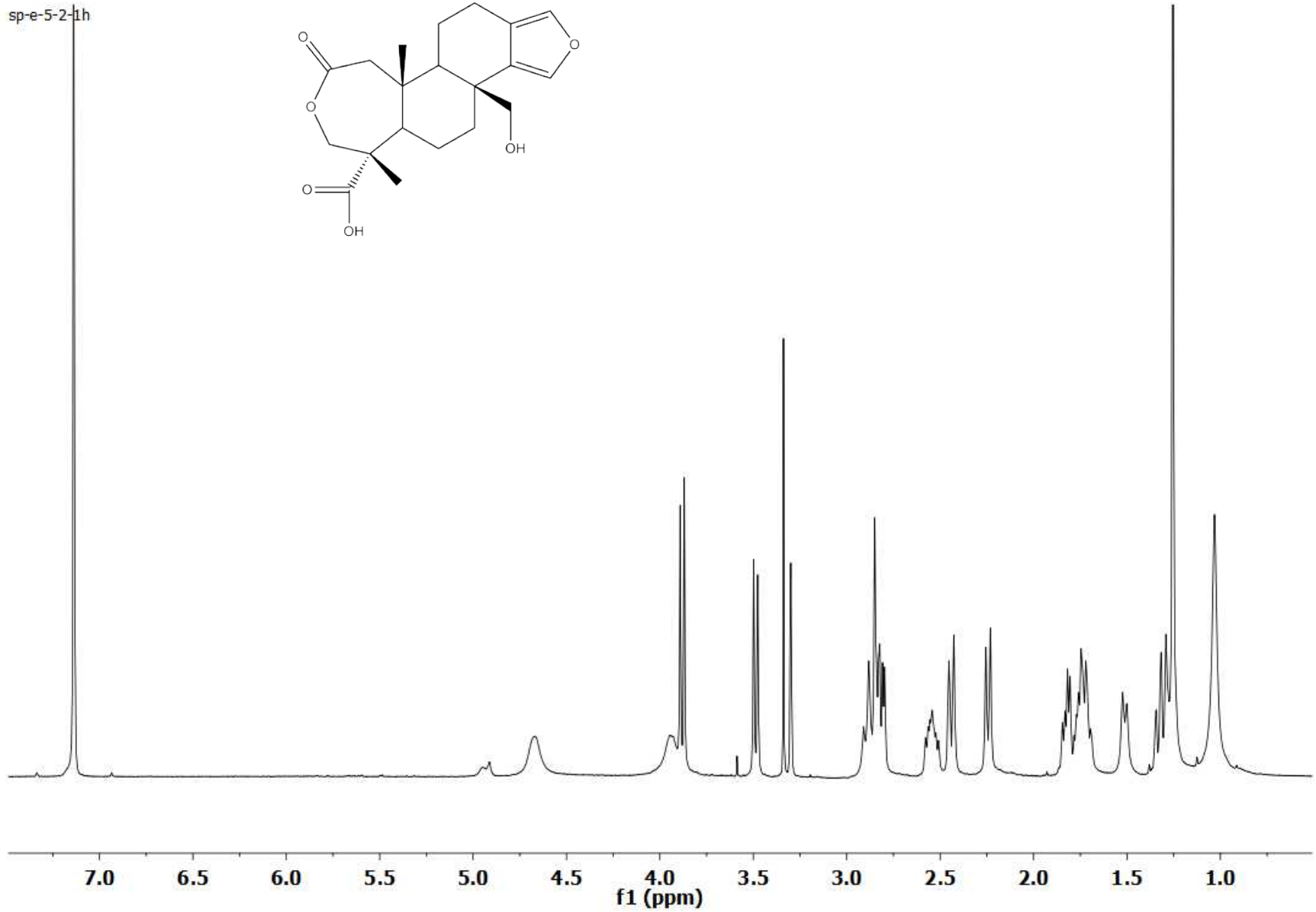

Appendix 25: ^{13}C NMR Spectrum of 17-hydroxy-4-epispongialactone A (**3.4**) (CD_3OD, 125 MHz)

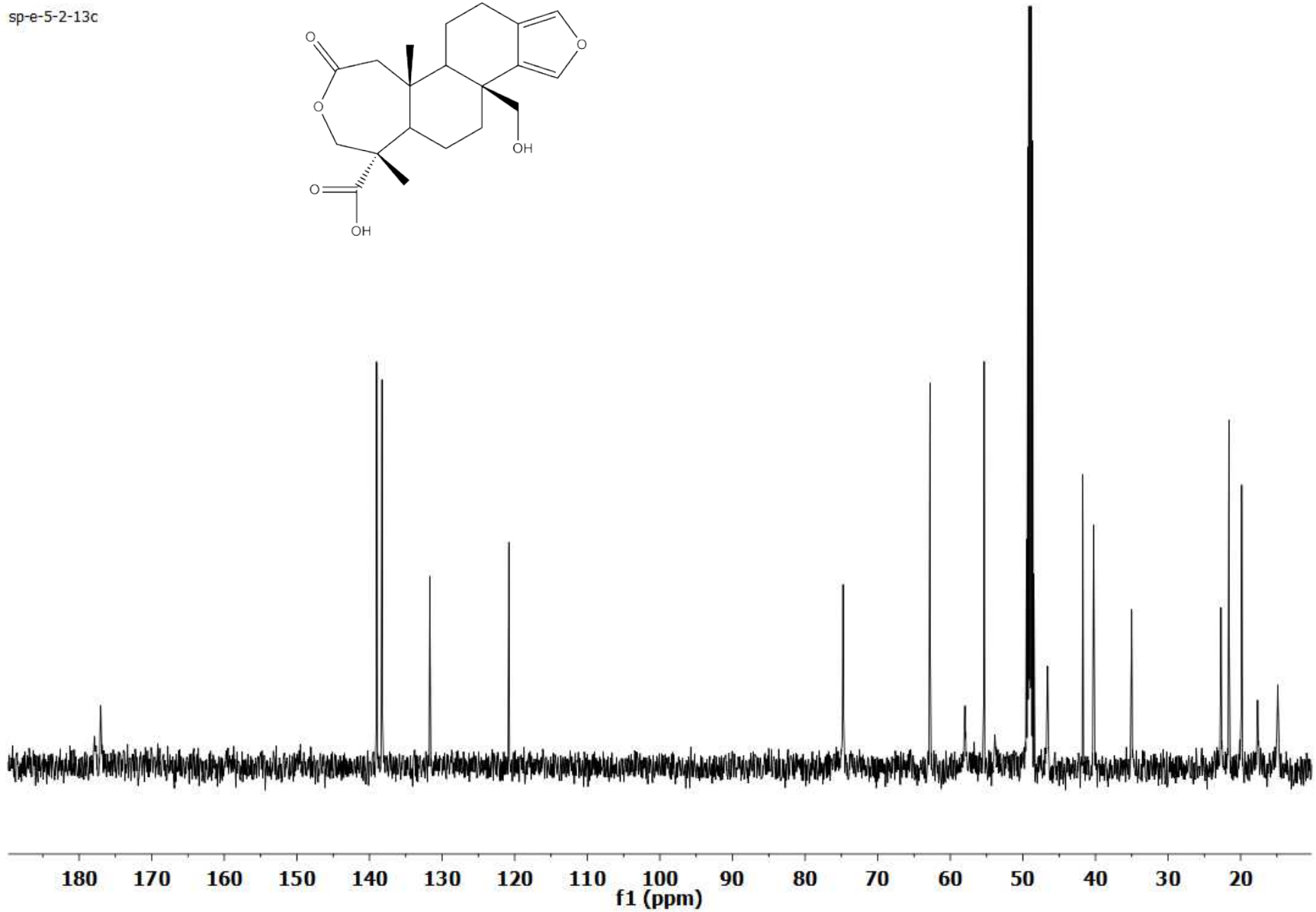

Appendix 26: NOE NMR Experiment of 17-hydroxy-4-epispongialactone A (**3.4**) at δ_H 1.25 (CD_3OD, 500 MHz)

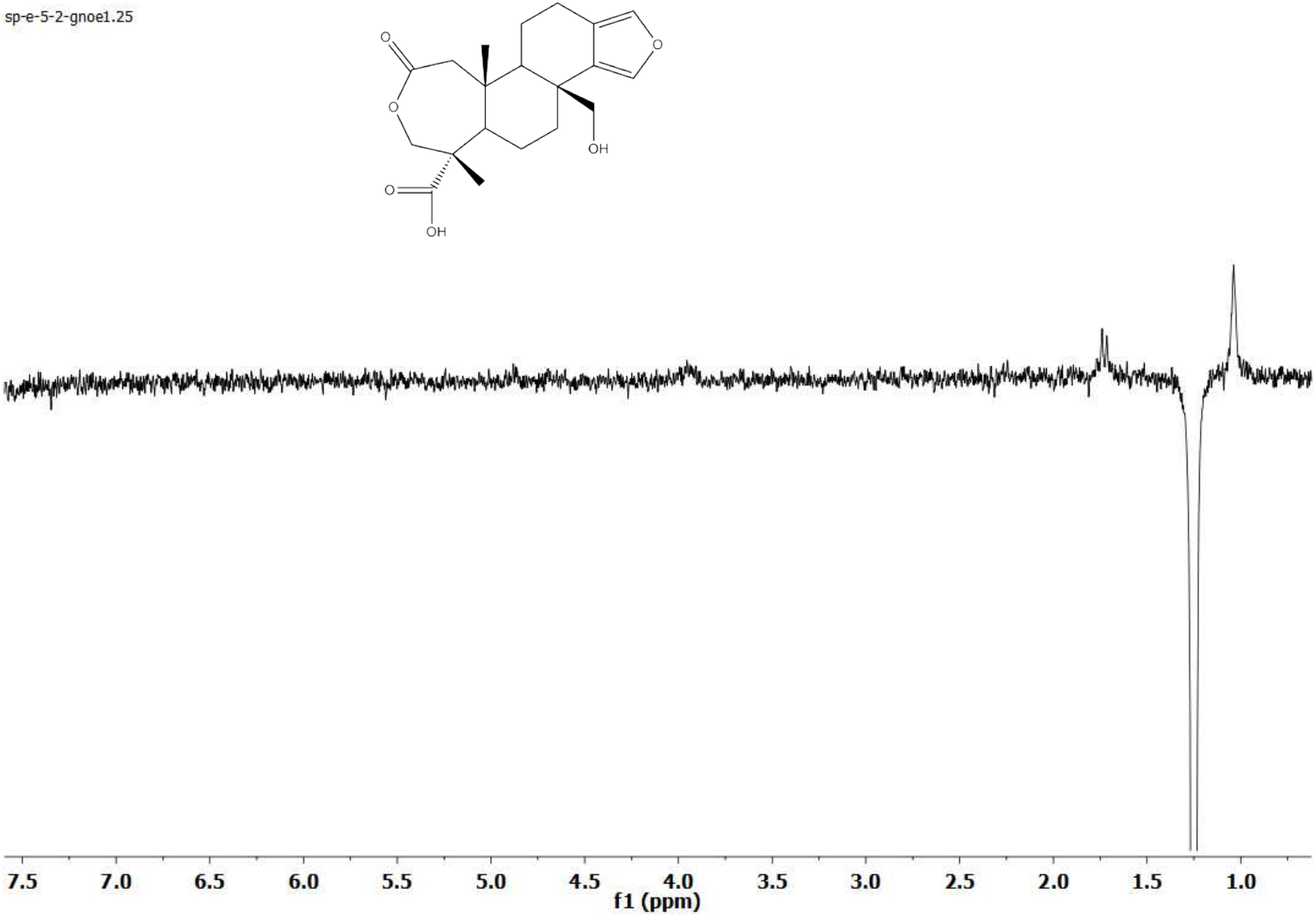

Appendix 27: A Table of ^{13}CNMR and ^{1}HNMR resonances of known compounds **2.4-2.6**

Postion	**2.4** δ_C, Type[a]	**2.4** δ_H, m (*J* Hz)[b]	**2.5** δ_C, Type[a]	**2.5** δ_H, m (*J* Hz)[b]	**2.6** δ_C, Type[a]	**2.6** δ_H, m (*J* Hz)[b]
1	112.3 CH	7.83, d (8.1)	112.0, CH	7.60, m	112.3, CH	7.64, d (8.3)
2	125.7, CH	7.55, t (7.6)	126.1, CH	7.50, td (7.0, 1.0)	125.8, CH	7.46, t (7.3)
3	120.6, CH	7.42, d (7.0)	121.0, CH	7.46, td (7.3, 1.0)	120.9, CH	7.43, t (7.3)
4	121.8, CH	8.45, d (7.9)	122.4, CH	8.55, d (7.5)	122.4, CH	8.51, d (8.0)
4a	122.0, qC		122.3, qC		122.3, qC	
4b	113.2, qC		115.1, qC		114.0, qC	
5	155.0, qC		155.4, qC		155.3, qC	
6	87.0, qC		87.7, qC		87.2, qC	
6a	120.3, qC		121.3, qC		119.8, qC	
6b	122.2, qC		122.6, qC		122.6, qC	
7	120.9, CH	9.00, d (8.0)	120.0, CH	9.04, d (8.0)	120.7, CH	9.02, d (8.0)
8	119.8, CH	7.35, t (7.5)	119.4, CH	7.38, ddd (8.0, 6.0, 2.0)	119.7, CH	7.36, t (7.3
9	126.1, CH	7.48, t (7.6)	126.4, CH	7.57, m	126.0, CH	7.48, t (7.6)
10a	141.4, qC		141.5, qC		141.1, qC	
10	109.4, CH	7.53, d (7.8)	109.8, CH	7.56, m	112.0, CH	7.63, d (7.9)
11a	122.3, qC		124.6, qC		123.0, qC	
11b	131.4, qC		130.2, qC		130.7, qC	
12a	140.6, qC		140.9, qC		140.3, qC	
CN	118.4, qC		118.6, qC		118.6, qC	
OMe	62.1, CH_3	4.34, s	62.3, CH_3	4.38, s	62.2, CH_3	4.37, s
NMe	31.6, CH_3	4.28, s	31.7, CH_3	4.16, s		

[a] Spectrum recorded at 125 MHz, in pyridine *d*-5
[b] Spectrum recorded at 500 MHz, in pyridine *d*-5

References:

[1] Moore, R. E.; Scheuer, P. J. *Science*. **1971**, 172, 495-498

[2] Spande, T. F.; Garraffo, H. M.; Edwards, M. W.; Yeh, H. J. C.; Pannell, L.; Daly, J. W. *J. Am. Chem. Soc.* **1992**, 114, 3475-3478

[3] Aboelsoud, N.H. *J. Med. Plants Res*. **2010**, 4, 82-86

[4] Karch, Steven B. A Brief History of Cocaine: From Inca Monarchs to Cali Cartels: 500 Years of Cocaine Dealing. Boca Raton, FL, CRC Press, 2006.

[5] Sertürner, F. W. A. *Trommsdorff. J. Pharm.* **1806**, *14*, 47-93

[6] Stone, E. *Phil. Trans.* **1763**, *53*, 195-200

[7] Fleming, A. *Br. J. Exp. Pathol.* **1929**, *10*, 226-236

[8] Duggar, B. M. *Ann. N. Y. Acad. Sci.* **1948**, *51*, 177-181

[9] National Center for Health Statistics. *Vital and Health Stat*. **1972** series 3 No. 16

[10] Hoyert, D. L. *NCHS Data Brief*. **2012**, No.88

[11] Wani, M. C.; Taylor, H. L.; Wall, M. E.; Coggon, P.; McPhail, A. T. *J. Am. Chem. Soc.* **1971**, *93*, 2325-2327

[12] Arcamone, F.; Franceschi, G.; Orezzi, P.; Cassinelli, G.; Barbieri, W.; Mondelli, R. *J. Am. Chem. Soc.* **1964**, *86*, 5334-5335

[13] Wall, M. E.;.Wani, M. C; Cook, C. E.; Palmer, K. H.; McPhail, A. T.; Sim, G. A. *J. Am. Chem. Soc.* **1966**; 88, 3888-3890.

[14] Klayman, D. L. *Science.* **1985**, *228*, 1049-1055

[15] Endo, A.; Kuroda, M.; Tanzawa, K. *FEBS Lett.* **1976**, *72*, 323-326

[16] Blunt, J.W.; Copp, B.R.; Hu, W.P.; Munro, M.H.G.; Northcote, P.T.; Prinsep, M. R. *Nat. Prod. Rep.* **2009**, 26, 170-244

[17] Food and Drug Administration (US). http://www.fda.gov/;

[18] Rinehart, K.L.; Holt, T.G.; Fregeau, N.L.; Stroh, J.G.; Keifer, P.A.; Sun, F.; Li, L.H.; Martin, D. G. *J. Org. Chem.* **1990**, 55, 4512-4515.

[19] Olivera, B.M.; Cruz, L.J.; de Santos, V.; LeCheminant, G.W.; Griffin, D.; Zeikus, R.; McIntosh, J.M.; Galyean, R.; Varga, J.; Gray, W.R.; et al. *Biochemistry* **1987**, 26, 2086–2090.

[20] Mayer, A.M.S.; Glaser, K.B.; Cuevas, C.; Jacobs, R.S.; Kem, W.; Little, R.D.; McIntosh, J.M.; Newman, D.J.; Potts, B.C.; Shuster, D.R. *Trends in Pharmacological Sciences.* **2010,** 31, 255-265

[21] Newman, D; Cragg, G. *J. Nat. Prod.***2012**, 75, 311-335

[22] Kellenberger, E.; Hofmann, A.; Quinn, R. J. *Nat. Prod. Rep.* **2011**, 28, 1483-1492

[23] McArdle, B. M.; Quinn, R. J. *ChemBioChem* **2007**, 8, 788-798.

[24] Koonin, E. V.; Wolf, Y. I.; Karev, G. P. *Nature.* **2002**, 420, 218-223

[25] Alzheimer's & Dementia. **2012**, 8, 131-168

[26]Maccioni, R..B.; Farias, G.; Morales, I. Navarrette, L. *Archives of Medical Research.* **2010,** 41, 226-231

[27] Lee, V. M.-Y.; Goedert, M.; Trojanowski, J. Q. *Annu. Rev. Neurosci.* **2001**, *24*, 1121-1159

[28] Grundke-Iqbal I.; Iqbal K.; Tung Y.C.; Quinlan H.M.; Binder L.I. *Proc Natl Acad Sci USA* **1986**, 83,4913-4917

[29] Maeda, S.; Sahara, N.; Saito, Y.; Murayama, S.; Ikai, A.; Takashima, A. *Biochemistry*. **2007**, 46, 3856-3861

[30] Fernandez J, Rojo LE, Kuljis R.O.; Maccioni. R.B. *J Alzheimers Dis* **2008**, 14, 329-333

[31] Hardy, J. Alzheimers Dis., **2006**, 9, 151–153.

[32] Hardy, J. *J. Neurochem.* **2009**, *110*, 1129-1134

[33] Sherrington, R et al. *Nature.* **1995**, 375, 754-60

[34] Fiuza, U-M.; Arias, A. M. *J. of Endocrinology*. **2007,** 194, 459–474

[35] Roberds, S. L. et al. *Hum. Mol. Genet*. **2001**, 10, 1317–1324

[36] Scarpini, E.; Schelterns, P.; Feldman, H. *Lancet Neurology* **2003**, 2, 539-547

[37] Alzheimer's Disease Medications Fact Sheet. NIH Publication No. 08-3431

[38] Cancer Facts & Figures 2012. *American Cancer Society*. **2013**, 1-64

[39] Santen, R.J.; Boyd, N.F.; Chlebowski, R.T.; Cuzick, J.; Dowsett, M.; Easton, D.; Forbes, J.F.; Hankinson, S.E.; Howell, A.; Ingle, J. *Endocr. Relat. Cancer*. **2007**, 14, 169–187

[40] Bocchinfuso, W.P.; Hively, W.P.; Couse, J.F; Varmus, H.E.; Korach, K.S. *Cancer Res*. **1999**, 59, 1869–1876

[41] Chen J.Q.; Cammarata, P.R.; Baines, C.P.; Yager, J.D. *Biochimica et Biophysica Acta* . **2009**, 1793, 1540–1570

[42] Lavigne, J.A.; Goodman, J.E.; Fonong, T.; Odwin, S.; He, P.; Roberts, D.W.; Yager, J. *Cancer Res*. **2001**, 61,

7488–7494

[43] Cavalieri, E.L.; Rogan, E.G. *J. Steroid Biochem Mol. Bio.* **2011,** 125, 169–180

[44] Li,R.; Bianchet, M. A.;Talalay, P.; Amzel, L. M. *Proc Natl Acad Sci USA* **1995**, 92, 8846-8850

[45] Mayhoub, A. S; Marler, L.; Kondratyuk, T.P.; Park, E.J.; Pezzuto, J.M.; Cushman, M. *Bioorg. Med. Chem.* **2012**, 20, 7030–7039

[46] Catella-Lawson, F.; Fitzgerald, G. *A. Drug Saf.* **1995**, 13, 69-75

[47] Vogel, V. G.; Costantino, J. P.; Wickerham, D. L.; Cronin, W. M. *J. Natl. Cancer Inst*. **2002**, 94, 1504

[48] Fisher, B.; Costantino, J. P.; Wickerham, D. L.; Redmond, C. K.; Kavanah, M.; Cronin, W. M.; Vogel, V.; Robidoux, A.; Dimitrov, N.; Atkins, J.; Daly, M.; Wieand, S.; Tan-Chiu, E.; Ford, L.; Wolmark, N. *J. Natl. Cancer Inst*. **1998**, 90, 1371-1388

[49] Chumsri, S.; Howes, T.; Bao, T.; Sabnis, G.; Brodie, A. *J. Steroid Biochem. Mol. Biol.* **2011**, 125, 13-22

[50] Xiao, H.; Parkin, K.L. Phytochemistry, **2007**, 68, 1059-1067

[51] Wargovich, M. J. *Cancer Lett*. **1997,** 114, 11–17

[52] Engene, N.; Rottacker, E.C.; Kastovsky, J.; Byrum, T.; Choi, H.; Ellisman, M.H.; Komarek, J.; Gerwick, W.H. *Int. J. Syst. Evol. Micr.* **2012**, 62, 1171-1178

[53] Gerwick, W. H.; Proteau, P. J.; Nagle, D. G.; Hamel, E.; Blokhin, A.; Slate, D. L. *J. Org. Chem*. **1994**, 59, 1243-1245

[54] Edwards D. J.; Marquez, B. L.; Nogle, L. M.; McPhail K.; Goeger, D. E.; Roberts, M. A.; Gerwick, W. H. Chem. Bio. **2004**, 11, 817-833

[55] Cardellina, J.H.; Marner, F.J.; Moore, R.E. *Science*. **1979**, 204, 193-195

[56] Annis, D. A.; Nazef, N.; Chuang, C.-C.; Scott, M. P.; Nash, H. M. *J. Am. Chem. Soc.* **2004**, 126, 15495-15503.

[57] Coan, K.E.D.; Shoichet, B.K. *J. Am. Chem. Soc.* **2008**, 130, 9606-9612

[58] Schoichet, B. K. *Drug Disc. Today.* **2006**, 11, 607-615

[59] *AntiMarin Database*, University of Canterbury: Christchurch, New Zealand; University of Gottingen, Gottingen, Germany: 2011. http://www.chem.canterbury.ac.nz/marinlit/marinlit.shtml

[60] Cardellina, J.H.; Dalietos, D.; Marner, F.J.; Mynderse, J.S.; Moore, R.E. *Phytochemistry*. **1978**, 17, 2091-2095

[61] Suntornchaswej, S.; Suwanborirux, K.; Koga, K.; Isobe, M. *Chem Asian J*. **2007**, 2, 114-22.

[62] Marner, F. J.; Moore. R. E. *J. Org. Chem.* **1977***,* 42, 2815-2819

[63] Knubel, G.; Larsen, L.K.; Moore, R.E.; Levine, I.A.; Patterson, G.M.L. *J. Antibiotics*. **1990**, 43, 1236-1239

[64] Furasaki, A.; Hashiba, N.; Matsumoto, T.; Hirano, A.; Iwai, Y.; Omura, S. *J.C.S. Chem. Comm*. **1978**, 800-801

[65] Steglich, W.; Steffan, B.; Kopanski, L.; Eckhardt, G. *Angew. Chem. Int. Ed. Engl*. **1980**, 19, 459-460

[66] Meksuriyen, D.; Cordell, G. A. *J. Nat. Prod.* **1988**, 51, 893-899

[67] Blunt, J.W.; Copp, B.R.; Hu, W.P.; Munro, M.H.G.; Northcote, P.T.; Prinsep, M. R. *Nat. Prod. Rep.* **2009**, 26, 170-244

[68] MarinLit search using the taxonomic genus *Spongia* and no species criteria. March 2013.

[69] Gunasekera, S.P. and Schmitz F.J. *J. Org. Chem*. **1991**, 56, 1250-1253

[70] Pretsch, E; Buhlmann, P; Badertscher, M. Structure Determination of Organic Compounds: Tables of Spectral Data. Springer, Heidleberg, 2009.

[71] Zeng, L.M. et al. *Acta Chimica Sinica*. **2001**, 59, 10, 1675-1679

[72] Kazlauskas, R.; Murphy, P. T.; Wells, R. J.; Noack, K.; Oberhansli, W. E.; Schonholzer, P. *Aust. J. Chem*. **1979**, 32, 867-880

[73] De Marino et al. *J. Nat. Prod*. **2000**, 63, 3, 322-326

[74] Park, S.K. et al. *J. Kor. Chem. Soc.* **1994**. 39, 4, 301-305

[75] Gunasekera, S.P. and Schmitz F.J. *J. Org. Chem*. **1991**, 56, 1250-1253

[76] Schumacher, M.; Dicato, M.; Diederich, M.. *J. Food Drug Anal.* **2012**, 20, 250-225

[77] Rüngeler, P., Castro, V., Mora, G., Gören, N., Vichnewski, W., Pahl, H. L., Merfort, I.; Schmidt, T. J. *Bioorg. Med. Chem.* **1999**, 7, 234-2352.

[78] Corey, E. J; Sneen, R. A. *J. Am. Chem. Soc*. **1956**, *78*, 6269-6278

[79] Naqvi, T. J. *Biomol. Screen*. **2004**, *9*, 298–408

[80] Gerhauser, C.; You, M.; Liu, J.; Moriarty, R. M.; Hawthorne, M.; Mehta, R. G.; Moon, R. C.; Pezzuto, J. M. *Cancer Res*. **1997**, 57, 272.

[81] Maiti, A.; Cuendet, M.; Croy, V. L.; Endringer, D. C.; Pezzuto, J. M.; Cushman, M. *J. Med. Chem*. **2007**, 50, 2799-2806.